

# **Holmium microparticles for intratumoral radioablation**

**Wouter Bult**

Thesis, University Utrecht

ISBN: 978-90-393-5458-1

© W. Bult, 2010

Cover Scanning electron micrograph of a single holmium acetylacetonate  
microsphere surrounded by holmium acetylacetonate nanoparticles.

Lay-out Karin van Rijnbach

Printed by Ipskamp Drukkers BV, Enschede, The Netherlands

Dit proefschrift werd (mede) mogelijk gemaakt met financiële steun van  
IDB Holland B.V.; G.E. Healthcare B.V.; De Lindeboom B.V.; MILabs; Phenom-World B.V.;  
Stichting ter bevordering van onderzoek in de ziekenhuisapotheek Groningen,  
Ziekenhuisapotheek UMCG; Veenstra Instruments.

# **Holmium microparticles for intratumoral radioablation**

**Holmium microdeeltjes voor intratumorale radioablatie**

(met een samenvatting in het Nederlands)

## **Proefschrift**

ter verkrijging van de graad van doctor  
aan de Universiteit Utrecht  
op gezag van de rector magnificus, prof. dr. J.C. Stoof,  
ingevolge het besluit van het college voor promoties  
in het openbaar te verdedigen  
op maandag 13 december 2010 des middags te 2.30 uur

door

**Wouter Bult**

geboren op 4 september 1979 te Putte

Promotoren: Prof. dr. ir. W.E. Hennink  
Prof. dr. P.R. Luijten

Co-promotoren: Dr. J.F.W. Nijsen  
Dr. A.D. van het Schip

Voor Rosemarie en Sophie



# Contents

<b>Chapter 1</b>	General introduction and outline of thesis	9
<b>Chapter 2</b>	Microsphere radioembolization of liver malignancies: current developments	17
<b>Chapter 3</b>	Microspheres with ultrahigh holmium content for radioablation of malignancies	41
<b>Chapter 4</b>	Radioactive holmium acetylacetonate microspheres for interstitial microbrachytherapy: an <i>in vitro</i> and <i>in vivo</i> stability study	57
<b>Chapter 5</b>	Interstitial microbrachytherapy using holmium-166 acetylacetonate microspheres: a feasibility study in feline liver cancer patients	75
<b>Chapter 6</b>	Intratumoral administration of holmium-166 acetylacetonate microspheres as a novel minimally-invasive treatment for small kidney tumors	89
<b>Chapter 7</b>	Holmium nanoparticles: preparation and <i>in vitro</i> characterization of a new device for radioablation of solid malignancies	105
<b>Chapter 8</b>	Summary and future perspectives	121
<b>Chapter 9</b>	Nederlandse Samenvatting	129
	List of Affiliations	135
	Curriculum Vitae and List of Publications	139
	Dankwoord	145







# Chapter 1

## General introduction and outline of thesis



## Introduction

Worldwide, cancer is the second cause of death, after cardiovascular diseases (1), and it is estimated that each year over 20 million new cases are presented (2). Solid tumors represent the majority (over 90%) of these new cases, and result in 12 million deaths each year (1, 2). Traditionally, surgical resection has been the preferred treatment since this modality can be considered curative (3). Unfortunately, not all tumors are eligible for curative resection, and surgery is associated with an increase in morbidity. External beam radiotherapy is also considered a potentially curative treatment option. However, not all oncological patients are eligible for this therapy due to motion of the tumor-bearing tissue or the adjacency of relatively radiosensitive organs. Although chemotherapeutic agents are becoming more and more effective, many of the clinically used chemotherapeutics require high tissue concentrations, which are frequently associated with systemic toxicity. To overcome these limitations and drawbacks, a number of minimally invasive treatment options have been proposed in the 1990s, including radiofrequency ablation (4), high-intensity focused ultrasound (5) and local administration of radionuclide labelled particles (6). These local ablative techniques have shown promising results in several types of solitary, solid unresectable tumors of different histotype, such as kidney tumors, brain tumors and liver malignancies (3, 6-8). Traditional treatment modalities are usually not an option for these tumor types due to their localisation and/or the function of the organ where the tumor is located. Thermal ablation techniques are associated with restrictions with respect to the number, location and size of the lesions. In addition, cooling by blood from adjacent vessels may lead to incomplete tumor ablation (9). Local administration of radionuclides can overcome the latter drawback, since tumor kill is not due to the transfer of heat but by ionizing radiation.

The intratumoral administration of particles labelled with the high-energy beta emitting radionuclide yttrium-90 ( $^{90}\text{Y}$ ) in 33 patients with hepatocellular carcinoma led to a size reduction in 90.6% of the tumors, and apparent complete tumor necrosis was observed in 8 patients (6). A drawback to this modality however, is the inability to visualize beta particles directly through nuclear imaging (10). Consequently, accurate dose calculations cannot be performed to predict efficacy and toxicity of the treatment. The administration of the high energy beta and gamma emitter holmium-166 ( $^{166}\text{Ho}$ ) has been proposed to overcome this shortcoming (11). Experiments in prostate cancer and melanoma rodent models have been performed in which the intratumoral administration of  $^{166}\text{Ho}$  was demonstrated to be both safe and efficacious (11-13). Intratumoral administration of  $^{166}\text{Ho}$  has been tested in humans by administering  $^{166}\text{Ho}$  chelated to chitosan to liver cancer patients (14). Complete tumor necrosis was observed in 77% (31 of 40 patients). The authors also reported a number of, mainly hematological, side effects in 11 of 40 patients that could be attributed to the release of  $^{166}\text{Ho}$  from the chitosan complex (14).  $^{166}\text{Ho}$  is an ideal isotope for intratumoral radioablation of solid malignancies because it has a favorable half-life and combines high-energy beta and low-energy gamma emission, which allow for therapy and nuclear imaging, respectively.

At the Nuclear Medicine Department of the University Medical Center Utrecht, work started in the mid-nineties on the development of poly(L-lactic acid) microspheres loaded with the radioisotope holmium-166 ( $^{166}\text{HoPLLAMS}$ ). These microspheres are intended for so-called transcatheter radioembolization of liver tumors, in which radioactive particles are administered through a catheter placed in the hepatic artery and subsequently lodge in and around tumors.  $^{166}\text{HoPLLAMS}$  were found to be radiochemically stable, both *in vitro* (15) and *in vivo* (16), and are currently under clinical investigation in patients with liver metastases (17). Although these particles also appear to be ideally suited for direct injection into solid malignancies, the specific activity is likely too low, since only 0.1 – 0.3 mL can be administered intratumorally per depot. Consequently, the holmium content of the  $^{166}\text{Ho}$  microspheres needs to be increased to become suitable for intratumoral treatment.

Development of a dedicated radioablation device requires preparation and characterization, followed by *in vitro* and *in vivo* stability studies, and efficacy experiments before a phase I clinical trial can be commenced. Preclinical studies on the development of a novel holmium containing radioablation device suitable for intratumoral treatment are presented in this thesis. In addition to the characterization of holmium-loaded microspheres, holmium-loaded nanoparticles are investigated to further extend the applicability of intratumoral radioablation and to address challenges encountered in the *in vivo* studies, like optimization of injection procedure and refinement of dosage delivery.

This thesis is organized as follows: **Chapter 2** describes the clinical status and new developments of yttrium-90 microsphere radioembolization of inoperable liver malignancies. Furthermore, the currently available preclinical literature on  $^{166}\text{HoPLLAMS}$  for radioembolization is reviewed. In addition to the transarterial administration, the direct intratumoral injection of radioactive devices is discussed. **Chapter 3** reports on the preparation and characterization of microspheres with a high holmium load, namely holmium acetylacetonate microspheres (HoAcAcMS). Light microscopy, scanning electron microscopy, and differential scanning calorimetry are used to characterize both non-radioactive and radioactive microspheres. Elemental analysis, Raman spectroscopy and X-ray powder diffraction are performed on non-radioactive microspheres. **Chapter 4** describes the results from both *in vitro* and *in vivo* stability tests on HoAcAcMS. After incubation of the microspheres in buffer, scanning electron microscopy, elemental analysis, infrared spectroscopy, and secondary ion mass spectrometry are performed. An *in vivo* stability study is carried out in VX2 carcinoma-bearing rabbits. In **Chapter 5**, the clinical effects of the intratumoral administration of  $^{166}\text{HoAcAcMS}$  in three house cats with spontaneous liver malignancies are assessed. In **Chapter 6**, the efficacy of intratumoral administration of  $^{166}\text{HoAcAcMS}$  is evaluated in a mouse kidney tumor model. In addition to the efficacy of  $^{166}\text{HoAcAcMS}$ , the *in vivo* multimodality imaging characteristics of the  $^{166}\text{HoAcAcMS}$  are investigated. **Chapter 7** reports on the preparation of HoAcAc nanospheres to further improve and extend the intratumoral applicability of holmium labeled particles. Scanning electron microscopy, elemental

analysis, infrared spectroscopy, differential scanning calorimetry, and short-term stability tests are performed to characterize the particles. **Chapter 8** presents a summary of the previous chapters and discusses the future directions of intratumoral radioablation using  $^{166}\text{Ho}$  laden micro- and nanoparticles.

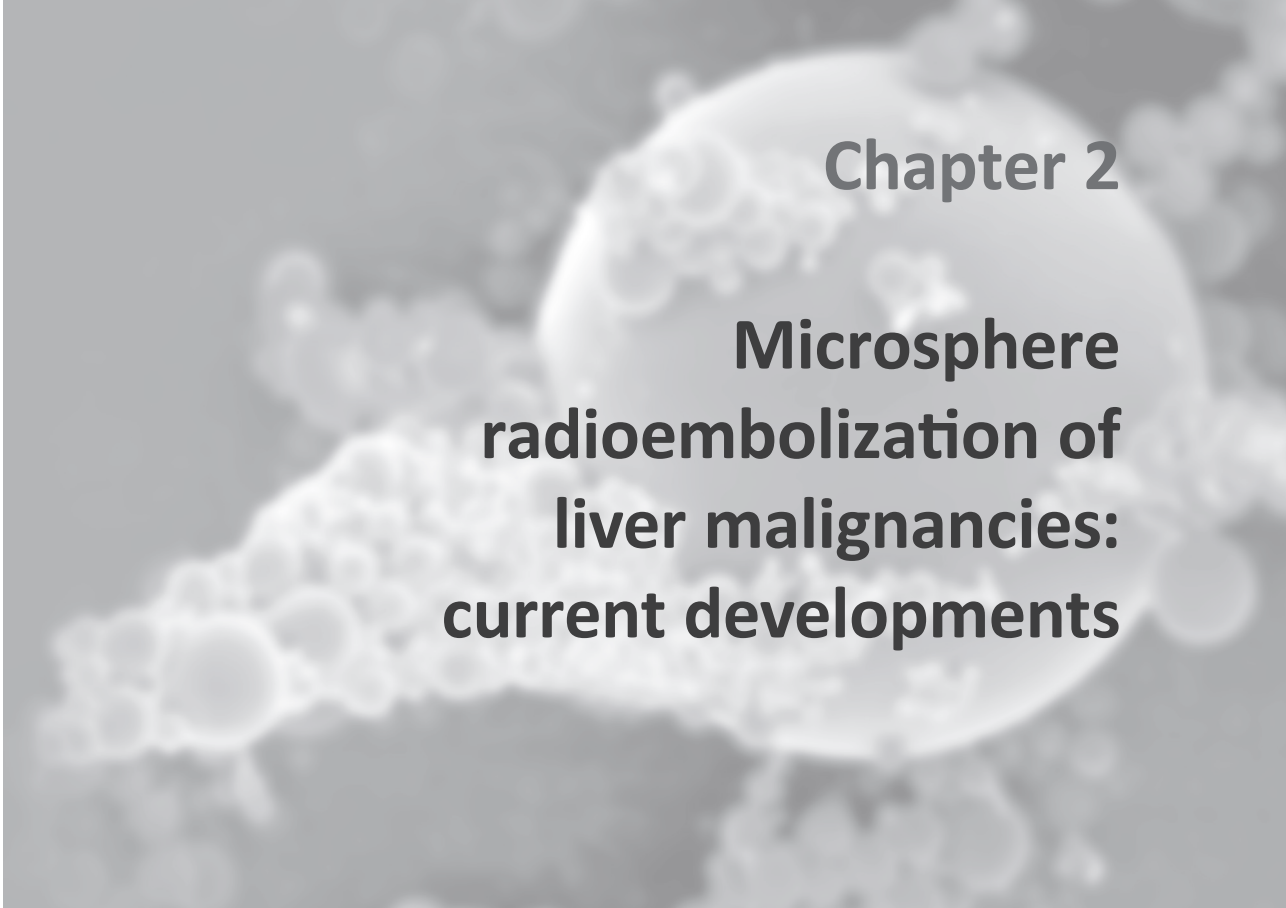
## References

1. A. Jemal, R. Siegel, E. Ward, Y. Hao, J. Xu, and M.J. Thun. Cancer statistics, 2009. *Ca Cancer J Clin.* 59:225-249 (2009).
2. D.M. Parkin, F. Bray, J. Ferlay, and P. Pisani. Global cancer statistics, 2002. *Ca Cancer J Clin.* 55:74-108 (2005).
3. J.E. Kennedy. High-intensity focused ultrasound in the treatment of solid tumours. *Nat Rev Cancer.* 5:321-327 (2005).
4. J.P. McGahan, P.D. Browning, J.M. Brock, and H. Tesluk. Hepatic ablation using radiofrequency electrocautery. *Invest Radiol.* 25:267-270 (1990).
5. H.G. Ter Haar, D. Sinnett, and I. Rivens. High intensity focused ultrasound--a surgical technique for the treatment of discrete liver tumours. *Phys Med Biol.* 34:1743-1750 (1989).
6. J.H. Tian, B.X. Xu, J.M. Zhang, B.W. Dong, P. Liang, and X.D. Wang. Ultrasound-guided internal radiotherapy using yttrium-90-glass microspheres for liver malignancies. *J Nucl Med.* 37:958-963 (1996).
7. D.A. Kunkle and R.G. Uzzo. Cryoablation or radiofrequency ablation of the small renal mass : a meta-analysis. *Cancer.* 113:2671-2680 (2008).
8. E. Liapi and J.F. Geschwind. Transcatheter and ablative therapeutic approaches for solid malignancies. *J Clin Oncol.* 25:978-986 (2007).
9. A.R. Gillams and W.R. Lees. Five-year survival following radiofrequency ablation of small, solitary, hepatic colorectal metastases. *J Vasc Interv Radiol.* 19:712-717 (2008).
10. S. Ho, W.Y. Lau, T.W. Leung, and P.J. Johnson. Internal radiation therapy for patients with primary or metastatic hepatic cancer: a review. *Cancer.* 83:1894-1907 (1998).
11. Y.S. Suzuki, Y. Momose, N. Higashi, A. Shigematsu, K.B. Park, Y.M. Kim, J.R. Kim, and J.M. Ryu. Biodistribution and kinetics of holmium-166-chitosan complex (DW-166HC) in rats and mice. *J Nucl Med.* 39:2161-2166 (1998).
12. J.D. Lee, W.I. Yang, M.G. Lee, Y.H. Ryu, J.H. Park, K.H. Shin, G.E. Kim, C.O. Suh, J.S. Seong, B.H. Han, C.W. Choi, E.H. Kim, K.H. Kim, and K.B. Park. Effective local control of malignant melanoma by intratumoural injection of a beta-emitting radionuclide. *Eur J Nucl Med Mol Imaging.* 29:221-230 (2002).
13. W.Y. Lee, E.Y. Moon, J. Lee, C.H. Choi, S.C. Nam, K.B. Park, J.M. Ryu, Y.H. Chung, S.J. Yoon, and D.K. Lee. Toxicities of <sup>166</sup>Holmium-chitosan in mice. *Arzneimittelforschung.* 48:300-304 (1998).
14. J.K. Kim, K.H. Han, J.T. Lee, Y.H. Paik, S.H. Ahn, J.D. Lee, K.S. Lee, C.Y. Chon, and Y.M. Moon. Long-term clinical outcome of phase IIb clinical trial of percutaneous injection with holmium-166/chitosan complex (Milican) for the treatment of small hepatocellular carcinoma. *Clin Cancer Res.* 12:543-548 (2006).
15. S.W. Zielhuis, J.F.W. Nijsen, G.C. Krijger, A.D. van het Schip, and W.E. Hennink. Holmium-loaded poly(L-lactic acid) microspheres: In vitro degradation study. *Biomacromolecules.* 7:2217-2223 (2006).
16. S.W. Zielhuis, J.F.W. Nijsen, J.H. Seppenwoolde, C.J.G. Bakker, G.C. Krijger, H.F. Dullens, B.A. Zonnenberg, P.P. van Rijk, W.E. Hennink, and A.D. van het Schip. Long-term toxicity of holmium-loaded poly(L-lactic acid) microspheres in rats. *Biomaterials.* 28:4591-4599 (2007).
17. M.L. Smits, J.F. Nijsen, M.A. van den Bosch, M.G. Lam, M.A.D. Vente, J.E. Huijbregts, A.D. van het Schip, M. Elschot, W. Bult, H.W. de Jong, P.C. Meulenhoff, and B.A. Zonnenberg. Holmium-166 radioembolization for the treatment of patients with liver metastases: design of the phase I HEPAR trial. *J Exp Clin Cancer Res.* 29:70 (2010).









# Chapter 2

## Microsphere radioembolization of liver malignancies: current developments

W. Bult, M.A.D. Vente, B.A. Zonnenberg, A.D. van het Schip, J.F.W. Nijsen

Based on Q J Nucl Med Mol Imaging. 2009 Jun;53(3):325-35

## Abstract

The worldwide incidence of hepatic malignancies, both primary and secondary, exceeds 1,000,000 new cases each year. The poor prognosis of patients suffering from hepatic malignancies has led to the development of a liver directed therapy which consists of intra-arterial administration of radioactive particles through a catheter. Yttrium-90 ( $^{90}\text{Y}$ ) microspheres are increasingly applied for this purpose, and up to now nearly all clinical experience with radioembolization has been obtained with these microspheres. The response rate is very promising in both patients with primary and metastatic liver malignancies. Currently, two commercially available  $^{90}\text{Y}$  microsphere devices are in use clinically, both as a first-line treatment and in a salvage setting.

Unfortunately, the use of a pure beta emitter like  $^{90}\text{Y}$  hampers acquisition of high quality nuclear images for pre-treatment work-up and follow-up. This issue was addressed by the development of holmium-166 ( $^{166}\text{Ho}$ ) and rhenium-188 ( $^{188}\text{Re}$ ) microspheres, which emit both beta particles for therapeutic purposes and gamma photons for nuclear imaging. Moreover, since holmium is paramagnetic it allows for magnetic resonance imaging.  $^{166}\text{Ho}$  loaded poly(L-lactic acid) microspheres have been thoroughly investigated in a preclinical setting, and recently the first clinical results for  $^{188}\text{Re}$  microspheres were reported.

This review provides an overview of the current status and (pre-)clinical developments of radioactive microspheres for treatment of liver malignancies. In addition, the intratumoral administration of radioactive particles as a radioablation device is discussed.

## Introduction

A worldwide cancer statistics survey showed that the estimated number of patients diagnosed with liver malignancies, either primary or secondary, was more than 1,000,000 each year (1). Primary liver cancer, hepatocellular carcinoma (HCC) and cholangiocarcinoma, is the sixth most common cancer in the world (2). Overall survival for patients suffering from primary liver malignancies is low, since the majority of patients are not eligible for potentially curative surgical resection, i.e. partial hepatectomy or orthotopic liver transplantation. The five-year survival rate is limited to only 3-5% (1, 2). A survival benefit has been reported for the multikinase inhibitor sorafenib, yet the use of systemic chemotherapy to treat primary liver cancer has been proven to be ineffective (3).

The liver is a common metastatic site for tumors in organs drained by the portal vein, including colorectal, pancreatic and stomach malignancies (4). Colorectal malignancies, its frequency ranking third in women and fourth in men (1), are especially prone to metastasize solely to the liver. Like primary hepatic malignancies, surgical resection is considered to be the only potentially curative option, yet only 10–20% of patients is eligible (5). Approximately 50% of patients with colorectal cancer will develop hepatic metastases during the course of their disease, and five-year survival is approximately 55% (1, 2, 6). Chemotherapeutic treatment of liver metastases has improved markedly the last couple of years, and chemotherapy protocols, combinations of 5-fluorouracil, leucovorin, oxaliplatin and/or irinotecan, are associated with a median survival of almost two years (7).

The vascular anatomy of the liver is different from other organs. Typically, the afferent blood vessel supplying the organ with oxygen-rich blood is an artery. The efferent blood vessel draining oxygen-poor blood from an organ is a vein. The liver, however, receives some of its blood from the hepatic artery, yet the bulk of the blood (over 70%) is supplied from the portal vein. Bierman *et al.* (8) were one of the first to establish the predominantly arterial blood supply to liver tumors. Since this discovery several techniques have been developed to selectively target liver tumors. These include the local administration of cytostatic drugs, like hepatic arterial infusion and isolated hepatic infusion, or intra-arterial embolization techniques such as transarterial chemoembolization and selective intra-arterial radioembolization therapy. In the latter, radioactive microspheres are administered through a catheter, and the microspheres lodge in and around the tumor. This technique has shown remarkable response rates (9) and currently over 15,000 patients have been treated with these microspheres. The aim of this review is to provide an overview of the currently available literature on the (pre-) clinical use of radioactive microspheres to treat liver malignancies.

## Radioactive microspheres as a treatment option

### Background

The concept of intra-arterial administration of radioactive microspheres was first explored by Blanchard *et al.* (10), who injected yttrium-90 ( $^{90}\text{Y}$ ,  $E_{\beta\text{max}} = 2.28$  MeV) (Table I) containing microspheres into the hepatic artery of tumor bearing rabbits. The results were promising, since all  $^{90}\text{Y}$  treated animals showed tumor size reduction. A number of experiments were conducted in different animal models, to determine the safety and efficacy of  $^{90}\text{Y}$  microspheres. In the 1960s (11, 12) and 1970s (13) the first patients (not exclusively patients with liver tumors) were treated with radioactive  $^{90}\text{Y}$  ceramic microspheres, with striking results, and halfway the 1980s, the first clinical trials were conducted on selected patient populations using the transcatheter radioembolization technique (14-17). However, this came to an abrupt halt when several patients died of myelosuppression due to leaching of  $^{90}\text{Y}$  from the microspheres and this device was withdrawn (16, 17).

### Yttrium microspheres

#### *$^{90}\text{Y}$ glass microspheres*

In order to eliminate the leaching problem, yttrium containing glass microspheres (TheraSphere<sup>®</sup>, MDS Nordion, Kanata, Canada) were developed and proposed for treatment of liver malignancies in 1986 (18). These microspheres have a mean diameter of  $25 \pm 10 \mu\text{m}$ , in which  $^{89}\text{Y}_2\text{O}_3$  is stably incorporated (19). The microspheres are neutron irradiated in a nuclear reactor to render them radioactive and since they are resistant to neutron irradiation, very high specific activities can be obtained (2500 Bq per sphere (20))(Table I). The *in vitro* release of yttrium was less than 0.13%, after 6 weeks of incubation in water or saline (21). The microspheres were tested in dogs, and were found to be well tolerated (22). Typically, 100 mg of TheraSphere<sup>®</sup> microspheres is administered to obtain a patient dose of up to 5 GBq. A disadvantage is the high density of these microspheres ( $3.3 \text{ g mL}^{-1}$  (19)), which could lead to premature intravascular settling (23, 24). The half-life of  $^{90}\text{Y}$  (64.1 h) allows for global distribution from one production site. TheraSphere<sup>®</sup> is registered as a Humanitarian Use Device by the FDA for use in radiation treatment or neoadjuvant to surgery or liver transplantation in patients with unresectable hepatocellular carcinoma (20). TheraSphere<sup>®</sup> has also been used for treatment of patients with hepatic metastases (9, 25).

#### *$^{90}\text{Y}$ resin microspheres*

The other  $^{90}\text{Y}$  device in clinical use is SIR-Spheres<sup>®</sup> (SIR-Spheres<sup>®</sup>, SIRTech Medical Ltd., Sydney, Australia). These microspheres likely consist of a cation exchange resin (Aminex 50W-X4 (Biorad, Hercules, CA, USA)) (26), with a diameter of  $32 \pm 10 \mu\text{m}$ , yet the exact chemical composition of SIR-Spheres is proprietary and therefore unknown (27). The resin microspheres are labeled with  $^{90}\text{Y}$  through ion-exchange, and have a relatively low specific activity (approximately 50 Bq/sphere) (28, 29). Unlike the incorporation of the radionuclide within the particle itself, ion

**Table I** Microsphere characteristics.

Microsphere	TheraSphere®	SIR-Sphere®	HoPLLAMS	Re-HSAM
Matrix material	Glass	Resin	PLLA	Albumin
Isotope		<sup>90</sup> Y	<sup>166</sup> Ho	<sup>188</sup> Re
Half-life (h)		64.1	26.8	16.9
γ-energy (keV)		-	81	155
β-energy (MeV)		2.28 (99.9%)	1.77 (48.7%) 1.85 (50.0%)	2.12 (79%)
Activity/sphere (Bq)	2500 (20)	50 (20)	≥ 450 (4)	≥ 100,000*
No. particles instilled	4 million (20)	50 million (20)	33 million (4)	300,000 (65)
Clinical experience	Yes	Yes	2009 <sup>f</sup>	Yes

\* Calculated value

<sup>f</sup> First patients enrolled in 2009.

exchange labeling is a reversible process and may lead to the release of <sup>90</sup>Y from the microspheres when using ionic solutions, like saline. Stability studies showed a <sup>90</sup>Y release of approximately 0.01 to 0.4% after 20 minutes incubation in water (26). However, <sup>90</sup>Y levels in blood and urine of patients have been reported to be less than 50 kBq L<sup>-1</sup>, without clinical side effects like myelosuppression (30). To deliver a typical patient dose of 3 GBq, around 30 to 60 million SIR-Spheres® have to be administered (31-33). Premature filling of tumor vessels can however lead to retrograde flow of microspheres (25). In these cases the calculated dose cannot be delivered (20, 34). SIR-Spheres® were granted premarket approval by the FDA in 2002, for treatment of colorectal cancer metastasized to the liver, with adjuvant floxuridine administered via the hepatic artery (35, 36), but patients with liver malignancies from other origins have also been treated (37, 38).

#### ***Pretreatment work-up and administration procedure***

Patients selected for microsphere treatment are subjected to selective celiac and mesenteric angiography, to accurately map out visceral arterial anatomy, and to identify aberrant vasculature. Arteries arising from the hepatic artery, e.g. the right gastric artery and the gastroduodenal artery, are prophylactically occluded using coils to isolate the hepatic arterial circulation (39). Venous phase imaging is performed to evaluate the status and to identify obstructions of the portal vein. Portal vein thrombosis is considered to be a contraindication for radioembolization with resin microspheres, since an obstruction of the portal vein can hamper the compensatory portal vein blood flow to maintain adequate perfusion of the liver (35, 36). Subsequently, <sup>99m</sup>Tc labeled albumin macroaggregates (<sup>99m</sup>Tc MAA) are administered (approximately 150 MBq), followed by single photon emission tomography (SPECT) to establish the degree of extrahepatic shunting. This is done by calculating the amount of <sup>99m</sup>Tc activity observed in the lungs or gastrointestinal

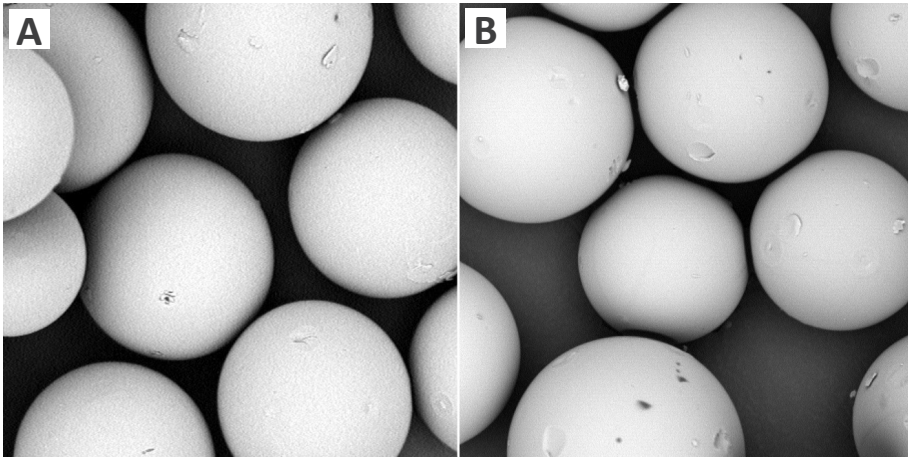


**Figure 1.** Scanning electron micrographs of HoPLLAMS. **A:** before neutron activation, **B:** after neutron activation.

tract relative to the total amount of activity injected (20). Depending on the degree of shunting to non-target organs, the intended administered dose is reduced, in case of  $^{90}\text{Y}$  resin microspheres. No resin microspheres should be administered, when a shunt fraction  $>20\%$  is observed (29). For  $^{90}\text{Y}$  glass microspheres, the shunt fraction should be  $<10\%$ , without adjustments to the dose administered. If the shunt fraction is  $>10\%$ , no microspheres are to be administered (20, 36). The  $^{99\text{m}}\text{Tc}$  MAA scan is also used to assess the intrahepatic distribution.

The  $^{90}\text{Y}$  resin microspheres are slowly injected via a correctly placed 3F catheter, using water for injection, alternated with a non-ionogenic contrast agent. The administration is stopped prematurely when stasis or retrograde flow of the contrast is observed under fluoroscopy to avoid side effects. During the administration of  $^{90}\text{Y}$  glass microspheres, no stasis or retrograde flow occurs, since a very limited number of microspheres is administered causing no macro-embolic effects (20). The microspheres are administered with saline, without the use of a contrast agent. Post administration a planar Bremsstrahlung scan may be acquired, to qualitatively assess the distribution of microspheres (20). Unfortunately, Bremsstrahlung does not allow for quantitative imaging and as a consequence, no accurate dose calculations can be performed (40). Recently, SPECT/CT has been used to improve the spatial resolution by correlating the nuclear images to the anatomical images (41).

### ***Clinical experience with $^{90}\text{Y}$ microspheres***

Intra-arterial radioembolization with radioactive microspheres, containing the high energy beta emitter  $^{90}\text{Y}$ , is increasingly applied in patients with unresectable hepatic malignancies. The majority of patients with liver malignancies have received  $^{90}\text{Y}$  radioembolization as salvage therapy, however nowadays microspheres are increasingly applied as first-line treatment in the US. Unfortunately, results from large phase III clinical trials have not been published yet. Recently, a meta-analysis of

the literature was published, which investigated the response rates after treatment of both HCC and colorectal liver metastases with either glass or resin based  $^{90}\text{Y}$  microspheres (9). Complete response, partial response and stable disease were defined as any response (AR). When  $^{90}\text{Y}$  microspheres were used as a salvage therapy in patients with colorectal liver metastases, an AR of 80% was found. When used concomitantly with chemotherapy as a first-line treatment, AR was up to 90%. The use of either glass or resin microspheres in patients with metastatic liver tumors did not show a significant difference in response. This can be attributed to the limited number of patients (8%) that was treated with glass microspheres (9). In patients with HCC, the authors did find a relationship between response and type of microspheres used. In patients with primary liver malignancies, the response was significantly higher when patients were treated with resin microspheres than patients treated with glass microspheres (0.89 vs. 0.78). Interestingly,  $^{90}\text{Y}$  glass microspheres are registered for primary liver tumors, whilst  $^{90}\text{Y}$  resin microspheres are registered for metastatic liver tumors (20).

The use of the resin microspheres is usually accompanied by the post embolisation syndrome, which consists of fatigue, nausea, fever, right upper quadrant pain and/or vomiting. These symptoms are transitory, and can be controlled by medication (9, 31).

## Holmium microspheres

### *Holmium-166 poly(L-lactic acid) microspheres*

Holmium containing poly(L-lactic acid) (PLLA) microspheres (HoPLLAMS) were proposed as suitable candidates for radioembolization treatment of hepatic malignancies, in the early 1990s by Mumper *et al.* (42, 43), and further investigated at the authors' nuclear medicine department (44, 45). These polymer microspheres are prepared by dissolving the lipophilic complex holmium acetylacetonate (HoAcAc) and PLLA in chloroform, followed by emulsification and subsequent evaporation of chloroform (44). The microspheres are made radioactive by neutron activation of holmium-165 ( $^{165}\text{Ho}$ ) to yield holmium-166 ( $^{166}\text{Ho}$ ) ( $E_{\beta\text{max}}$  1.77 (48.7%) and 1.85 (50.5%) MeV) (46) (Fig. 1). Besides beta particles, holmium emits gamma photons (81 keV (6.7%)), suitable for nuclear imaging (Table I).

In addition to the nuclear characteristics, holmium is highly paramagnetic and can consequently be visualized by magnetic resonance imaging (MRI) (47). HoPLLAMS show a high transverse relaxation rate, resulting in blackening on a  $T_2^*$  weighted image. Holmium is therefore, like iron, a negative contrast agent. Moreover, holmium has a high linear attenuation coefficient, allowing for visualization through X-ray computed tomography (CT) (47). Holmium has a higher X-ray attenuation coefficient than iodine, which is one of the most widely used CT contrast agents (47).  $^{166}\text{Ho}$  can be regarded as a true multimodality imaging element.

The HoPLLAMS described by Mumper *et al.* (42), had a holmium content of 9%, whereas the holmium content of the microspheres developed by Nijssen *et al.* was 17% (42, 44). This increased holmium loading would enable the delivery of tumoricidal amounts of activity to patients in a routine setting, and allow sufficient time for transport of the microspheres from the reactor to a treatment centre (42,

44). The HoPLLAMS are resilient to neutron irradiation for up to 6 hours (flux  $5 \times 10^{12} \text{ cm}^{-2} \text{ s}^{-1}$ ) attaining approximately 17 GBq  $^{166}\text{Ho}$  (600 mg of HoPLLAMS) end-of-bombardment (48-50). The beta energy of  $^{166}\text{Ho}$  is slightly lower than that of  $^{90}\text{Y}$  and the physical half-life is shorter (26.8 h for  $^{166}\text{Ho}$  vs. 64.1 h for  $^{90}\text{Y}$ ). Hence, the absorbed radiation dose per Bq of  $^{166}\text{Ho}$  is lower than of  $^{90}\text{Y}$  ( $^{166}\text{Ho}$ : 8.7 mGy MBq $^{-1}$ ;  $^{90}\text{Y}$ : 28 mGy MBq $^{-1}$ ). For an equivalent radiation dose on tissue, roughly three times the amount of radioactivity of  $^{166}\text{Ho}$  has to be administered compared to  $^{90}\text{Y}$  (4, 42). An advantage of the short half-life of  $^{166}\text{Ho}$  is the higher dose rate compared to  $^{90}\text{Y}$ , since more energy is deposited in a shorter timeframe (51, 52). Conversely, the relatively short half-life of  $^{166}\text{Ho}$  requires separate neutron irradiation of each patient dose, and a short logistical line to get the dose from the reactor to the patient in time.

Albeit somewhat laborious, the separate neutron irradiation per patient dose in the final container has a distinct advantage in terms of radiation safety and sterility of the product. The technician does not receive an additional dose on the hands, since no transfer is needed from the shipping vial to the administration vial (33). A product is regarded sterile when a radiation dose of at least 25 kGy is absorbed in the final container (53). Neutron irradiation is associated with an absorbed radiation dose in excess of 5,000 kGy, and therefore the HoPLLAMS can be considered to be sterile according to the European Pharmacopoeia (Ph.Eur.) (49). The presence of residual solvents in the final product should also meet the requirements set out by the Ph.Eur. The limit stipulated by the Ph.Eur. is considered to be the maximum daily intake. In the case of HoPLLAMS, chloroform is used, the limit for which is 60 ppm in the final product (53). It was demonstrated that chloroform was completely removed from the microspheres by radiolysis during neutron irradiation (54).

The stability of HoPLLAMS was studied by measuring the long term release of  $^{166\text{m}}\text{Ho}$  from neutron activated microspheres for 52 weeks by incubation of HoPLLAMS in phosphate buffer (55). The cumulative release was approximately 0.7%, and it was demonstrated that microspheres had degraded to the insoluble holmium lactate, which retained the holmium after degradation. The HoPLLAMS have been produced under GMP conditions and are considered to be suitable for application in human subjects (56).

### ***Preclinical experience with holmium microspheres***

Holmium microspheres have not yet been used in a clinical setting, though a number of pre-clinical animal experiments have been performed.

A non-survival biodistribution study in rats was performed in which it was demonstrated that the  $^{166}\text{HoPLLAMS}$  deposition was confined to the liver and that in the tumorous tissue the radioactivity concentration was six times higher than in the non-target liver tissue (57). This finding was similar to the tumor-to-liver ratio of  $^{90}\text{Y}$  microspheres in human patients (30). To demonstrate that  $^{166}\text{HoPLLAMS}$  have a tumoricidal effect, an efficacy study in VX2 carcinoma bearing rabbits was performed. This was studied by administering  $^{166}\text{HoPLLAMS}$  or  $^{165}\text{HoPLLAMS}$  into the hepatic artery (58). All animals in the  $^{166}\text{HoPLLAMS}$  group showed an arrest in tumor growth and histology revealed that the tumors were necrotic. These experiments



showed that  $^{166}\text{Ho}$ PLLAMS preferentially accumulate in and around the tumor, and that a therapeutic effect is observed whilst sparing healthy tissue.

Apart from *in vitro* release experiments, acute, mid- and long-term effects were studied after implantation of decayed  $^{166}\text{Ho}$ PLLAMS in the liver of healthy Wistar rats (59). The animals were monitored for a period of up to 18 months. Toxicity was studied by evaluating clinical and biochemical parameters, and tissue response was investigated based on post-mortem examinations. In addition, the *in vivo* holmium release was studied by subjecting bone tissue to neutron activation analysis. Since holmium is a calcium-analogue it will accumulate in bone, and the holmium content in bone should therefore be increased if leaching from the microspheres had occurred (60). No clinical and biochemical toxic effects were observed. In accordance with the *in vitro* release results, no leaching of holmium had occurred *in vivo*. It was concluded that decayed  $^{166}\text{Ho}$ PLLAMS do not provoke any toxic reaction and can be applied safely *in vivo*.

A comprehensive toxicity study in healthy, non-tumor bearing pigs was conducted in which up to 6.5 GBq of  $^{166}\text{Ho}$ PLLAMS was administered via the hepatic artery, which corresponded with absorbed liver doses in excess of 120 Gy (61). The porcine model was selected, since this is one of the most anthropomorphic laboratory animal species, and pigs are more suitable for the catheterization procedure compared to smaller laboratory animals (61). The animals were monitored clinically, biochemically, and hematologically for one or two months. No signs of the post-embolisation syndrome were observed in these animals. A transient rise in aspartate aminotransferase levels post  $^{166}\text{Ho}$ PLLAMS administration was observed, which is an indicator for the presence of ischemic/necrotic liver tissue. No abnormalities were observed in the other blood parameters. After termination, a pathological examination was undertaken. Typical pathological findings were moderate to marked atrophy to one or more liver lobes with a compensatory hyperplasia of other liver lobes (61). The authors did observe toxicity caused by inadvertent delivery of  $^{166}\text{Ho}$ PLLAMS to the stomach due to retrograde flow. This was prevented in the remaining experiments by administering the microspheres in a 50% v/v mixture of saline and iodinated contrast. This study demonstrated that pigs can withstand liver absorbed doses up to 160 Gy, and that hepatic arterial embolization with  $^{166}\text{Ho}$ PLLAMS is not associated with clinically relevant side effects, if administered correctly. A phase I clinical study in patients with unresectable liver tumors has commenced in 2009 at the authors' medical center.

## Rhenium microspheres

### *Rhenium-186 and -188 microspheres*

Hafeli (62, 63) and Wunderlich (64) have proposed rhenium 186/188 microspheres as an alternative for  $^{90}\text{Y}$  containing microspheres (62-64).  $^{186}\text{Re}$  is a combined beta and gamma emitter ( $E_{\beta_{\text{max}}}$  1.07 MeV;  $E_{\gamma}$  137 keV) (62), with a half-life of 89.2 h.  $^{188}\text{Re}$  has a half-life of 16.9 h, and emits both beta particles and gamma rays ( $E_{\beta_{\text{max}}}$  2.12 MeV;  $E_{\gamma}$  155 keV) (63) (Table I).  $^{186}\text{Re}/^{188}\text{Re}$  glass,  $^{186}\text{Re}/^{188}\text{Re}$  poly(L-lactic acid) RePLLAMS and  $^{188}\text{Re}$  human serum albumin microspheres ( $^{188}\text{Re}$ -HSAM) were proposed as

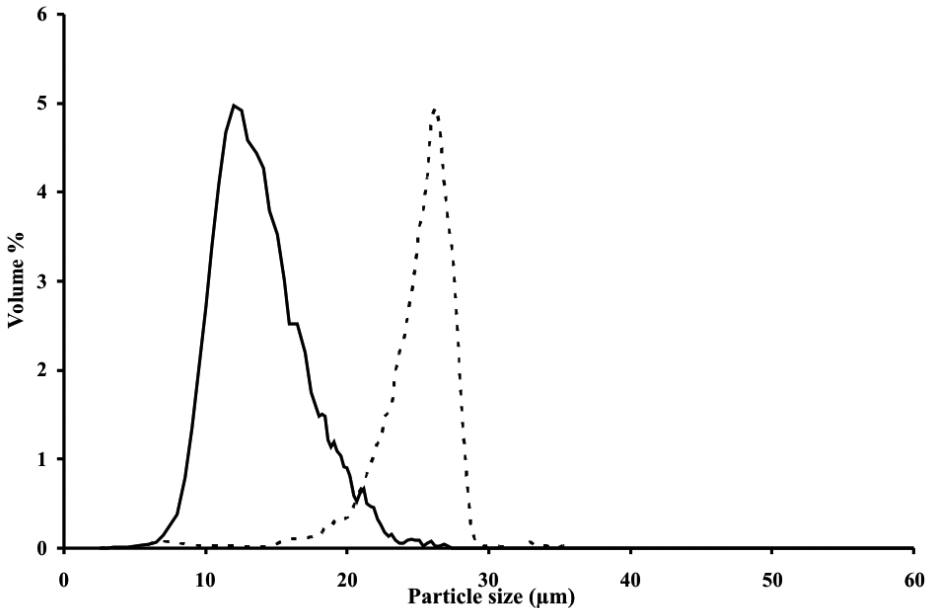


**Figure 2.** Size distribution measured using a coulter counter. The solid line represents the size distribution of macroaggregated albumin (Technescan® LyoMAA, Mallinckrodt Medical B.V., Petten, The Netherlands), the dotted line represents the size distribution of SIR-Spheres®.

possible carriers. In both the glass microspheres and PLLA microspheres, rhenium is incorporated in non-radioactive form, followed by neutron activation. The naturally occurring element rhenium consists of two isotopes,  $^{185}\text{Re}$  (37.4%) and  $^{187}\text{Re}$  (62.6%) (46), resulting in  $^{186}\text{Re}/^{188}\text{Re}$  after neutron activation (62, 63). It was reported that neutron irradiation of RePLLAMS leads to damage to the microspheres, making them unsuitable for application in a clinical setting (63). Other disadvantages of  $^{186}\text{Re}/^{188}\text{Re}$  microspheres are the different physical half-lives, different energies and different abundancies, which lead to impractical and difficult dosimetric calculations. The  $^{186}/^{188}\text{Re}$  glass and polymer microspheres have not been tested in humans, while a single study in a small number of patients has been published for  $^{188}\text{Re}$ -HSAM microspheres (65). The  $^{188}\text{Re}$ -HSAM are prepared by adding carrier free  $^{188}\text{Re}$  sodium perrhenate from a  $^{188}\text{W}/^{188}\text{Re}$  generator to human serum albumin microspheres (Rotop Pharmaka AG, Radeberg, Germany), followed by a reduction step of perrhenate (66). The microspheres were found to retain more than 90% of  $^{188}\text{Re}$  after 30 h of incubation in plasma (66). Similar to  $^{166}\text{Ho}$ , four to five fold higher  $^{188}\text{Re}$  activities need to be administered to obtain an equivalent absorbed dose as  $^{90}\text{Y}$  (65).

#### ***Clinical experience rhenium-188 microspheres***

Radioembolization with  $^{188}\text{Re}$ -HSAM has been tested in ten patients (65). Three patients suffered from HCC, and the remaining seven suffered from colorectal liver metastases. Patients received  $13.6 \pm 4.7$  GBq of  $^{188}\text{Re}$ -HSAM ( $2\text{-}3 \times 10^5$  microspheres).

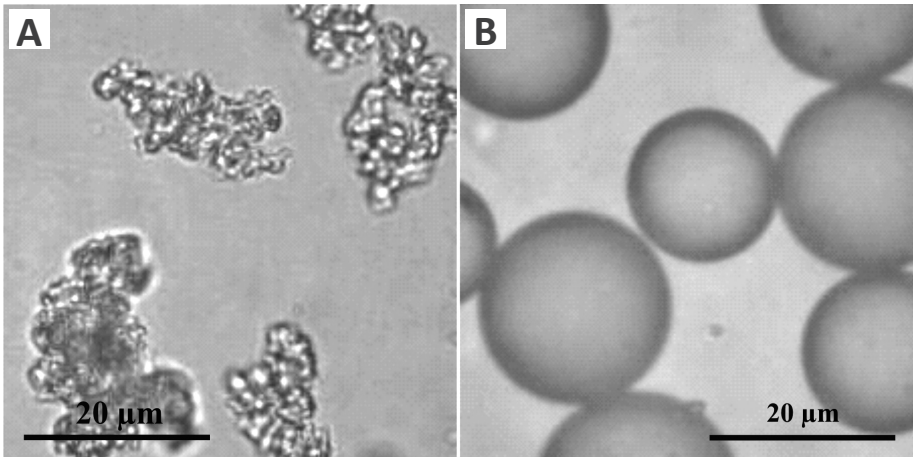


**Figure 3.** Light micrographs showing **A:** Macroaggregated albumin (Technescan® LyoMAA, Mallinckrodt Medical B.V., Petten, The Netherlands), and **B:** SIR-Spheres®.

Retrograde flow was monitored for by administering the microspheres using a 50% v/v mixture of saline and iodinated contrast agent. Two patients (20%) showed partial response, five patients (50%) had stable disease, and in three (30%) patients disease progression was observed. Owing to the small size and heterogeneity of the patient group, no conclusive effects could be determined and a larger patient cohort is warranted, to evaluate the effect of radioembolization with  $^{188}\text{Re}$ -HSAM on hepatic malignancies. The treatment was well tolerated in three patients, while the other seven patients displayed transient toxicity, e.g. nausea, emesis, fever, fatigue, abdominal pain (65), which was unrelated to the dose administered (up to 20.5 GBq).

## Challenges to improve microsphere radioembolization

The use of  $^{90}\text{Y}$  radioembolization for treatment of inoperable liver malignancies is undeniably very promising. However, there are some challenges to be met, to further improve efficacy and safety of radioembolization using microspheres.

### $^{99\text{m}}\text{Tc}$ MAA for imaging of expected biodistribution

In the 1960s, the expected biodistribution of  $^{90}\text{Y}$  microspheres was assessed by administering ceramic microspheres labeled with ytterbium-169 ( $^{169}\text{Yb}$ ,  $E_{\gamma}$  198 keV; half-life 32.0 days (46)), after which radioembolization was performed using the same ceramic microspheres labeled with  $^{90}\text{Y}$  (12). In the late 1970s Grady *et al.* placed the catheter in the hepatic artery via laparotomy. Proper position of the catheter was checked by infusion of a fluorescent dye (fluorescein) and ultraviolet light. Yet the authors commented that the use of gamma emitting microspheres would be beneficial (13).

It was not until the late 1980s when  $^{99\text{m}}\text{Tc}$  labeled human serum albumin microspheres were introduced to predict the  $^{90}\text{Y}$  glass microspheres biodistribution

(16). The  $^{99m}\text{Tc}$  scans and post administration Bremsstrahlung scans revealed similar distribution patterns (16, 67). Other groups utilized  $^{99m}\text{Tc}$  MAA to visualize possible extrahepatic shunting of  $^{90}\text{Y}$  resin microspheres (30, 68). Since then,  $^{99m}\text{Tc}$  MAA have been used to predict  $^{90}\text{Y}$  microspheres distribution.

Unfortunately, the  $^{99m}\text{Tc}$  MAA scan often approximates the microsphere distribution poorly. This is due to a number of dissimilarities between the  $^{99m}\text{Tc}$  MAA and the  $^{90}\text{Y}$  microspheres (69). The number of particles administered, the size, shape and density of the MAA are different from  $^{90}\text{Y}$  microspheres. The number of particles used to predict the biodistribution ( $1 - 2 \times 10^5$  particles) is significantly lower than the number of  $^{90}\text{Y}$  microspheres applied (resin:  $30 - 60 \times 10^6$ ; glass:  $4 - 5 \times 10^6$  particles), while the density of MAA ( $1.1 \text{ g mL}^{-1}$ ) (70) is lower than that of  $^{90}\text{Y}$  microspheres (resin:  $1.6 \text{ g mL}^{-1}$ ; glass:  $3.3 \text{ g mL}^{-1}$ ).

The size of MAA particles ranges between  $10 - 100 \mu\text{m}$  (mean  $15 \mu\text{m}$ ) (53), while  $^{90}\text{Y}$  microspheres have a mean particle size of around  $30 \mu\text{m}$  (Fig. 2). There is also a major difference in shape (Fig. 3). This might be resolved by using human serum albumin microspheres (66) labeled with  $^{99m}\text{Tc}$  as a scout dose, since these particles would have approximately the same size and shape.

It has also been reported in the literature that there is a time-dependent degradation of  $^{99m}\text{Tc}$  MAA, leading to reduction in particle size and free  $^{99m}\text{Tc}$ -pertechnetate, which can lead to inaccurate prediction of  $^{90}\text{Y}$  microsphere distribution (69). Moreover, no correlation between  $^{99m}\text{Tc}$  MAA and treatment response (tumor marker data, CT data or survival time) was observed after the administration of  $^{90}\text{Y}$  resin microspheres (71). These factors show that  $^{99m}\text{Tc}$  MAA particles are not the optimal  $^{90}\text{Y}$  microsphere analog.

### **$^{166}\text{Ho}$ -PLLAMS for imaging of expected biodistribution**

In 1994, Turner *et al.* explored the value of  $^{166}\text{Ho}$  resin microspheres as a predictor of the biodistribution of a treatment dose of the same microspheres (72). They administered a scout dose of  $^{166}\text{Ho}$  resin microspheres (8.5 mg; 174 MBq) into a pig, followed by a "treatment" dose (16 mg; 325 MBq)  $^{166}\text{Ho}$  microspheres. SPECT scans were acquired, and the absorbed doses calculated in the regions of interest. The holmium microspheres could be used both as a predictor of biodistribution of  $^{166}\text{Ho}$  microspheres and for quantitative SPECT measurements. However, the reduced image quality caused by scatter and Bremsstrahlung posed a challenge for image reconstruction.

The use of  $^{166}\text{Ho}$  microspheres was further investigated at the authors' medical center. A Monte Carlo based reconstruction method was developed to enhance the accuracy of the reconstructed activity distribution maps (73). This method allows for accurate absorbed dose calculations (28). It is anticipated that in a clinical setting a patient dose of  $^{166}\text{Ho}$ PLLAMS will consist of 600 mg with a maximum of 15 GBq  $^{166}\text{Ho}$ . The pretreatment scout dose is planned to be approximately 10% (60 mg) of the total amount of microspheres administered. This was tested in a pig study as well (74). Using SPECT, the biodistribution of a scout dose of  $^{166}\text{Ho}$ PLLAMS (60 mg; 250 MBq) was compared to the biodistribution of a treatment dose of  $^{166}\text{Ho}$ PLLAMS (540 mg; 250 MBq). If catheter placement had been identical, the distribution of the

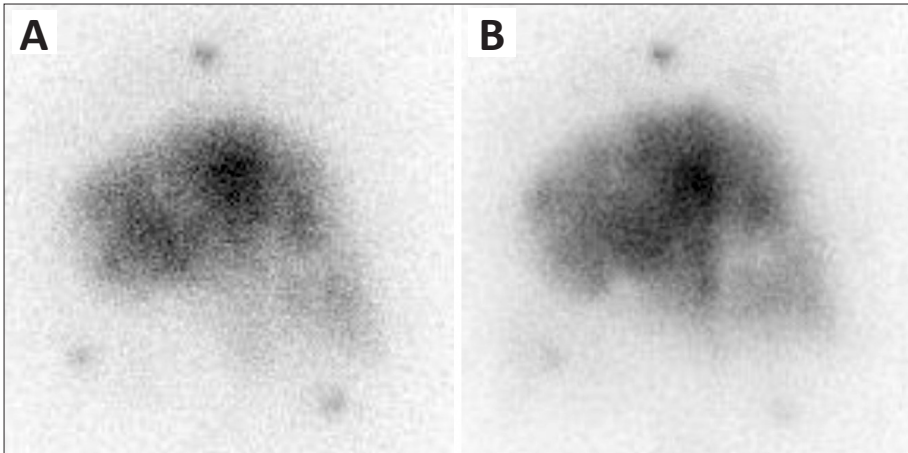


**Figure 4.** Planar scintigraphs from a non-tumor bearing pig. **A:** Scintigraph of the scout dose  $^{166}\text{HoPLLAMS}$  (60 mg). **B:** Scintigraph of the combined scout/treatment dose  $^{166}\text{HoPLLAMS}$  (600 mg).

scout dose and treatment dose were nearly identical (Fig. 5). It was concluded that a scout dose of  $^{166}\text{HoPLLAMS}$  can be used to correctly predict the biodistribution of a treatment dose. Currently, the predictive value of the scout dose for dosimetry is being investigated.

#### Positron emitters for imaging of expected biodistribution

Positron emitting isotopes, like copper-64 ( $^{64}\text{Cu}$ ), yttrium-86 ( $^{86}\text{Y}$ ) and zirconium-89 ( $^{89}\text{Zr}$ ) have been coupled to resin based microspheres to allow for visualization and quantification of the  $^{90}\text{Y}$  microspheres through positron emission tomography (PET) (28). Unfortunately, copper readily binds quantitatively to albumin, as a consequence of which  $^{64}\text{Cu}$  is released from the microsphere surface and is bound by albumin in the body upon administration. In an experiment carried out in rats, >95% of the label was homogeneously distributed throughout the body, rendering the microspheres unsuitable for biodistribution assessment. The  $^{86}\text{Y}$  and  $^{89}\text{Zr}$  containing resin microspheres were found to be stable in vivo in these rat experiments (28). Besides positrons  $^{86}\text{Y}$  emits photons which increase background noise deteriorating contrast (75). This confounds the determination of the shunt fraction (27). The half-life (78.4 h) of  $^{89}\text{Zr}$  exceeds that of  $^{90}\text{Y}$  (64.1 h), and therefore the presence of  $^{89}\text{Zr}$  may influence the post-treatment  $^{90}\text{Y}$  scan (27).

Fluorine-18 ( $^{18}\text{F}$ ) labeled resin microspheres have also been proposed (27).  $^{18}\text{F}$  microspheres were shown to have a limited stability in rabbits. Approximately 15% of the  $^{18}\text{F}$  had leached from the microspheres within 45 min post injection. This renders these microspheres unsuitable for PET quantification of extrahepatic shunting.

## Magnetic Resonance Imaging in transcatheter radioembolization

### MR tracking of microspheres

Currently, X-ray fluoroscopy in combination with a radiopaque iodinated contrast agent is used for correct positioning of the catheter in the hepatic artery and for coiling of aberrant vessels prior to microsphere administration. This procedure can take up to two hours, resulting in a significant radiation burden for the patient and the intervention radiologist. Since HoPLLAMS can be tracked using MRI, due to the paramagnetic nature of holmium, MR guided administration of HoPLLAMS was proposed by Nijsen *et al.* (76) and by Seppenwoolde *et al.* (77, 78) (Fig. 5).

In the experimental setup of Nijsen *et al.* HoPLLAMS were administered to VX2 tumor-bearing rabbits via the hepatic artery (76). Rabbits were subjected to MR imaging before and after the administration of HoPLLAMS. In this way they were able to visualize the accumulation of HoPLLAMS in and around the tumor using MRI.

In order to investigate the MR guided catheterization and administration of HoPLLAMS experiments were conducted in healthy pigs under real-time MR guidance (78). After positioning of a custom made catheter fitted with MR markers, microspheres were administered and their biodistribution qualitatively assessed using MR. Real-time MR guided administration and biodistribution visualization both proved feasible. MR compatible catheters and guide wires should be more widely available before clinical application will be feasible.

Gupta and co-workers suggested iron labeled glass microspheres as an analog for  $^{90}\text{Y}$  glass microspheres to allow for real-time MR tracking (69). VX2 tumor-bearing rabbits were selectively catheterized under X-ray fluoroscopy and microspheres were administered under MR guidance to visualize the accumulation in and around the tumor. The results were promising, however, more preclinical studies are warranted to compare the biodistribution patterns of iron and yttrium labeled glass microspheres.

### MR quantification of HoPLLAMS

Apart from quantitative SPECT, MRI can also be used for quantification of HoPLLAMS or iron labeled microspheres since there is a strong correlation between the amount of microspheres administered (in mg) and the transverse relaxation rate  $R_2^*$  (77). The feasibility of MR quantification of HoPLLAMS was demonstrated in ex-vivo non-tumor-bearing rabbit livers after administration of known amounts of HoPLLAMS. MR scans were acquired and processed for quantification (77). Unfortunately, an underestimation of the amount of microspheres was observed when over 40 mg of HoPLLAMS was administered.  $^{166}\text{Ho}$ PLLAMS were also administered in vivo to tumor-bearing rabbits, followed by MR imaging and gamma scintigraphy. It appeared that diffusion sensitivity compromised the holmium specific MR sequence, due to the relatively long echo time associated with spin echo sequences. Another MR sampling technique was proposed to overcome this problem by using a shorter echo time, which allows for more accurate sampling of highly paramagnetic artifacts (79). By using this so-called MGEFID sequence a good correspondence was observed



**Figure 5.** T<sub>2</sub>\* weighted coronal scan showing a non-tumor bearing pig. The outline of the liver is highlighted. HoPLLAMS appear as blackening in the liver, as indicated by the arrows.

between injected and measured amount of microspheres after administration of up to 70 mg of HoPLLAMS into an excised rabbit liver (140 g). This amount of microspheres corresponds to a human dose of HoPLLAMS of approximately 700 mg. MR quantification of HoPLLAMS is therefore considered feasible.

## Intratumoral injections

Microsphere radioembolization is a very effective technique for the treatment of inoperable liver tumors, mainly due to the high tumor-to-non-tumor ratio that is achieved. Unfortunately, contraindications for liver radioembolization exist. Patients with a life expectancy of less than three months are withheld treatment, since the side effects that are associated with radioembolization might outweigh the benefits (80, 81). Obviously, patients need to have an adequate liver function to be able to tolerate this liver-directed radiation treatment (80, 81). Unresectable colorectal liver metastases are a major indication for radioembolization. However, the chemotherapy regimens nowadays typically used in patients with metastatic colorectal cancer also include bevacizumab (82) or cetuximab (83) and, unfortunately, the long-term

use of these anti-vascular agents can result in tumor feeding vessels too frail for microspheres to be deposited peri- and endotumorally (84). Post-angiography exclusion criteria include portal vein thrombosis, extrahepatic  $^{99m}\text{Tc}$  MAA deposition exceeding 20% that cannot be reduced by lobar infusion, the addition of balloon catheters or additional coils (80, 85). Moreover, vascular abnormalities that cannot be corrected by preventive coiling could result in significant reflux of hepatic arterial blood to the stomach, pancreas or duodenum and are therefore excluded from radioembolization.

Patients with unresectable liver malignancies, who, for either one of the abovementioned reasons, are not amenable for radioembolization, might benefit from local ablative techniques such as radiofrequency ablation and high-intensity focussed ultrasound. These techniques locally apply heat to induce tumor kill (86, 87), and have shown promising results in patients with liver tumors. Restrictions associated with thermal ablation are the number, location and size of the lesions. Also, the cooling by blood from adjacent vessels, the so-called 'heat sink phenomenon' (88), may lead to incomplete tumor ablation. In order to overcome the latter limitation, it could be postulated that instead of applying heat, a dose of ionizing radiation brought upon the tumors by beta emitting microspheres is used, not, however, administered *via* the hepatic artery, but injected *directly* into the lesions. Whereas liver radioembolization is also known as intra-arterial microbrachytherapy (89), this technique may be described as a type of interstitial microbrachytherapy.

Intratumoral administration of  $^{90}\text{Y}$  glass microspheres was performed by Tian *et al.* in 33 patients with unresectable liver malignancies, mostly (27/33) HCC (90). Patients had a limited number ( $\leq 3$ ) of lesions with a diameter not exceeding 5 cm in most cases (90). Treatment was repeated maximally five times. The  $^{90}\text{Y}$  microspheres (74-92.5 MBq in 0.1-0.3 mL iodinated oil) were administered percutaneously under ultrasound guidance. The iodinated oil prevented the precipitation of the microspheres from the solution. The high specific activity of the  $^{90}\text{Y}$  glass microspheres (see Table I) allowed for the delivery to the compact tumor tissue of tumoricidal doses because small numbers of microspheres were required. The results were promising: 90.6% of the tumors treated showed a size reduction, and apparent complete tumor necrosis was observed in 8 patients. Although these results were very promising, the extrahepatic delivery of microspheres, especially to the lungs, in six patients, and the lack of accurate dose estimations were posed as problems to be overcome (91).

Kim and colleagues conducted a phase II study on interstitial microbrachytherapy with  $^{166}\text{Ho}$  labelled chitosan (92). The radioisotope  $^{166}\text{Ho}$  was selected because it also emits gamma photons, permitting scintigraphic imaging which allows confirmation of the *in vivo* distribution. Forty patients with single HCC lesions  $\leq 3$  cm in diameter were enrolled. The intratumoral injections were carried out percutaneously under ultrasound guidance, with a planned dose of 740 MBq  $\text{cm}^{-1}$  and an average delivered dose of 1,850 MBq  $^{166}\text{Ho}$  per lesion. Complete tumor necrosis was achieved in 77.5% of the patients, as assessed by CT. This is a notable result, yet, due to leakage of holmium from the chitosan, 11 patients (27.5%) developed hematologic side effects, requiring hospitalization in two of them. Holmium is a bone seeking element; if



administered intravenously, over 55% of the injected dose is incorporated in bone within 4 days (93). The toxicity after intratumoral administration of  $^{166}\text{Ho}$ -chitosan might therefore be attributed to the irradiation of the bone marrow after uptake of unbound holmium in the skeleton.

In itself,  $^{166}\text{Ho}$  is ideally suited for the intratumoral approach, just not if complexed in chitosan.  $^{166}\text{Ho}$  has a favorable half-life and combines beta and gamma emission. The intratumoral administration of HoPLLAMS might be a safe alternative, since neither release of holmium was found after long-term incubation in buffer nor were there any signs of holmium leakage after 18 months *in vivo* (55, 59). The maximum specific activity of HoPLLA microspheres (~450 Bq per sphere, Table I) however, might not suffice for interstitial administration, since the overall injection volume is limited to 0.1-0.3 mL. Holmium acetylacetonate microspheres (HoAcAcMS) were formed that contain 2.6 times more holmium per sphere than HoPLLAMS (94). This allows for the delivery of tumoricidal doses in small volumes, since the activity per sphere is also increased 2.6 fold to approximately 1,100 Bq per sphere. The microspheres have a high stability both *in vitro* and *in vivo*. Besides characterisation of HoAcAcMS, preclinical studies are being carried out to investigate the therapeutic potential of these microspheres. This includes efficacy studies in animals with solid tumors of different origin and histotype, like, for instance, small kidney tumors.

## Conclusions

The use of beta emitting microspheres has shown to be an attractive treatment for inoperable liver malignancies.  $^{90}\text{Y}$  microspheres, either glass or resin based, are increasingly applied and clinical experience with radioactive microspheres has almost uniquely been obtained with these microspheres. Unfortunately, the use of a pure beta emitter like  $^{90}\text{Y}$  hampers acquisition of high quality nuclear images for pre-treatment work-up and follow-up.

Microspheres containing the combined beta and gamma emitter  $^{166}\text{Ho}$  were proposed to further improve liver-directed treatment with radioactive microspheres. The microsphere size, tumor-to-liver ratio and beta energy are nearly identical. The microspheres are therefore expected to exert a comparable therapeutic effect as the  $^{90}\text{Y}$  microspheres, yet there are some distinct differences in the pre- and post-administration procedures. The anticipated biodistribution of a therapeutic dose of  $^{166}\text{HoPLLAMS}$  is visualized using a scout dose of these microspheres. The administration procedure of  $^{166}\text{HoPLLAMS}$  will be performed under fluoroscopic guidance by administering the microspheres in a 50% mixture of saline and non-ionogenic contrast. Consequently, retrograde flow of microspheres is instantly visualized in order to prevent side effects. The absorbed dose delivered by  $^{166}\text{HoPLLAMS}$  can accurately be determined by SPECT which enables pre- and post-treatment dosimetric calculations. Furthermore, MR tracking of microspheres, MR guided administration and MR quantification are feasible due to the paramagnetic nature of holmium. A phase I dose escalation trial in patients with unresectable, chemorefractory liver tumors using  $^{166}\text{HoPLLAMS}$  has commenced in 2009.

## References

1. D.M. Parkin, F. Bray, J. Ferlay, and P. Pisani. Global cancer statistics, 2002, *Ca Cancer J Clin.* 55:74-108 (2005).
2. F. Kamangar, G.M. Dores, and W.F. Anderson. Patterns of cancer incidence, mortality, and prevalence across five continents: defining priorities to reduce cancer disparities in different geographic regions of the world, *J Clin Oncol.* 24:2137-2150 (2006).
3. J.M. Llovet and J. Bruix. Molecular targeted therapies in hepatocellular carcinoma, *Hepatology.* 48:1312-1327 (2008).
4. M.A.D. Vente, M.G.G. Hobbelink, A.D. van het Schip, B.A. Zonnenberg, and J.F.W. Nijssen. Radionuclide liver cancer therapies: from concept to current clinical status, *Anticancer Agents Med Chem.* 7:441-459 (2007).
5. E. Vibert, L. Canedo, and R. Adam. Strategies to treat primary unresectable colorectal liver metastases, *Semin Oncol.* 32:33-39 (2005).
6. G. Steele, Jr. and T.S. Ravikumar. Resection of hepatic metastases from colorectal cancer. Biologic perspective, *Ann Surg.* 210:127-138 (1989).
7. D.S. Zuckerman and J.W. Clark. Systemic therapy for metastatic colorectal cancer: current questions, *Cancer.* 112:1879-1891 (2008).
8. H.R. Bierman, R.L. Byron, Jr., K.H. Kelley, and A. Grady. Studies on the blood supply of tumors in man. III. Vascular patterns of the liver by hepatic arteriography in vivo, *J Natl Cancer Inst.* 12:107-131 (1951).
9. M.A.D. Vente, M. Wondergem, I. van der Tweel, I. M.A. van den Bosch, B.A. Zonnenberg, M.G. Lam, A.D. van het Schip, and J.F. Nijssen. Yttrium-90 microsphere radioembolization for the treatment of liver malignancies: a structured meta-analysis, *Eur Radiol.* 19:951-959 (2009).
10. R.J. Blanchard, I. Grotenhuis, J.W. Lafave, C.W. Frye, and J.F. Perry, Jr. Treatment of Experimental Tumors; Utilization of Radioactive Microspheres, *Arch Surg.* 89:406-410 (1964).
11. I.M. Ariel. Treatment of inoperable primary pancreatic and liver cancer by the intra-arterial administration of radioactive isotopes ( $^{90}\text{Y}$  radiating microspheres). *Annals of Surgery* [8], 267-278. 1965.
12. I.M. Ariel and G.T. Pack. Treatment of inoperable cancer of the liver by intra-arterial radioactive isotopes and chemotherapy, *Cancer.* 20:793-804 (1967).
13. E.D. Grady. Internal radiation therapy of hepatic cancer. *Dis.Col.& Rect.* 22, 371-375. 1979.
14. G.J. Ehrhardt and D.E. Day. Therapeutic use of  $^{90}\text{Y}$  microspheres, *Int J Rad Appl Instrum B.* 14:233-242 (1987).
15. M.J. Herba, F.F. Illescas, M.P. Thirlwell, G.J. Boos, L. Rosenthal, M. Atri, and P.M. Bret. Hepatic malignancies: improved treatment with intraarterial Y-90, *Radiology.* 169:311-314 (1988).
16. S. Houle, T.K. Yip, F.A. Shepherd, L.E. Rotstein, K.W. Sniderman, E. Theis, R.H. Cawthorn, and K. Richmond-Cox. Hepatocellular carcinoma: pilot trial of treatment with Y-90 microspheres, *Radiology.* 172:857-860 (1989).
17. R.V. Mantravadi, D.G. Spigos, W.S. Tan, and E.L. Felix. Intraarterial yttrium 90 in the treatment of hepatic malignancy, *Radiology.* 142:783-786 (1982).
18. A.S. Kennedy, C. Nutting, D. Coldwell, J. Gaiser, and C. Drachenberg. Pathologic response and microdosimetry of ( $^{90}\text{Y}$ ) microspheres in man: review of four explanted whole livers, *Int J Radiat Oncol Biol Phys.* 60:1552-1563 (2004).
19. J.C. Andrews, S.C. Walker, R.J. Ackermann, L.A. Cotton, W.D. Ensminger, and B. Shapiro. Hepatic radioembolization with yttrium-90 containing glass microspheres: preliminary results and clinical follow-up, *J Nucl Med.* 35:1637-1644 (1994).
20. R. Murthy, R. Nunez, J. Szklaruk, W. Erwin, D.C. Madoff, S. Gupta, K. Ahrar, M.J. Wallace, A. Cohen, D.M. Coldwell, A.S. Kennedy, and M.E. Hicks. Yttrium-90 microsphere therapy for hepatic malignancy: devices, indications, technical considerations, and potential complications, *Radiographics.* 25 Suppl 1:S41-S55 (2005).
21. E.M. Erbe and D.E. Day. Chemical durability of  $\text{Y}_2\text{O}_3\text{-Al}_2\text{O}_3\text{-SiO}_2$  glasses for the in vivo delivery of beta radiation, *J Biomed Mater Res.* 27:1301-1308 (1993).
22. I. Wollner, C. Knutsen, P. Smith, D. Prieskorn, C. Chrisp, J. Andrews, J. Juni, S. Warber, J. Klevering, J. Crudup, and W. Ensminger. Effects of hepatic arterial yttrium 90 glass microspheres in dogs, *Cancer.* 61:1336-1344 (1988).

23. J.F.W. Nijssen, A.D. van het Schip, W.E. Hennink, D.W. Rook, P.P. van Rijk, and J.M.H. De Klerk. Advances in nuclear oncology: Microspheres for internal radionuclide therapy of liver metastases, *Current Medicinal Chemistry*. 9:73-82 (2002).
24. H.N. Wagner, Jr., B.A. Rhodes, Y. Sasaki, and J.P. Ryan. Studies of the circulation with radioactive microspheres, *Invest Radiol*. 4:374-386 (1969).
25. K. Sato, R.J. Lewandowski, J.T. Bui, R. Omary, R.D. Hunter, L. Kulik, M. Mulcahy, D. Liu, H. Chrisman, S. Resnick, A.A. Nemcek, Jr., R. Vogelzang, and R. Salem. Treatment of Unresectable Primary and Metastatic Liver Cancer with Yttrium-90 Microspheres (TheraSphere(R)): Assessment of Hepatic Arterial Embolization, *Cardiovasc Intervent Radiol*. 29:522-529 (2006).
26. B.N. Gray. Patent application WO 02/34300 A1. Polymer based radionuclide containing particulate material. 2002.
27. R.G. Selwyn, M.A. Avila-Rodriguez, A.K. Converse, J.A. Hampel, C.J. Jaskowiak, J.C. McDermott, T.F. Warner, R.J. Nickles, and B.R. Thomadsen. 18F-labeled resin microspheres as surrogates for 90Y resin microspheres used in the treatment of hepatic tumors: a radiolabeling and PET validation study, *Phys Med Biol*. 52:7397-7408 (2007).
28. M.A. Avila-Rodriguez, R.G. Selwyn, J.A. Hampel, B.R. Thomadsen, O.T. Dejesus, A.K. Converse, and R.J. Nickles. Positron-emitting resin microspheres as surrogates of 90Y SIR-Spheres: a radiolabeling and stability study, *Nucl Med Biol*. 34:585-590 (2007).
29. S.P. Kalva, A. Thabet, and S. Wicky. Recent advances in transarterial therapy of primary and secondary liver malignancies, *Radiographics*. 28:101-117 (2008).
30. M.A. Burton, B.N. Gray, P.F. Klemp, D.K. Kelleher, and N. Hardy. Selective internal radiation therapy: distribution of radiation in the liver, *Eur J Cancer Clin Oncol*. 25:1487-1491 (1989).
31. A.S. Kennedy, D. Coldwell, C. Nutting, R. Murthy, D.E. Wertman, Jr., S.P. Loehr, C. Overton, S. Meranze, J. Niedzwiecki, and S. Sailer. Resin (90)Y-microsphere brachytherapy for unresectable colorectal liver metastases: Modern USA experience, *Int J Radiat Oncol Biol Phys*. 65:412-425 (2006).
32. R. Murthy, H. Xiong, R. Nunez, A.C. Cohen, B. Barron, J. Szklaruk, D.C. Madoff, S. Gupta, M.J. Wallace, K. Ahrar, and M. E. Hicks. Yttrium 90 resin microspheres for the treatment of unresectable colorectal hepatic metastases after failure of multiple chemotherapy regimens: preliminary results, *J Vasc Interv Radiol*. 16:937-945 (2005).
33. Sirtex Medical Ltd. SIR-Spheres Product Package insert. [SSL-US-07]. 1-9-2006.
34. G. Popper, T. Helmlinger, W. Munzing, R. Schmid, T.F. Jacobs, and K. Tatsch. Selective internal radiation therapy with SIR-Spheres in patients with nonresectable liver tumors, *Cancer Biother Radiopharm*. 20:200-208 (2005).
35. B. Atassi, A.K. Bangash, A. Bahrani, G. Pizzi, R.J. Lewandowski, R.K. Ryu, K.T. Sato, V.L. Gates, M.F. Mulcahy, L. Kulik, F. Miller, V. Yaghmai, R. Murthy, A. Larson, R.A. Omary, and R. Salem. Multimodality imaging following 90Y radioembolization: a comprehensive review and pictorial essay, *Radiographics*. 28:81-99 (2008).
36. R.J. Lewandowski, K.T. Sato, B. Atassi, R.K. Ryu, A.A. Nemcek, Jr., L. Kulik, J.F. Geschwind, R. Murthy, W. Rilling, D. Liu, L. Bester, J.I. Bilbao, A.S. Kennedy, R.A. Omary, and R. Salem. Radioembolization with 90Y microspheres: angiographic and technical considerations, *Cardiovasc Intervent Radiol*. 30:571-592 (2007).
37. A.S. Kennedy, W.A. Dezarn, P. McNeillie, D. Coldwell, C. Nutting, D. Carter, R. Murthy, S. Rose, R.R. Warner, D. Liu, H. Palmedo, C. Overton, B. Jones, and R. Salem. Radioembolization for unresectable neuroendocrine hepatic metastases using resin 90Y-microspheres: early results in 148 patients, *Am J Clin Oncol*. 31:271-279 (2008).
38. J.E. Stuart, B. Tan, R.J. Myerson, J. Garcia-Ramirez, S.M. Goddu, T.K. Pilgram, and D.B. Brown. Salvage radioembolization of liver-dominant metastases with a resin-based microsphere: initial outcomes, *J Vasc Interv Radiol*. 19:1427-1433 (2008).
39. L.M. Kulik, B.I. Carr, M.F. Mulcahy, R.J. Lewandowski, B. Atassi, R.K. Ryu, K.T. Sato, A. Benson, III, A.A. Nemcek, Jr., V.L. Gates, M. Abecassis, R.A. Omary, and R. Salem. Safety and efficacy of 90Y radiotherapy for hepatocellular carcinoma with and without portal vein thrombosis, *Hepatology*. 47:71-81 (2008).
40. M. Sandström, M. Lubberink, and H. Lundquist. Quantitative SPECT with Yttrium-90 for Radionuclide Therapy Dosimetry, *European Journal of Nuclear Medicine*. 32: (2007).
41. R. Mansberg, N. Sorensen, V. Mansberg, and W.H. Van der. Yttrium 90 Bremsstrahlung SPECT/CT scan demonstrating areas of tracer/tumour uptake, *Eur J Nucl Med Mol Imaging*. 34:1887 (2007).

42. R.J. Mumper, U.Y. Ryo, and M. Jay. Neutron-activated holmium-166-poly (L-lactic acid) microspheres: a potential agent for the internal radiation therapy of hepatic tumors, *J Nucl Med.* 32:2139-2143 (1991).
43. R.J. Mumper and M. Jay, M. Biodegradable Radiotherapeutic Polyester Microspheres: Optimization and in-vitro / in-vivo Evaluation. *J.Contr.Rel.* 18, 193-204. 1992.
44. J.F.W. Nijsen, B.A. Zonnenberg, J.R. Woittiez, D.W. Rook, I.A. Swildens-van Woudenberg, P.P. van Rijk, and A.D. van het Schip. Holmium-166 poly lactic acid microspheres applicable for intra-arterial radionuclide therapy of hepatic malignancies: effects of preparation and neutron activation techniques, *Eur J Nucl Med.* 26:699-704 (1999).
45. J.F.W. Nijsen, M.J. van Steenberg, H. Kooijman, H. Talsma, L.M. Kroon-Batenburg, M. van de Weert, P.P. van Rijk, A. De Witte, A.D. van het Schip, and W.E. Hennink. Characterization of poly(L-lactic acid) microspheres loaded with holmium acetylacetonate, *Biomaterials.* 22:3073-3081 (2001).
46. D.R. Lide, ed., *CRC Handbook of Chemistry and Physics*, 89th Edition (Internet Version 2009), CRC Press/Taylor and Francis, Boca Raton, FL.
47. P.R. Seevinck, J.H. Seppenwoolde, T.C. de Wit, J.F. Nijsen, F.J. Beekman, A.D. van het Schip, and C.J. Bakker. Factors affecting the sensitivity and detection limits of MRI, CT, and SPECT for multimodal diagnostic and therapeutic agents, *Anticancer Agents Med Chem.* 7:317-334 (2007).
48. S.W. Zielhuis, J.F.W. Nijsen, R. Figueiredo, B. Feddes, A.M. Vredenberg, A.D. van het Schip, and W.E. Hennink. Surface characteristics of holmium-loaded poly(l-lactic acid) microspheres, *Biomaterials.* 26:925-932 (2005).
49. M.A.D. Vente, J.F. Nijsen, R.R. de, M.J. van Steenberg, C.N. Kaaijk, M.J. Koster-Ammerlaan, P.F. de Leege, W.E. Hennink, A.D. van het Schip, and G.C. Krijger. Neutron activation of holmium poly(L-lactic acid) microspheres for hepatic arterial radio-embolization: a validation study, *Biomed Microdevices.* 11:763-772 (2009).
50. J.F.W. Nijsen, A.D. van het Schip, M.J. van Steenberg, S.W. Zielhuis, L.M. Kroon-Batenburg, M. van de Weert, P.P. van Rijk, and W.E. Hennink. Influence of neutron irradiation on holmium acetylacetonate loaded poly(L-lactic acid) microspheres, *Biomaterials.* 23:1831-1839 (2002).
51. R.G. Dale. Dose-rate effects in targeted radiotherapy, *Phys Med Biol.* 41:1871-1884 (1996).
52. R.P. Spencer. Short lived radionuclides in therapy, *Int J Rad Appl Instrum B.* 14:537-538 (1987).
53. European Pharmacopoeia, Directorate for the Quality of Medicines & HealthCare of the Council of Europe (EDQM), Strasbourg, 2008.
54. S.W. Zielhuis, J.F.W. Nijsen, L. Dorland, G.C. Krijger, A.D. van het Schip, and W.E. Hennink. Removal of chloroform from biodegradable therapeutic microspheres by radiolysis, *Int J Pharm.* 315:67-74 (2006).
55. S.W. Zielhuis, J.F.W. Nijsen, G.C. Krijger, A.D. van het Schip, and W.E. Hennink. Holmium-loaded poly(L-lactic acid) microspheres: In vitro degradation study, *Biomacromolecules.* 7:2217-2223 (2006).
56. S.W. Zielhuis, J.F.W. Nijsen, R. de Roos, G.C. Krijger, P.P. van Rijk, W.E. Hennink, and A.D. van het Schip. Production of GMP-grade radioactive holmium loaded poly(l-lactic acid) microspheres for clinical application, *Int J Pharm.* 311:69-74 (2006).
57. J.F.W. Nijsen, D. Rook, C.J.W.M. Brandt, R. Meijer, H. Dullens, B.A. Zonnenberg, J.M.H. De Klerk, P.P. van Rijk, W.E. Hennink, and A.D. van het Schip. Targeting of liver tumour in rats by selective delivery of holmium-166 loaded microspheres: a biodistribution study, *Eur J Nucl Med.* 28:743-749 (2001).
58. J.F.W. Nijsen. Radioactive holmium poly(L-lactic acid) microspheres for treatment of hepatic malignancies: efficacy in rabbits. PhD Thesis, Utrecht University, 2001, pp 109-122.
59. S.W. Zielhuis, J.F.W. Nijsen, J.H. Seppenwoolde, C.J.G. Bakker, G.C. Krijger, H.F. Dullens, B.A. Zonnenberg, P.P. van Rijk, W.E. Hennink, and A.D. van het Schip. Long-term toxicity of holmium-loaded poly(L-lactic acid) microspheres in rats, *Biomaterials.* 28:4591-4599 (2007).
60. P.W. Durbin, M.H. Williams, M. GEE, R.H. Newman, and J.G. Hamilton. Metabolism of the lanthanons in the rat, *Proc Soc Exp Biol Med.* 91:78-85 (1956).
61. M.A.D. Vente, J.F.W. Nijsen, T.C. de Wit, J.H. Seppenwoolde, G.C. Krijger, P.R. Seevinck, A. Huisman, B.A. Zonnenberg, T.S.G.A.M. Van den Ingh, and A.D. van het Schip. Clinical effects of transcatheter hepatic arterial embolization with holmium-166 poly(L-lactic acid) microspheres in healthy pigs, *Eur J Nucl Med Mol Imaging.* 35:1259-1271 (2008).

62. U.O. Hafeli, S. Casillas, D.W. Dietz, G.J. Pauer, L.A. Rybicki, S.D. Conzone, and D.E. Day. Hepatic tumor radioembolization in a rat model using radioactive rhenium (<sup>186</sup>Re/<sup>188</sup>Re) glass microspheres, *Int J Radiat Oncol Biol Phys.* 44:189-199 (1999).
63. U.O. Hafeli, W.K. Roberts, G.J. Pauer, S.K. Kraeft, and R.M. Macklis. Stability of biodegradable radioactive rhenium (Re-<sup>186</sup> and Re-<sup>188</sup>) microspheres after neutron-activation, *Appl Radiat Isot.* 54:869-879 (2001).
64. G. Wunderlich, J. Pinkert, M. Andreeff, M. Stintz, F.F. Knapp, Jr., J. Kropp, and W.G. Franke. Preparation and biodistribution of rhenium-188 labeled albumin microspheres B 20: a promising new agent for radiotherapy, *Appl Radiat Isot.* 52:63-68 (2000).
65. K. Liepe, C. Brogsitter, J. Leonhard, G. Wunderlich, R. Hliscs, J. Pinkert, G. Folprecht, and J. Kotzerke. Feasibility of high activity rhenium-188-microsphere in hepatic radioembolization, *Jpn J Clin Oncol.* 37:942-950 (2007).
66. G. Wunderlich, A. Drews, and J. Kotzerke. A kit for labeling of [<sup>188</sup>Re] human serum albumin microspheres for therapeutic use in nuclear medicine, *Appl Radiat Isot.* 62:915-918 (2005).
67. F.A. Shepherd, L.E. Rotstein, S. Houle, T.C. Yip, K. Paul, and K.W. Sniderman. A phase I dose escalation trial of yttrium-90 microspheres in the treatment of primary hepatocellular carcinoma, *Cancer.* 70:2250-2254 (1992).
68. B.N. Gray, M.A. Burton, D.K. Kelleher, J. Anderson, and P. Klemp. Selective internal radiation (SIR) therapy for treatment of liver metastases: measurement of response rate, *J Surg Oncol.* 42:192-196 (1989).
69. T. Gupta, S. Virmani, T.M. Neidt, B. Szolc-Kowalska, K.T. Sato, R.K. Ryu, R.J. Lewandowski, V.L. Gates, G.E. Woloschak, R. Salem, R.A. Omary, and A.C. Larson. MR Tracking of Iron-labeled Glass Radioembolization Microspheres during Transcatheter Delivery to Rabbit VX2 Liver Tumors: Feasibility Study, *Radiology.* 249:845-854 (2008).
70. S.N. Rao, S.P. Basu, C.G. Sanny, R.V. Manley, and J.A. Hartsuck. Preliminary x-ray investigation of an orthorhombic crystal form of human plasma albumin, *J Biol Chem.* 251:3191-3193 (1976).
71. A. Dhabuwala, P. Lamerton, and R.S. Stubbs. Relationship of <sup>99m</sup>Tc-MAA uptake by colorectal liver metastases to response following Selective Internal Radiation Therapy (SIRT), *BMC Nucl Med.* 5:7 (2005).
72. J.H. Turner, P.G. Claringbold, P.F. Klemp, P.J. Cameron, A.A. Martindale, R.J. Glancy, P.E. Norman, E.L. Hetherington, L. Najdovski, and R.M. Lambrecht. <sup>166</sup>Ho-microsphere liver radiotherapy: a preclinical SPECT dosimetry study in the pig, *Nucl Med Commun.* 15:545-553 (1994).
73. T.C. de Wit, J. Xiao, J.F. Nijsen, A.D. van Het Schip, S.G. Staelens, P.P. van Rijk, and F.J. Beekman. Hybrid scatter correction applied to quantitative holmium-166 SPECT, *Phys Med Biol.* 51:4773-4787 (2006).
74. M.A.D. Vente, T.C. de Wit, M.A. van den Bosch, W. Bult, P.R. Seevinck, B.A. Zonnenberg, H.W. de Jong, G.C. Krijger, C.J. Bakker, A.D. van het Schip, and J.F. Nijsen. Holmium-166 poly(L-lactic acid) microsphere radioembolisation of the liver: technical aspects studied in a large animal model, *Eur Radiol.* 20:862-869 (2010).
75. H.G. Buchholz, H. Herzog, G.J. Forster, H. Reber, O. Nickel, F. Rosch, and P. Bartenstein. PET imaging with yttrium-86: comparison of phantom measurements acquired with different PET scanners before and after applying background subtraction, *Eur J Nucl Med Mol Imaging.* 30:716-720 (2003).
76. J.F.W. Nijsen, J.H. Seppenwoolde, T. Havenith, C. Bos, C.J.G. Bakker, and A.D. van het Schip. Liver tumors: MR imaging of radioactive holmium microspheres—phantom and rabbit study, *Radiology.* 231:491-499 (2004).
77. J.H. Seppenwoolde, J.F.W. Nijsen, L.W. Bartels, S.W. Zielhuis, A.D. van het Schip, and C.J. Bakker. Internal radiation therapy of liver tumors: Qualitative and quantitative magnetic resonance imaging of the biodistribution of holmium-loaded microspheres in animal models, *Magn Reson Med.* 53:76-84 (2004).
78. J.H. Seppenwoolde, L.W. Bartels, W.R. van der, J.F.W. Nijsen, A.D. van het Schip, and C.J. Bakker. Fully MR-guided hepatic artery catheterization for selective drug delivery: a feasibility study in pigs, *J Magn Reson Imaging.* 23:123-129 (2006).
79. P.R. Seevinck, J.H. Seppenwoolde, J.J.M. Zwanenburg, J.F.W. Nijsen, and C.J.G. Bakker. FID Sampling Superior to Spin-Echo Sampling for T-2\*-Based Quantification of Holmium-Loaded Microspheres: Theory and Experiment, *Magnetic Resonance in Medicine.* 60:1466-1476 (2008).

80. Sirtex Medical Ltd. SIRTEx Medical Training Manual. 2008.
81. M.L. Smits, J.F. Nijsen, M.A. van den Bosch, M.G. Lam, M.A.D. Vente, J.E. Huijbregts, A.D. van het Schip, M. Elschot, W. Bult, H.W. de Jong, P.C. Meulenhoff, and B.A. Zonnenberg. Holmium-166 radioembolization for the treatment of patients with liver metastases: design of the phase I HEPAR trial, *J Exp Clin Cancer Res.* 29:70 (2010).
82. M. Klinger, D. Tamandl, S. Eipeldauer, S. Hacker, B. Herberger, K. Kaczirek, M. Dorfmeister, B. Gruenberger, and T. Gruenberger. Bevacizumab improves pathological response of colorectal cancer liver metastases treated with XELOX/FOLFOX, *Ann Surg Oncol.* 17:2059-2065 (2010).
83. E. Van Cutsem, C.H. Kohne, E. Hitre, J. Zaluski, C.R. Chang Chien, A. Makhson, G. D'Haens, T. Pinter, R. Lim, G. Bodoky, J.K. Roh, G. Folprecht, P. Ruff, C. Stroh, S. Tejpar, M. Schlichting, J. Nippgen, and P. Rougier. Cetuximab and chemotherapy as initial treatment for metastatic colorectal cancer, *N Engl J Med.* 360:1408-1417 (2009).
84. R. Murthy, C. Eng, S. Krishnan, D.C. Madoff, A. Habbu, S. Canet, and M.E. Hicks. Hepatic yttrium-90 radioembolotherapy in metastatic colorectal cancer treated with cetuximab or bevacizumab, *J Vasc Interv Radiol.* 18:1588-1591 (2007).
85. L. Bester and R. Salem. Reduction of arteriohepatovenous shunting by temporary balloon occlusion in patients undergoing radioembolization, *J Vasc Interv Radiol.* 18:1310-1314 (2007).
86. J.E. Kennedy. High-intensity focused ultrasound in the treatment of solid tumours, *Nat Rev Cancer.* 5:321-327 (2005).
87. E. Liapi and J.F. Geschwind. Transcatheter and ablative therapeutic approaches for solid malignancies, *J Clin Oncol.* 25:978-986 (2007).
88. A.R. Gillams and W.R. Lees. Five-year survival following radiofrequency ablation of small, solitary, hepatic colorectal metastases, *J Vasc Interv Radiol.* 19:712-717 (2008).
89. R. Salem and K.G. Thurston. Radioembolization with 90Yttrium microspheres: a state-of-the-art brachytherapy treatment for primary and secondary liver malignancies. Part 1: Technical and methodologic considerations, *J Vasc Interv Radiol.* 17:1251-1278 (2006).
90. J.H. Tian, B.X. Xu, J.M. Zhang, B.W. Dong, P. Liang, and X.D. Wang. Ultrasound-guided internal radiotherapy using yttrium-90-glass microspheres for liver malignancies, *J Nucl Med.* 37:958-963 (1996).
91. S. Ho, W.Y. Lau, T.W. Leung, and P.J. Johnson. Internal radiation therapy for patients with primary or metastatic hepatic cancer: a review, *Cancer.* 83:1894-1907 (1998).
92. J.K. Kim, K.H. Han, J.T. Lee, Y.H. Paik, S.H. Ahn, J.D. Lee, K.S. Lee, C.Y. Chon, and Y.M. Moon. Long-term clinical outcome of phase IIb clinical trial of percutaneous injection with holmium-166/chitosan complex (Milican) for the treatment of small hepatocellular carcinoma, *Clin Cancer Res.* 12:543-548 (2006).
93. P.W. Durbin. Metabolic characteristics within a chemical family, *Health Phys.* 2:225-238 (1960).
94. W. Bult, P.R. Seevinck, G.C. Krijger, T. Visser, L.M. Kroon-Batenburg, C.J. Bakker, W.E. Hennink, A.D. van het Schip, and J.F. Nijsen. Microspheres with ultrahigh holmium content for radioablation of malignancies, *Pharm Res.* 26:1371-1378 (2009).







A grayscale microscopic image showing numerous spherical microspheres of varying sizes. Some are in sharp focus, while others are blurred in the background, creating a sense of depth. The spheres appear to have a textured or porous surface.

## Chapter 3

# Microspheres with ultrahigh holmium content for radioablation of malignancies

W. Bult, P.R. Seevinck, G.C. Krijger, T. Visser, L.M.J. Kroon-Batenburg,  
C.J.G. Bakker, W.E. Hennink, A.D. van het Schip, J.F.W. Nijsen

## Abstract

**Purpose:** The aim of this study was to develop microspheres with an ultra high holmium content which can be neutron activated for radioablation of malignancies. These microspheres are proposed to be delivered selectively through either intratumoral injections into solid tumors, or administered via an intravascularly placed catheter.

**Methods:** Microspheres were prepared by solvent evaporation, using holmium acetylacetonate (HoAcAc) crystals as the sole ingredient. Microspheres were characterized using light and scanning electron microscopy, coulter counter, titrimetry, infrared and Raman spectroscopy, differential scanning calorimetry, x-ray powder diffraction, magnetic resonance imaging (MRI) and x-ray computed tomography (CT).

**Results:** Microspheres thus prepared displayed a smooth surface. The holmium content of the HoAcAc microspheres (HoAcAcMS; 45% (w/w)) was higher than the holmium content of the starting material, HoAcAc crystals (33% (w/w)). This was attributed to the loss of acetylacetonate from the HoAcAc complex, during rearrangement of acetylacetonate around the holmium ion. The increase of the holmium content allows for the detection of (sub)microgram amounts of microspheres using MRI and CT.

**Conclusions:** HoAcAcMS with an ultra high holmium content were prepared. These microspheres are suitable for radioablation of tumors by intratumoral injections or treatment of liver tumors through transcatheter administration.

### Key words

Holmiumacetylacetonate, Intratumoral, Microspheres, Multimodality, Radioablation

## Introduction

Worldwide, primary liver cancer (hepatocellular carcinoma or cholangio-carcinoma) is the sixth most common cancer, and each year over 600,000 new cases are presented. A limited number of patients is eligible for surgical resection (partial hepatectomy or liver transplantation), limiting the five year survival rate to only 3-5% (1, 2). The use of systemic chemotherapy has been proven ineffective, however recently a survival benefit of several months has been reported for the oral multikinase inhibitor sorafenib (3).

The liver is also a common site of metastasis, and more than 50% of patients with primary malignancies will develop hepatic metastases. A very common type of cancer to metastasize solely to the liver is colorectal carcinoma. Each year over 1,000,000 new cases of colorectal cancer are presented and the mortality is approximately 500,000 patients per year. Five year survival of patients in the developed world with colorectal cancer is approximately 55%, with main prognostic factors being the extent of lymphatic spread, the number and resectability of liver metastases (1, 2). Surgical resection, considered to be the only curative treatment option, is only eligible in 10 to 20% of patients (4). Currently applied chemotherapy protocols (e.g. FOLFOX or FOLFORI, 5-fluorouracil/leucovorin combined with oxaliplatin or irinotecan, respectively, in combination with the angiogenesis inhibitor bevacizumab) are associated with a survival of patients with unresectable liver metastases of nearly two years (5, 6).

Intra-arterial radioembolisation with radioactive microspheres (glass- or resin-based) containing the high-energy beta emitter yttrium-90 ( $^{90}\text{Y}$ ) is currently increasingly applied in patients with unresectable hepatic malignancies. This  $^{90}\text{Y}$  radioembolisation treatment has shown very high response rates (up to 91%), in both salvage setting and as a first-line treatment option (7, 8). The lack of (quantitative) imaging options for  $^{90}\text{Y}$  (9) has led to the development of holmium-166 loaded poly(L-lactic acid) microspheres ( $^{166}\text{Ho}$ PLLAMS), since  $^{166}\text{Ho}$  emits gamma rays and beta particles that can be used for nuclear imaging and therapy, respectively (10-12). Moreover, holmium is highly paramagnetic and has a high linear attenuation coefficient allowing for visualization by magnetic resonance imaging (MRI) and X-ray computed tomography (CT), respectively (13, 14).

Unfortunately, restrictions to inclusion to this intra-arterial transcatheter radioembolisation approach exist. For example, in patients who have been heavily pretreated with bevacizumab or cetuximab, the tumor feeding vessels may be too feeble for the microspheres to be deposited peri- and endotumorally (15). Efficacy may also be diminished in patients with hypovascular liver tumors. Furthermore, patients with portal vein thrombosis are excluded from treatment with the resin microspheres (16). Extensive liver cirrhosis and poor general health may also hamper the use of this treatment option.

Especially in patients with a limited number of unresectable intrahepatic tumors, not eligible for transcatheter radioembolisation, intratumoral injections of radioactive microspheres might be an option. This approach has been explored in patients with liver tumors using  $^{90}\text{Y}$  glass microspheres, showing a response rate

in 90% of patients (17). Direct intratumoral injection requires small deposits of radioactive microspheres in compact tumor tissue, limiting the overall injection volume to 0.1–0.3 mL (17, 18). Consequently, the amount of activity per injection should be very high.

The purpose of this study was to prepare holmium loaded microspheres, using holmium acetylacetonate (HoAcAc) crystals as the sole starting material, without the use of PLLA as matrix forming polymer, to increase the content of holmium per sphere in order to obtain microspheres suitable for intratumoral application.

## Materials and methods

### Materials

All chemicals are commercially available and were used as obtained. Acetylacetone, 2,4-pentanedione (AcAc; >99.9%), ammoniumhydroxide ( $\text{NH}_4\text{OH}$ ; 29.3% in water), chloroform (HPLC-grade), phosphorus pentoxide (Sicapent®), polyvinyl alcohol (PVA, average MW 30,000 – 70,000) and Pluronic F68® (PEO<sub>100</sub>PPO<sub>65</sub>PEO<sub>100</sub>; MW 9,840–14,600) were purchased from Sigma Aldrich (Steinheim, Germany). Holmium CertiPUR ICP standard and hexamethylenetetramine were purchased from Merck (Darmstadt, Germany). Seakem LE Agarose was purchased from Lonza (Basel, Switzerland). Holmium (III) chloride hexahydrate ( $\text{HoCl}_3 \cdot 6\text{H}_2\text{O}$ ; 99.95%) was purchased from Metall Rare Earth Ltd (Shenzhen, China).

### Preparation of HoAcAcMS

The holmium acetylacetonate microspheres (HoAcAcMS) were prepared using a solvent evaporation process. HoAcAc crystals were prepared as previously described by Nijssen *et al.* (10). HoAcAc crystals were dissolved in chloroform (186 g, 5.5% (w/w)) and emulsified in an aqueous PVA solution (1 L, 2% (w/w)). The chloroform/water emulsion was continuously stirred at a preset stirring speed (300–500 rpm). To evaporate chloroform, the mixture was thermostated at 25°C and a constant flow of nitrogen ( $12 \text{ L min}^{-1}$ ) was applied. After 40 hours of evaporation the formed microspheres were collected by centrifugation and washed five times with water. The washed microspheres were sieved using an electronic sieve vibrator, (EMS 755) and ultrasonic processor (UDS 751; Topaz GmbH, Dresden, Germany) as described by Zielhuis *et al.* (19). The microspheres were dried at room temperature for 24 hours, followed by drying at 50°C for 48 hours.

### Size distribution, holmium content and surface characteristics

The size distribution of the sieved fractions and dried fractions was determined using a Coulter counter (Multisizer 3, Beckman Coulter, Mijdrecht, The Netherlands), equipped with an orifice of 100  $\mu\text{m}$ .

The holmium content of the microspheres was determined by complexometric titration with EDTA as described by Zielhuis *et al.* (19), and Inductively Coupled Plasma Optical Emission spectroscopy (ICP OES). Samples were measured at three different wavelengths (339.898, 345.600 and 347.426 nm) in an Optima 4300 CV (PerkinElmer; Norwalk, USA).

Elemental analysis of carbon, hydrogen, oxygen and holmium of the HoAcAc crystals and HoAcAcMS was performed by H. Kolbe, Mülheim an der Ruhr, Germany.

Scanning electron Microscopy (SEM) micrographs were acquired using a PHENOM (Phenom-World BV, Eindhoven, The Netherlands) electron microscope. Samples were mounted on an aluminum stub, and coated with a Pt layer of 6 nm.

### **Raman spectroscopy**

Raman spectroscopy was performed on a Kaiser RXN spectrometer equipped with a 70 mW 785 nm diode laser for excitation, a holographic grating for dispersion and a Peltier cooled Andor CCD camera for detection.

### **Differential scanning calorimetry**

Modulated Differential Scanning Calorimetry (mDSC) measurements were performed using a DSC Q1000 (TA Instruments Inc., New Castle, DE, USA). The modulation amplitude was set at 1°C per minute. Samples were heated from 20 to 220°C with a heating rate of 2°C min<sup>-1</sup>.

### **X-ray diffraction**

X-ray diffraction patterns were obtained on a Nonius k-CCD diffractometer, with a sealed tube using MoK $\alpha$  radiation with a graphite monochromator. Powder patterns were recorded to a maximum scattering angle (2 $\theta$ ) 22°. The samples were contained in boroglass capillaries.

### **Neutron activation**

Neutron activation was performed in the pneumatic rabbit system operational at a research reactor facility (Department of Radiation, Radionuclides and Reactors, Delft University of Technology, Delft, The Netherlands). Samples were irradiated for three or six hours with a thermal neutron flux of  $5 \times 10^{12}$  n cm<sup>-2</sup> s<sup>-1</sup>. The radioactive <sup>166</sup>Ho was left to decay for one month, to ensure safe handling of HoAcAcMS.

### **Multimodality imaging characteristics**

To determine the sensitivity of MRI and CT for the HoAcAcMS, phantom experiments were carried out on MRI and CT. The phantom used to determine MRI and CT sensitivity consisted of agarose (2% (w/w)) gel samples in which HoAcAcMS were homogeneously dispersed (loadings ranged from 0 to 4 mg microspheres per mL agarose) in plastic tubes (diameter 10 mm, length 100 mm). MR imaging was performed using a 1.5 T clinical MR scanner (Intera, Philips Medical Systems, Best, The Netherlands). To determine the  $r_2^*$  relaxivity, which represents the MR sensitivity of the HoAcAcMS, transverse images were made using a multiple gradient echo MR sequence with 15 echos, an echo spacing of 1.39 msec a repetition time of 500 msec, a field of view (FOV) of 128 mm, a voxel size of 1x1x10 mm, two signal averages and a 60° flip angle. Monoexponential signal decay was assumed. Data processing was performed as described by Seevinck *et al.* (14). A second agarose gel phantom was constructed for qualitative imaging. This gel consisted of 2%

(w/w) agarose, with pockets for the administration of a suspension of HoAcAcMS to obtain depots of 1  $\mu\text{g}$  to 1 mg. The imaging parameters were similar to the imaging parameters mentioned before, except for the slice thickness, which was 1 mm.

To mimic potential *in vivo* imaging applications, depots of HoAcAcMS were injected in an *ex vivo* rabbit liver. The excised liver was flushed with water, and placed in an aqueous solution containing  $\text{MnCl}_2$  ( $19.2 \text{ mg L}^{-1}$ ), to reduce the relaxation time of the water. Fifty microlitre of a suspension of HoAcAcMS was administered to the liver, to obtain depots of 1, 5 and 10  $\mu\text{g}$  microspheres. The imaging parameters were similar to the imaging parameters mentioned before. For the MR images displayed in Fig. 5A, D, E and F an echo time of 20 ms was used.

Quantitative X-ray CT imaging was performed on a clinical 64 slice CT scanner (Brilliance, Philips Medical Systems, Best, The Netherlands). The sample tubes were positioned co-axially to the main axis of the scanner. Using the methods described by Seevinck *et al.*, a linear regression curve was constructed to determine the sensitivity of X-ray CT for HoAcAcMS (14).

## Results and discussion

### Size distribution, holmium content and surface characteristics

We found that HoAcAcMS could be obtained of HoAcAc crystals without using PLLA as a matrix forming polymer using a solvent evaporation technique.

The size distribution, surface morphology of the microspheres were characterized using Coulter Counter, light microscopy and SEM, both before and after neutron activation. The particle size distribution was rather broad, from 5 to 40  $\mu\text{m}$ , with an average microsphere size of 15  $\mu\text{m}$  when the microspheres were prepared at 500 rpm. The average particle size could be tailored by altering the stirring rate during emulsifying and increased from 15  $\mu\text{m}$  at 500 rpm to 20  $\mu\text{m}$  at 400 rpm and 26  $\mu\text{m}$  at 300 rpm. The size distribution should be narrow to control the biodistribution of the microspheres and to reduce possible shunting of small microspheres to non-target organs after administration. Therefore, a sieving step is necessary to obtain a more confined size distribution. More than 93% of the microspheres had a size between 15 – 20  $\mu\text{m}$  after sieving. No changes in microsphere size distribution were observed after neutron activation, which is an indication that small fragments due to radiation damage were absent. Light and scanning electron microscopy showed that spherical particles with a smooth surface were formed (Figs. 1 A and B). Neither surface damage nor agglomeration was observed after neutron activation of the microspheres. After neutron activation for 3 or even 6 hours, the surface of the microspheres only showed small crevices. However, no large fragments were present (Fig. 1 C). This, in combination with the size distribution results, indicates that the microspheres are resistant to neutron irradiation.

The holmium content of the HoAcAcMS, as determined by complexometric titration, ICP OES and elemental analysis was found to be  $45.0 \pm 0.5\%$  (w/w), which is significantly higher than the holmium content of the HoAcAc crystals, being 31.2% (w/w) (Table I). Also, the density of the HoAcAcMS ( $1.90 \text{ g mL}^{-1}$ ) was higher than the density reported for HoAcAc crystals ( $1.77 \text{ g mL}^{-1}$  (20)). In the HoAcAc crystals,

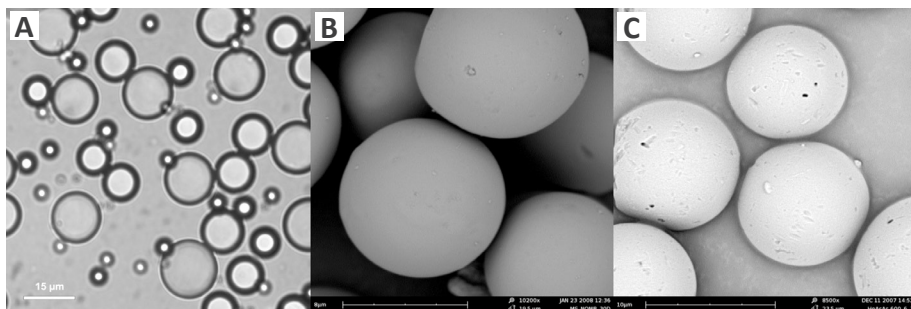


**Figure 1** A) Light micrograph of HoAcAcMS before sieving (mean size 15  $\mu\text{m}$ ), B) scanning electron micrograph of non activated HoAcAcMS and C) scanning electron micrograph of HoAcAcMS after 6 hours of neutron activation.

holmium is surrounded by three acetylacetonate ligands, and three water molecules (10, 20). The increase in holmium content of the HoAcAcMS was explained by a loss of one or more acetylacetonate ligands caused by a structural rearrangement of the acetylacetonate ligands around holmium. This hypothesis was further investigated by determining the elemental composition of the microspheres and Raman spectroscopy.

The substantially higher holmium content per sphere (17.0% (w/w) for the HoPLLAMS vs. 45.0% (w/w) for the HoAcAcMS) results in a significant increase in radioactivity per sphere from 29 MBq  $\text{mg}^{-1}$  for HoPLLAMS (12) to 76 MBq  $\text{mg}^{-1}$  for HoAcAcMS (6 h neutron activation; thermal neutron flux of  $5 \times 10^{12} \text{ n cm}^{-2} \text{ s}^{-1}$ ). Clinical results after intratumoral injection of  $^{90}\text{Y}$  glass microspheres showed that 74 MBq  $^{90}\text{Y}$  is sufficient to evoke a tumoricidal effect on a tumor of 3 cm (17). The injected volume of the microsphere suspension to such a tumor is limited to typically 0.1 – 0.3 mL (18). Based on the radiation characteristics of  $^{166}\text{Ho}$  and  $^{90}\text{Y}$  it can be calculated that a tumoricidal dose of  $^{166}\text{Ho}$  activity (230 MBq per 3 mg) can be delivered in this volume using HoAcAcMS for intratumoral administration (12).

### Raman spectroscopy

Infrared and Raman spectroscopy was performed to ascertain the presence of acetylacetonate in the microspheres. The Raman spectra of the HoAcAc crystals and the HoAcAcMS were virtually identical (Fig. 2), which implies that holmium is surrounded by acetylacetonate in both the HoAcAc crystals and the HoAcAcMS. These findings are in agreement with the infrared measurements on HoAcAcMS that showed the same peak characteristics as for HoAcAc crystals previously reported (21). The increase of the holmium content, found by elemental analysis, complexometric titration and ICP OES can therefore only be explained by a rearrangement of acetylacetonate groups around the holmium(III) ion. Taking into account that holmium is surrounded by acetylacetonate ligands, and the results from the elemental analysis (Table I), we propose that per holmium ion one and a half acetylacetonate and two water molecules are present in the HoAcAcMS. The change of the acetylacetonate coordination should, in principle, be reflected

**Table I.** Calculated and measured elemental composition of HoAcAc crystals and proposed and measured composition of HoAcAcMS (in % w/w).

Element	HoAcAc Crystals $\text{Ho}(\text{AcAc})_3 \cdot 3\text{H}_2\text{O}$		HoAcAcMS $\text{Ho}_2(\text{AcAc})_3 \cdot 4\text{H}_2\text{O}$	
	Calculated	Measured <sup>a</sup>	Proposed <sup>b</sup>	Measured
C	34.9	36.5	25.8	27.0
H	5.3	5.0	4.2	3.8
O	27.9	27.1	22.9	24.2
Ho	31.9	31.2	47.2	45.0

[a] Data taken from Nijssen *et al.* (10).

[b] Structure of HoAcAcMS is proposed based on measured elemental composition and Raman spectroscopy.

in an intensity decrease of the Ho---O bending band, but since the position of this vibration is expected around  $100 \text{ cm}^{-1}$  (22), it is most likely filtered out with the Rayleigh scattering. The hypothesized structure of the HoAcAcMS is depicted in figure 3. As can be seen in this figure, acetylacetonate forms a bridge between two holmium(III) ions by coordinating each carbonyl to another holmium(III) ion forming a network. This bridging effect of chelates between metal ions has been proposed for metal catalysts after gradual removal of the solvent (23). The water observed in elemental analysis (Table I) is likely coordinated to the holmium(III) ion, as previously reported for HoAcAc crystals (20). An important observation that supports the network formation between holmium and acetylacetonate is that HoAcAcMS, in contrast to HoAcAc crystals, did not dissolve in chloroform.

### Differential Scanning Calorimetry

The thermal behaviour of HoAcAc crystals and HoAcAcMS was investigated using modulated differential scanning calorimetry (mDSC). Representative mDSC scans of the holmium acetylacetonate crystals and microspheres are shown in figure 4, and relevant data are summarized in Table II. The thermogram for HoAcAc crystals shows an endotherm with a peak maximum at  $123 \pm 7^\circ\text{C}$ . This endotherm was ascribed to the loss of water from the complex, leading to the collapse of the crystalline structure of the crystals (21). HoAcAcMS show a distinctly different thermogram. We observed an endotherm at approximately  $194 \pm 2^\circ\text{C}$ , which is likely due to the loss of water from the structure. Interestingly, after heating to  $200^\circ\text{C}$  the microspheres were still intact, and the surface of the microspheres showed minor signs of damage. In contrast, heating of the HoAcAc crystals to  $200^\circ\text{C}$  lead to completely molten material, which is in agreement with literature (24). The resistance of microspheres to heating to  $200^\circ\text{C}$  is also an indication that a network is formed. Moreover, this resistance to heat allows for dry heat sterilization (25), making the microspheres suitable for *in vivo* use. DSC analysis of neutron activated HoAcAcMS showed an endotherm at  $199 \pm 3^\circ\text{C}$ , which is likely associated with the loss of water, which was also observed for the non activated microspheres.



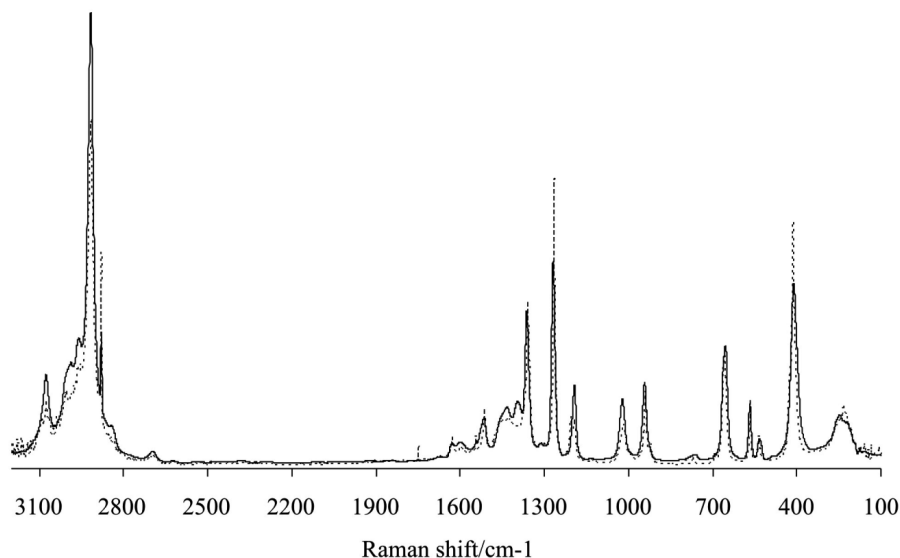


Figure 2. Raman spectra of HoAcAcMS (solid line) and HoAcAc crystals (dotted line).

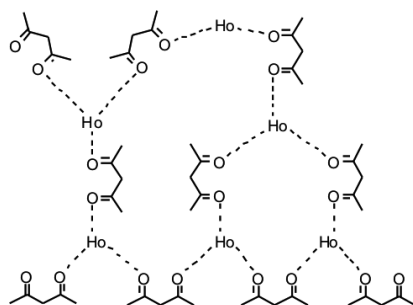


Figure 3. The proposed interaction of acetylacetonate with holmium(III) ion in HoAcAcMS (coordinated water molecules not shown). Each acetylacetonate carbonyl oxygen coordinates with a separate holmium(III) ion, linking two holmium(III) ions.

### X-ray diffraction

The internal structure of the HoAcAc crystals and HoAcAcMS was studied using X-ray diffraction. The HoAcAc crystals have a crystalline structure (21), with a powder pattern reflecting the periodicity of the crystal structure. The pattern for the HoAcAcMS shows no sharp peaks at a higher diffraction angle. This indicates the absence of repetitive intermolecular interactions, which is typical for amorphous structures. The broad peak in the HoAcAcMS diffraction pattern at a diffraction angle of approximately  $11^\circ$  can be attributed to the distance of two holmium atoms separated by one acetylacetonate molecule, which is approximately  $4.5 \text{ \AA}$ . Since holmium has a large scattering power due to the relatively high number of electrons, the high intensity peak at a diffraction angle of approximately  $3.2^\circ$  is ascribed to the Ho-Ho contact in its amorphous form, corresponding to a bond length of approximately  $15.5 \text{ \AA}$  (21).

**Table II.** Summary of DSC data of HoAcAc crystals and HoAcAcMS both non neutron activated and neutron activated ( $n = 6 - 8$ ).

	Onset $T_{max}$ ( $^{\circ}\text{C}$ ) <sup>a</sup>	$T_{max}$ ( $^{\circ}\text{C}$ ) <sup>b</sup>	$\Delta H$ (J/g) <sup>c</sup>
HoAcAc Crystals	$118 \pm 7$	$123 \pm 7$	$115 \pm 9$
HoAcAcMS	$188 \pm 2$	$194 \pm 2$	$25 \pm 5$
Neutron activated HoAcAcMS	$190 \pm 3$	$199 \pm 3$	$12 \pm 11$

[a] Onset  $T_{max}$ : onset of the endotherm

[b]  $T_{max}$ : peak maximum of the endotherm

[c]  $\Delta H$ : enthalpy of the endotherm

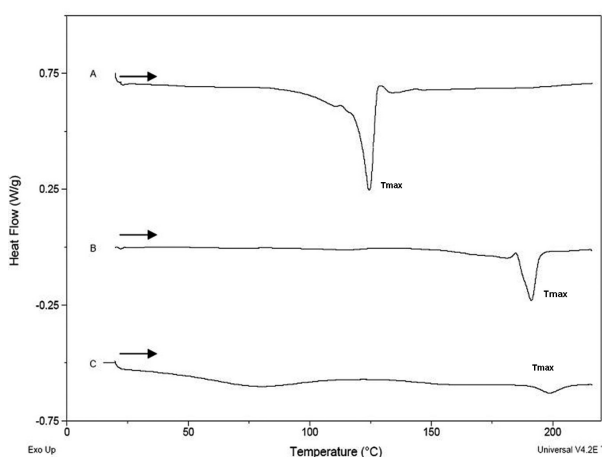


**Figure 4.** mDSC thermograms of **A)** HoAcAc crystals, **B)** HoAcAcMS and **C)** neutron activated (6 hours) HoAcAcMS.  $T_{max}$  is the maximum peak of the endotherm.

### Multimodality imaging characteristics

The paramagnetic nature and the high linear attenuation coefficient of holmium allows for multimodality imaging of non-radioactive HoPLLAMS.

To investigate if the multimodality imaging characteristics enhanced with an increase of the holmium concentration, the HoPLLAMS were homogeneously dispersed in an agarose gel matrix. The paramagnetic nature of holmium locally induces a magnetic field inhomogeneity, leading to an enhanced MRI signal decay in gradient echo images (13). The resulting  $r_2^*$  relaxivity of the HoPLLAMS with a holmium load of 45% (w/w), is  $264 \pm 5.7 \text{ s}^{-1} \text{ mg}^{-1} \text{ mL}$ , which is substantially higher than the  $r_2^*$  value for the HoPLLAMS with a holmium load of 17% (w/w) ( $92 \pm 3.2 \text{ s}^{-1} \text{ mg}^{-1} \text{ mL}$ ) (26). This increase of the  $r_2^*$  relaxivity represents an enhanced sensitivity of MRI to the HoPLLAMS, as compared with HoPLLAMS, which can be explained by the increased holmium weight content per sphere.

Quantitative CT of the agarose phantom resulted in a mass attenuation coefficient at 120 kV of  $15.6 \text{ HU mg}^{-1} \text{ mL}$  for HoAcAcMS, which is substantially increased, when compared to the mass attenuation coefficient of HoPLLAMS of  $6.7 \text{ HU mg}^{-1} \text{ mL}$  at 120 kV (14). This increase in CT sensitivity, like the increase of sensitivity of MRI to the HoAcAcMS, can be attributed to the increase in holmium content.

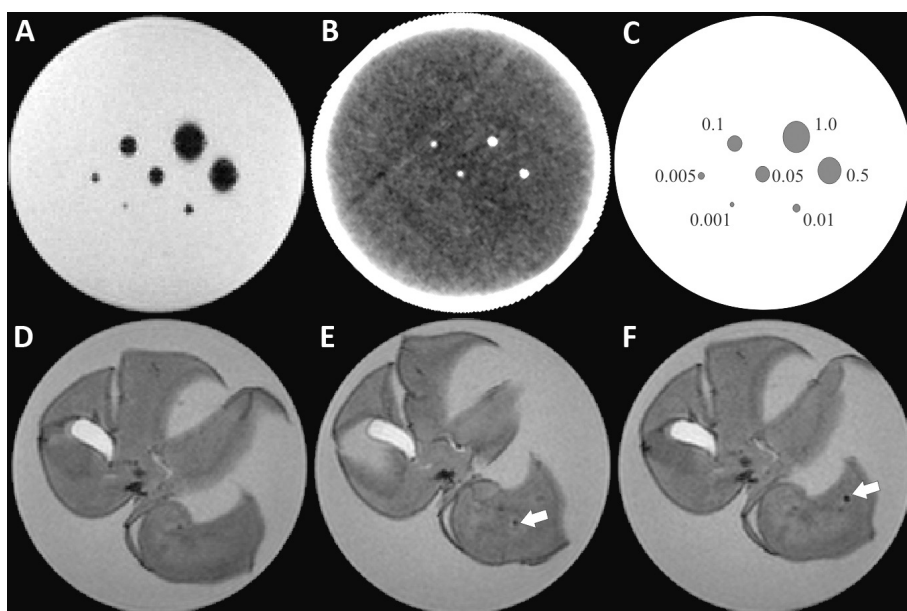


**Figure 5.** A) Gradient echo MRI image of agarose phantom with different depots of HoAcAcMS, B) CT image of agarose phantom with different depots of HoAcAcMS, C) schematic representation of agarose phantom with different depots of HoAcAcMS, including the amount of microspheres in milligram, D) MRI image of rabbit liver before administration of HoAcAcMS, E) MRI image of rabbit liver after administration of 5 µg HoAcAcMS, indicated by arrow, F) MRI image of rabbit liver after administration of 10 µg HoAcAcMS, indicated by arrow.

To demonstrate the feasibility of visualization of microgram amounts of HoAcAcMS, using MRI and CT, decreasing amounts of HoAcAcMS (1 mg to 1 µg) in clusters were imaged *in vitro* as well as *ex vivo*. The enhanced  $r_2^*$  relaxivity of the HoAcAcMS allowed for the detection of 1 µg of HoAcAcMS in the gel (Fig. 5A). The same setup was used for CT measurements, and the increased Ho content per sphere resulted in detection of 50 µg HoAcAcMS (Figs. 5B and 5C). We used an excised rabbit liver (Fig. 5D), with depots of 1, 5 and 10 µg HoAcAcMS to investigate the *ex vivo* imaging characteristics on MRI. The inhomogeneity of the *ex vivo* rabbit liver resulted in the detection of depots from 5 µg onwards (Figs. 5E and F).

Unlike the  $^{90}\text{Y}$  microspheres, which lack the MR imaging possibilities, holmium microspheres can be visualized directly therefore allow for tracking of the microspheres long after the radioactive  $^{166}\text{Ho}$  has decayed, and thus establish the *in vivo* fate of the microspheres after intratumoral injection in a non invasive manner using MRI. The detection of microgram amounts of HoAcAcMS will also enable MRI guided administration of the particles, allowing for accurate positioning of the depots in tumor tissue, whilst refraining healthy tissue from radiation damage.

### Clinical perspective

The two currently available  $^{90}\text{Y}$  microspheres are glass-based (TheraSphere®, MDS Nordion, Kanata, Canada) or resin-based (SIR-Spheres®, SIRTech Medical Ltd., Sydney,

Australia). The glass microspheres have a very high specific activity (2.5 kBq/microsphere), and are registered as a Humanitarian Use Device by the FDA for use in radiation treatment or neoadjuvant to surgery or transplantation in patients with unresectable hepatocellular carcinoma (27). The resin based microspheres have a relatively low specific activity 40 Bq/sphere, and were granted premarket approval by the FDA in 2002 (27).

With regard to the transcatheter approach, the HoAcAcMS might be considered for treatment of patients with hypovascular liver malignancies. This is due to the specific activity of the  $^{166}\text{HoAcAcMS}$  which is in the range of the specific activity of the glass  $^{90}\text{Y}$  microspheres. The obvious advantage of the  $^{166}\text{HoAcAcMS}$  lies in multimodality imaging.

Moreover, the high specific activity of the  $^{166}\text{HoAcAcMS}$  will allow for the delivery of a tumoricidal dose through intratumoral injections. This approach is thought to be applicable not only in patients with liver malignancies, but also in patients with solid tumors in other organs, e.g. brain, kidney and lungs.

However, before a phase I clinical study is allowed to be conducted, several issues need to be addressed. First, the pharmaceutical quality needs to be investigated, e.g. stability testing. Secondly, the *in vivo* toxicity needs to be assessed. The toxicity is expected to be minor, since holmium is a relatively non toxic metal (28). Finally, the therapeutic efficacy of the  $^{166}\text{HoAcAcMS}$  needs to be evaluated in tumor bearing animals.

## Conclusion

In conclusion, the present study demonstrates that microspheres with an ultra high holmium content can be prepared from HoAcAc crystals as the sole starting material, without the use of a polymeric matrix, using a solvent evaporation process. The resulting microspheres have a smooth surface, and are resistant to neutron activation with a thermal neutron flux ( $5 \times 10^{12} \text{ n cm}^{-2} \text{ s}^{-1}$ ) and heating to 200°C. The mean particle size can be tailored for different tumor treatment approaches by adapting the processing parameters. The size increased from 15 to 26  $\mu\text{m}$  when lowering the stirring rate from 500 to 300 rpm during emulsifying. The HoAcAcMS have an unexpectedly high holmium content of 45% (*w/w*) which is substantially higher when compared to the HoPLLAMS (17% (*w/w*)). Moreover, the holmium content in HoAcAcMS is higher than in the HoAcAc crystals (31% (*w/w*)), which is attributed to a rearrangement of acetylacetonate molecules around the holmium(III) ion, resulting in the loss of one and a half coordinating acetylacetonate molecules per holmium(III) ion. The data of this study suggest that acetylacetonate acts as a bridge between holmium(III) ions, forming an amorphous network. The increased holmium content leads to a 2.6 fold higher radioactivity per sphere (29 MBq  $\text{mg}^{-1}$  for HoPLLAMS vs. 76 MBq  $\text{mg}^{-1}$  for HoAcAcMS), which allows for tumoricidal radioactive doses in small volumes necessary for direct intratumoral injection. Additionally, the increased holmium content leads to a higher sensitivity for MRI and CT imaging, enabling detection of microgram amounts of microspheres *in vivo*.

## Acknowledgements

This research was financially supported by the Dutch Technology Foundation STW under grant UGT 6069. We thank mr. R. de Roos and mr. A.J. de Graaf M.Sc. for their assistance in preparing the microspheres, Dr. W.A.M. van Maurik and Dr. W.H. Müller from EMSA, Faculty of Biology Utrecht University for assistance in SEM image acquisition and mr. M.J. van Steenbergen for his assistance with the DSC measurements.

## References

1. F. Kamangar, G.M. Dores, and W.F. Anderson. Patterns of cancer incidence, mortality, and prevalence across five continents: defining priorities to reduce cancer disparities in different geographic regions of the world, *J Clin Oncol*. 24:2137-2150 (2006).
2. D.M. Parkin, F. Bray, J. Ferlay, and P. Pisani. Global cancer statistics, 2002, *Ca Cancer J Clin*. 55:74-108 (2005).
3. J.M. Llovet and J. Bruix. Molecular targeted therapies in hepatocellular carcinoma, *Hepatology*. 48:1312-1327 (2008).
4. E. Vibert, L. Canedo, and R. Adam. Strategies to treat primary unresectable colorectal liver metastases, *Semin Oncol*. 32:33-39 (2005).
5. H.S. Hochster, L.L. Hart, R.K. Ramanathan, B.H. Childs, J.D. Hainsworth, A.L. Cohn, L. Wong, L. Fehrenbacher, Y. Abubakr, M.W. Saif, L. Schwartzberg, and E. Hedrick. Safety and efficacy of oxaliplatin and fluoropyrimidine regimens with or without bevacizumab as first-line treatment of metastatic colorectal cancer: results of the TREE Study, *J Clin Oncol*. 26:3523-3529 (2008).
6. D.S. Zuckerman and J.W. Clark. Systemic therapy for metastatic colorectal cancer: current questions, *Cancer*. 112:1879-1891 (2008).
7. M.A.D. Vente, M. Wondergem, I. van der Tweel, M.A.A.J. van den Bosch, B.A. Zonnenberg, M.G.E.H. Lam, A.D. van het Schip, and J.F.W. Nijsen. Yttrium-90 microsphere radioembolization for the treatment of liver malignancies: a structured meta-analysis, *Eur Radiol*. In Press (2008).
8. G. van Hazel, A. Blackwell, J. Anderson, D. Price, P. Moroz, G. Bower, G. Cardaci, and B. Gray. Randomised phase 2 trial of SIR-Spheres plus fluorouracil/leucovorin chemotherapy versus fluorouracil/leucovorin chemotherapy alone in advanced colorectal cancer, *J Surg Oncol*. 88:78-85 (2004).
9. T. Gupta, S. Virmani, T.M. Neidt, B. Szolc-Kowalska, K.T. Sato, R.K. Ryu, R.J. Lewandowski, V.L. Gates, G.E. Woloschak, R. Salem, R.A. Omary, and A.C. Larson. MR Tracking of Iron-labeled Glass Radioembolization Microspheres during Transcatheter Delivery to Rabbit VX2 Liver Tumors: Feasibility Study, *Radiology*. 249:845-854 (2008).
10. J.F.W. Nijsen, B.A. Zonnenberg, J.R. Woittiez, D.W. Rook, I.A. Swildens-van Woudenberg, P.P. van Rijk, and A.D. van het Schip. Holmium-166 poly lactic acid microspheres applicable for intra-arterial radionuclide therapy of hepatic malignancies: effects of preparation and neutron activation techniques, *Eur J Nucl Med*. 26:699-704 (1999).
11. S.W. Zielhuis, J.F. Nijsen, J.H. Seppenwoolde, C.J. Bakker, G.C. Krijger, H.F. Dullens, B.A. Zonnenberg, P.P. van Rijk, W.E. Hennink, and A.D. van het Schip. Long-term toxicity of holmium-loaded poly(L-lactic acid) microspheres in rats, *Biomaterials*. 28:4591-4599 (2007).
12. M.A.D. Vente, J.F. Nijsen, T.C. de Wit, J.H. Seppenwoolde, G.C. Krijger, P.R. Seevinck, A. Huisman, B.A. Zonnenberg, T.S.G.A.M. Van den Ingh, and A.D. van het Schip. Clinical effects of transcatheter hepatic arterial embolization with holmium-166 poly(L-lactic acid) microspheres in healthy pigs, *Eur J Nucl Med Mol Imaging*. 35:1259-1271 (2008).
13. S. Fossheim, C. Johansson, A.K. Fahlvik, D. Grace, and J. Klaveness. Lanthanide-based susceptibility contrast agents: assessment of the magnetic properties, *Magn Reson Med*. 35:201-206 (1996).
14. P.R. Seevinck, J.H. Seppenwoolde, T.C. de Wit, J.F. Nijsen, F.J. Beekman, A.D. van het Schip, and C.J. Bakker. Factors affecting the sensitivity and detection limits of MRI, CT, and SPECT for multimodal diagnostic and therapeutic agents, *Anticancer Agents Med Chem*. 7:317-334 (2007).
15. A.S. Kennedy. Dosimetry Update, Presented at the emerging trends in radioembolisation using microspheres, clinical workshop, Chicago, IL, 4-5 May 2007.
16. L.M. Kulik, B.I. Carr, M.F. Mulcahy, R.J. Lewandowski, B. Atassi, R.K. Ryu, K.T. Sato, A. Benson, III, A.A. Nemcek, Jr., V.L. Gates, M. Abecassis, R.A. Omary, and R. Salem. Safety and efficacy of 90Y radiotherapy for hepatocellular carcinoma with and without portal vein thrombosis, *Hepatology*. 47:71-81 (2008).
17. J.H. Tian, B.X. Xu, J.M. Zhang, B.W. Dong, P. Liang, and X.D. Wang. Ultrasound-guided internal radiotherapy using yttrium-90-glass microspheres for liver malignancies, *J Nucl Med*. 37:958-963 (1996).
18. W.Y. Lin, S.C. Tsai, J.F. Hsieh, and S.J. Wang. Effects of 90Y-microspheres on liver tumors: comparison of intratumoral injection method and intra-arterial injection method, *J Nucl Med*. 41:1892-1897 (2000).

19. S.W. Zielhuis, J.F.W. Nijsen, R. Figueiredo, B. Feddes, A.M. Vredenberg, A.D. van het Schip, and W.E. Hennink. Surface characteristics of holmium-loaded poly(L-lactic acid) microspheres, *Biomaterials*. 26:925-932 (2005).
20. H. Kooijman, F. Nijsen, A.L. Spek, and A.D. van het Schip. Diaquatrakis(pentane-2,4-dionato-O,O')holmium(III) monohydrate and diaquatrakis(pentane-2,4-dionato-O,O')holmium(III) 4-hydroxypentan-2-one solvate dihydrate, *Acta Crystallogr C*. 56:156-158 (2000).
21. J.F.W. Nijsen, M.J. van Steenberg, H. Kooijman, H. Talsma, L.M. Kroon-Batenburg, M. van de Weert, P.P. van Rijk, A. De Witte, A.D. van het Schip, and W.E. Hennink. Characterization of poly(L-lactic acid) microspheres loaded with holmium acetylacetonate, *Biomaterials*. 22:3073-3081 (2001).
22. A.M.A. Bennett, G.A. Foulds, and D.A. Thornton. The Ir and H-1, C-13 Nmr-Spectra of the Nickel(II), Copper(II) and Zinc(II) Complexes of 2,4-Pentanedione, 4-Imino-2-Pentanone, 4-Thioxo-2-Pentanone and 2,4-Pentanedithione - A Comparative-Study, *Polyhedron*. 8:2305-2311 (1989).
23. A.J. Dillen, R.J.A.M. Terode, D.J. Lensveld, J.W. Geus, and K.P. de Jong. Synthesis of supported catalysts by impregnation and drying using aqueous chelated metal complexes, *J Catal*. 216:257-264 (2003).
24. G.W. Pope, J.F. Steinbach, and W.F. Wagner. Characteristics of the solvates of the rare-earth acetylacetonates, *Journal of Inorganic and Nuclear Chemistry*. 20:304-313 (1961).
25. European Pharmacopoeia, 6<sup>th</sup> Edition, Supplement 6.1, Directorate for the Quality of Medicines & HealthCare of the Council of Europe, Strassbourgh, 2008.
26. J.F. Nijsen, J.H. Seppenwoolde, T. Havenith, C. Bos, C.J. Bakker, and A.D. van het Schip. Liver tumors: MR imaging of radioactive holmium microspheres--phantom and rabbit study, *Radiology*. 231:491-499 (2004).
27. M.A.D. Vente, M.G. Hobbelink, A.D. van het Schip, B.A. Zonnenberg, and J.F. Nijsen. Radionuclide liver cancer therapies: from concept to current clinical status, *Anticancer Agents Med Chem*. 7:441-459 (2007).
28. P. Arvela. Toxicity of rare-earths. *Progress in Pharmacology* 2, 73-113. (1979).





## Chapter 4

# Radioactive holmium acetylacetonate microspheres for interstitial microbrachytherapy: an *in vitro* and *in vivo* stability study

W. Bult, H. de Leeuw, O.M. Steinebach, H.T. Wolterbeek, R.M.A. Heeren,  
C.J.G. Bakker, A.D. van het Schip, W.E. Hennink, J.F.W. Nijsen

Submitted

## Abstract

The clinical application of holmium acetylacetonate microspheres (HoAcAcMS) for the intratumoral radionuclide treatment of solid malignancies requires a thorough understanding of their stability. For that reason, an *in vitro* and an *in vivo* stability study with HoAcAcMS was conducted. HoAcAcMS, before and after neutron irradiation, were incubated in a phosphate buffer at 37°C for 6 months. The *in vitro* release of holmium in this buffer after six months was 0.5%. Elemental analysis, scanning electron microscopy, infrared spectroscopy and time of flight secondary ion mass spectrometry were performed on the HoAcAcMS. After four days in buffer the acetylacetonate ligands were replaced by phosphate, without altering the particle size and surface morphology. HoAcAcMS before and after neutron irradiation were administered intratumorally in VX2 tumor-bearing rabbits. No holmium was detected in the faeces, urine, femur and blood of the rabbits. Histological examination of the tumor revealed clusters of intact microspheres amidst necrotic tissue after thirty days.

**Keywords:** holmium, microspheres, *in vivo*, VX2 carcinoma, brachytherapy

## Introduction

Worldwide, cancer is the second cause of death, after cardiovascular diseases (1), and it is estimated that each year over 20 million new cases are presented (2). The majority (over 90%) of these new cases are solid tumors, and each year over 12 million people die from solid tumors (1, 2). Traditionally, surgery has been the preferred treatment of solid malignancies, since this treatment can be considered curative (3), but, unfortunately, not all tumors are eligible for curative resection. In the 1990s minimally invasive treatment options were proposed as treatment of inoperable solid malignancies, to offer a potentially curative treatment and to reduce the morbidity associated with surgery. These minimally invasive treatments, which are increasingly applied nowadays, include radiofrequency ablation (4), high intensity focused ultrasound (5) and local administration of radionuclides (6, 7). Intratumorally administered high energy beta emitting yttrium-90 ( $^{90}\text{Y}$ ) glass microspheres have been successfully tested in humans (6). Also, intratumoral administration of holmium-166 ( $^{166}\text{Ho}$ ) chelated to chitosan, an *in situ* gel forming device, has been tested in hepatocellular carcinoma patients with small ( $\leq 3$  cm) solitary lesions (8). Complete tumor necrosis was observed in 31 of 40 patients, yet the release of holmium from the injection site led to haematologic side effects in 11 of 40 patients. To further optimize the intratumoral application of  $^{166}\text{Ho}$ , holmium microspheres with an ultra high holmium load were proposed as a radioablation device for solid malignancies (9). These microspheres were suitable to deliver sufficient radiation after intratumoral administration, and their efficacy was tested in a renal cell carcinoma tumor-bearing mouse model (10). The microsphere treated tumors did not show a significant growth ( $141 \pm 99 \text{ mm}^3$  at time of treatment versus  $104 \pm 95 \text{ mm}^3$  after two weeks), whereas the tumor size in the saline treated control group increased dramatically (from  $122 \pm 33 \text{ mm}^3$  to  $4150 \pm 300 \text{ mm}^3$  two weeks post-injection).

The purpose of the present study was to investigate the long-term *in vitro* stability of these radioactive holmium acetylacetonate microspheres ( $^{166}\text{HoAcAcMS}$ ). The holmium release from the HoAcAcMS was measured and the surface morphology and the chemical composition of the HoAcAcMS were investigated upon incubation of both non-neutron activated and neutron activated radioactive HoAcAcMS in phosphate buffer at  $37^\circ\text{C}$  for up to 26 weeks. The *in vivo* stability was assessed in VX-2 tumor-bearing rabbits, after intratumoral administration of both non-activated HoAcAcMS and neutron-activated HoAcAcMS. The rabbits were followed for one month, during which blood, urine and faeces were collected to determine the excretion of holmium. Histology was performed on tumor tissue, and the holmium content in the femur was determined.

## Materials and Methods

### Materials

All chemicals were commercially available and used as received. Acetylacetone (2,4-pentanedione (AcAc; >99%)), ammonium hydroxide ( $\text{NH}_4\text{OH}$ ; 29.3% in water), chloroform ( $\text{CHCl}_3$ ; HPLC-grade), holmium phosphate (anhydrous ( $\text{HoPO}_4$ ; >99.99%), poly(vinyl alcohol) (PVA; average MW 30,000 – 70,000, 88% hydrolyzed) and poloxamer 188 (Pluronic F68, average MW 8350) were purchased from Sigma Aldrich (Steinheim, Germany). Di-sodium hydrogen phosphate dihydrate ( $\text{Na}_2\text{HPO}_4 \cdot 2\text{H}_2\text{O}$ ; 99%), ethanol (absolute), holmium CertiPUR ICP Standard (1.00 g  $\text{L}^{-1}$ ), sodium azide ( $\text{NaN}_3$ ; 99%) and sodium dihydrogen phosphate dihydrate ( $\text{NaH}_2\text{PO}_4 \cdot 2\text{H}_2\text{O}$ ; 99%) were purchased from Merck (Darmstadt, Germany). Holmium chloride hexahydrate ( $\text{HoCl}_3 \cdot 6\text{H}_2\text{O}$ ) was obtained from Metall rare earth (Shenzhen, China). Dexmedetomidine (Dexdomitor) and carprofen (Rimadyl) were obtained from Pfizer Animal Health B.V. (Capelle a/d IJssel, The Netherlands) and Isoflurane (IsoFlo) was obtained from Abbott Animal Health (Hoofddorp, The Netherlands).

### Preparation and neutron irradiation of HoAcAcMS

HoAcAcMS with a size of 15  $\mu\text{m}$  were prepared by a solvent evaporation process previously described (9). The HoAcAcMS (300 or 600 mg) were weighed in high density polyethylene vials (Type A, Posthumus plastics (Beverwijk, the Netherlands)). Neutron irradiations were performed in the pneumatic rabbit system operational at the research reactor facility of the Reactor Institute Delft (Delft University of Technology, The Netherlands) (11). Samples were irradiated for either 3 h or 6 h with a thermal neutron flux of  $5 \times 10^{12} \text{ n cm}^{-2} \text{ s}^{-1}$ , and the radioactive  $^{166}\text{Ho}$  was left to decay for 1 month in closed vials.

### *In vitro* degradation of the microspheres

The release of  $\text{Ho}^{3+}$ -ions from HoAcAcMS was determined as described by Zielhuis *et al.* (12). Neutron irradiated microsphere samples (50 mg) were suspended in 100  $\mu\text{l}$  of 2% PluronicF68 aqueous solution and incubated in test tubes containing 5 mL isotonic phosphate buffer (116 mM, 39 mmol of  $\text{NaH}_2\text{PO}_4 \cdot 2\text{H}_2\text{O}$  and 77 mmol of  $\text{Na}_2\text{HPO}_4 \cdot 2\text{H}_2\text{O}$  in 1 L, pH 7.4) with 0.05%  $\text{NaN}_3$  to prevent bacterial growth. All samples were prepared in duplicate. The tubes were placed in a water bath at 37°C and continuously shaken and at predetermined time points (1 day, 4 days, 1, 2, 4, 8, 12 and 24 weeks) the test tubes were centrifuged, and the supernatant was collected. The microspheres were washed three times with water for injection and dried at 50°C. The microspheres and the supernatant were used for further analysis.

### Particle surface morphology

Surface morphology of the HoAcAcMS after incubation was studied using a Phenom (Phenom-World BV, Eindhoven, The Netherlands) scanning electron microscope. The samples were placed on aluminium stubs and sputter coated with a 6 nm Pt layer, and images were acquired at a voltage of 5 kV.

### **Elemental analysis**

The holmium, carbon, oxygen, hydrogen and phosphorous content was determined before and after incubation of HoAcAcMS in phosphate buffer by H. Kolbe (Mulheim an der Ruhr, Germany).

### **Infrared spectroscopy**

Fourier Transform Infrared spectroscopy was used to ascertain the presence of acetylacetonate in the microspheres. Infrared spectra of dried microspheres were acquired on a BIO-RAD FTS6000 FT-IR (BIO-RAD, Cambridge, MA, USA). The spectra were recorded from 400 – 4000  $\text{cm}^{-1}$  using KBr pellets, by accumulating 256 scans per spectrum.

### **Secondary ion mass spectrometry**

Time of flight secondary ion mass spectrometry (TOF-SIMS) analysis was performed to obtain mass spectral information about the molecular composition and distribution on the surface of the microspheres before and after incubation in buffer (13). Samples were fixed on a conductive carbon sticker on a stainless steel sample holder, and measured using a TRIFT II mass spectrometer (Physical Electronics, Eden Prairie, MN) equipped with a Au primary ion gun. 22 keV  $\text{Au}^+$  primary ions were used for analysis. SIMS spectra were measured both in the positive and the negative secondary ion mode with a secondary ion energy of 7 keV.

### ***In vivo* degradation study**

#### ***Animal model***

All experimental protocols and procedures were approved by the local experimental animal welfare committee and conform to national and European regulations for animal experimentation. Eight adult female New Zealand White rabbits of approximately 3.5 kg were purchased from Harlan (Horst, The Netherlands). The animals were housed individually to allow for urine and faeces collection and were fed approximately 100 g complete diet pellets for rabbits. Water was supplied *ad libitum*.

#### ***Tumor cells***

The VX2 cell line was a kind gift from dr. R.J.J. van Es (Department of Oral and Maxillofacial Surgery, University Medical Centre Utrecht, Utrecht, The Netherlands) (14). The VX2 cells were propagated by subcutaneous passage in the rabbit hind limb. After dissecting the tumor, small portions of viable tumor (2 mm in diameter) were selected for intrahepatic implantation as described by Nijssen *et al.* (15).

#### ***Analgesia, sedation and euthanasia***

Analgesia during and two days post laparotomy was achieved with carprofen s.c. 4  $\text{mg kg}^{-1}$  bodyweight. General anaesthesia was induced by ketamine i.m. at 30  $\text{mg kg}^{-1}$  bodyweight and xylazine i.m. at 4  $\text{mg kg}^{-1}$  bodyweight. Anaesthesia was maintained

by inhalation of isoflurane (1.5-2.0% O<sub>2</sub>/air (1:1)). For post-administration imaging, the animals were sedated using dexmedetomidine at 50 mg kg<sup>-1</sup> and ketamine at 15 mg kg<sup>-1</sup>. The animals were euthanized by intravenous injection of 600 mg pentobarbital.

### ***Tumor implantation***

A subxiphoid laparotomy was performed by ventral mid-line incision, in order to expose the liver lobes. Three tumor pieces were implanted into the left lateral liver lobe with an intravenous catheter (Abbocath – T 16G, Hospira, Donegal Town, Ireland). After implantation of tumor tissue, the puncture wound in the liver was sealed with tissue glue (Histoacryl, B. Braun, Melsungen, Germany). Thereafter the abdominal muscle layer and skin layers were sutured in separate layers using Vicryl 3.0 (Johnson&Johnson Intl., St-Stevens-Woluwe, Belgium).

### ***Dose preparation***

Neutron irradiation of approximately 60 mg HoAcAcMS for one hour resulted in an activity of approximately 600 MBq <sup>166</sup>HoAcAcMS. The <sup>166</sup>HoAcAcMS were suspended in 1.2 mL of sterile water containing 2% PluronicF68 and 10% ethanol abs. to obtain a final concentration of 50 mg mL<sup>-1</sup> (= 500 MBq <sup>166</sup>HoAcAcMS mL<sup>-1</sup>). The microspheres were suspended by gentle agitation and repeatedly drawing them up and down with a syringe. Subsequently, approximately 200 μL (= 100 MBq or 10 mg <sup>166</sup>HoAcAcMS) was taken up in 29 G insulin syringes (Becton Dickinson Ultra Fine, Breda, the Netherlands), and the activity was measured using a dose calibrator (VDC-404, Veenstra Instruments, Joure, The Netherlands). As a control, a suspension of non-radioactive microspheres was prepared in a similar concentration of microspheres (50 mg mL<sup>-1</sup>). Approximately 200 μL (or 10 mg) was taken up in 29 G insulin syringes.

### ***Administration of <sup>166</sup>HoAcAcMS***

Fourteen days post implantation the tumor reached a size of approximately 2 cm<sup>3</sup> and a second subxiphoid laparotomy was performed. Prior to administration of the microspheres, the syringe was agitated vigorously to obtain a homogeneous microsphere suspension. One hundred μL of non-radioactive (= 5 mg), or radioactive HoAcAcMS (= 50 MBq, which corresponds to 5 mg) suspension was administered intratumorally. The syringes were measured in a dose calibrator before and after administration, to determine the injected amount of activity. Following the intratumoral administration of <sup>166</sup>HoAcAcMS, the animals were subjected to planar gamma scintigraphy (Forte, Philips Medical Systems, Best, The Netherlands) and CT imaging (Brilliance 64, Philips Medical Systems, Best, The Netherlands) to confirm the selective deposition of microspheres in the tumor.

### ***Release profile of the <sup>166</sup>HoAcAcMS***

The urine and faeces of the animals were collected at the same time each day during the first week after administration. Venous blood samples (1 mL) were taken before, just after, five days after and ten days after administration of HoAcAcMS.

Blood was centrifuged at 3000 rpm for 10 min at 4°C and the serum was collected and stored at -20°C for further analysis. The serum levels of alkaline phosphatase (ALP) as an indicator of biliary toxicity, alanine aminotransferase (ALAT), aspartate amino transferase (ASAT) and gamma glutamyltransferase ( $\gamma$ -GT) as indicators of hepatocellular toxicity and albumin as indicator for liver function were analysed on a UniCel DxC 800 Clinical System (Beckman Coulter B.V., Woerden, The Netherlands). In addition, the serum holmium levels were measured using inductively coupled plasma – optical emission spectroscopy (ICP OES).

### **Histology**

Rabbits were euthanized four weeks after administration of HoAcAcMS. After termination, the lungs, heart, stomach, liver, kidneys, and a femur were excised and fixed in a 4% formalin solution. The tumor bearing liver was dissected and embedded in paraffin. After haematoxylin-eosin staining the liver and tumor tissue was histologically evaluated, to verify the presence of microspheres in the tumor and liver.

### **Determination of holmium concentration**

The holmium concentration in buffer, serum, urine, faeces and bone samples was determined using ICP OES. Buffer samples were prepared by diluting 100  $\mu$ L of supernatant to 5 mL nitric acid (5% w/v). Approximately one gram of urine or faeces sample was destructed overnight using 5 mL nitric acid (30%). After overnight destruction the samples were centrifuged at 4000g for 10 min and 1 mL of supernatant was diluted to 5 mL with nitric acid (5% w/v). The bone was separated from the marrow of the femur samples. Approximately 500 mg bone sample was weighed accurately, and was destructed in 4 mL aqua regia (one volume of nitric acid (65% w/w) mixed with three volumes hydrochloric acid (36% w/w)) under heating to 100°C. After evaporation to dryness, the residue was dissolved in 5 mL nitric acid (5% w/v). All samples were measured at three different wavelengths (339.898 nm, 345.600 nm and 347.426 nm respectively) by ICP OES, using an Optima 4300 (PerkinElmer, Norwalk, USA). Analytical calibration curves from the holmium ICP standard solution were used to assess the precision and accuracy of the measurements.

## **Results and discussion**

Microsphere characteristics of the HoAcAcMS used in these experiments were in accordance with previous work (9). The microspheres had a holmium load of  $45 \pm 1\%$ , and a size of 15  $\mu$ m (97% of the microspheres between 10 and 20  $\mu$ m) after sieving. As previously observed, no differences in size distribution were observed before and after neutron irradiation, irrespective of irradiation time (9).

The *in vitro* release profile of holmium from the microspheres incubated in phosphate buffer is shown in Figure 1. As can be observed, the release of holmium was below 0.5% after 6 months. This is comparable to the holmium release ( $0.7 \pm 0.2\%$ ) reported for holmium loaded poly(L-lactic acid) microspheres (HoPLLAMS)

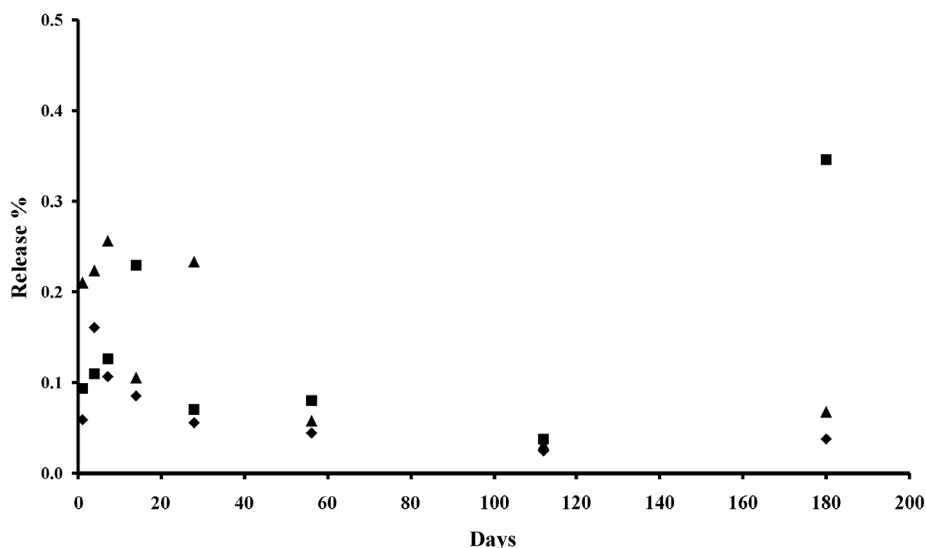


**Figure 1.** Release of holmium from HoAcAcMS (diamonds) and  $^{166}\text{HoAcAcMS}$  irradiated for either 3 hours (triangles) or 6 hours (squares) during incubation in phosphate buffer for 6 months. The data are presented as the mean of two measurements.

in the same buffer (12). The HoPLLAMS are considered radiochemically stable and are currently under clinical investigation in a phase I study for treatment of liver malignancies (16).

Electron microscopic inspection of the HoAcAcMS after incubation in phosphate buffer showed clusters of microspheres amidst buffer. The microspheres remained intact, irrespective of the neutron irradiation time and incubation time (Fig. 2). The surface of the microspheres was still smooth after 26 weeks in buffer. This finding is in contradistinction to neutron irradiated HoPLLAMS incubated in a similar buffer (12) which showed a rough surface after 12 weeks of incubation and started to disintegrate after 24 weeks incubation. This disintegration was attributed to hydrolysis of the poly(L-lactic acid), leading to the formation of holmium lactate (12).

The HoAcAcMS were subjected to elemental analysis to determine their composition after incubation in phosphate buffer (Table I). Interestingly, a quantitative exchange of acetylacetonate by phosphate was observed within 4 days of incubation. To confirm the exchange of acetylacetonate by phosphate, IR analysis was performed. The characteristic peaks of holmium acetylacetonate around  $1518\text{ cm}^{-1}$  are present in the samples before and after one day of incubation in buffer. The intensity of this peak reduces in time and after one month it could not be observed anymore. Interestingly, after 4 days a broad peak around  $1100\text{ cm}^{-1}$  appeared, which can be attributed to stretching bands of phosphate groups (17).

TOF-SIMS analysis of HoAcAcMS before and after incubation in buffer showed spherical particles in total ion count mode (Fig. 3). The resulting mass spectrum showed differences between HoAcAcMS incubated in phosphate buffer and



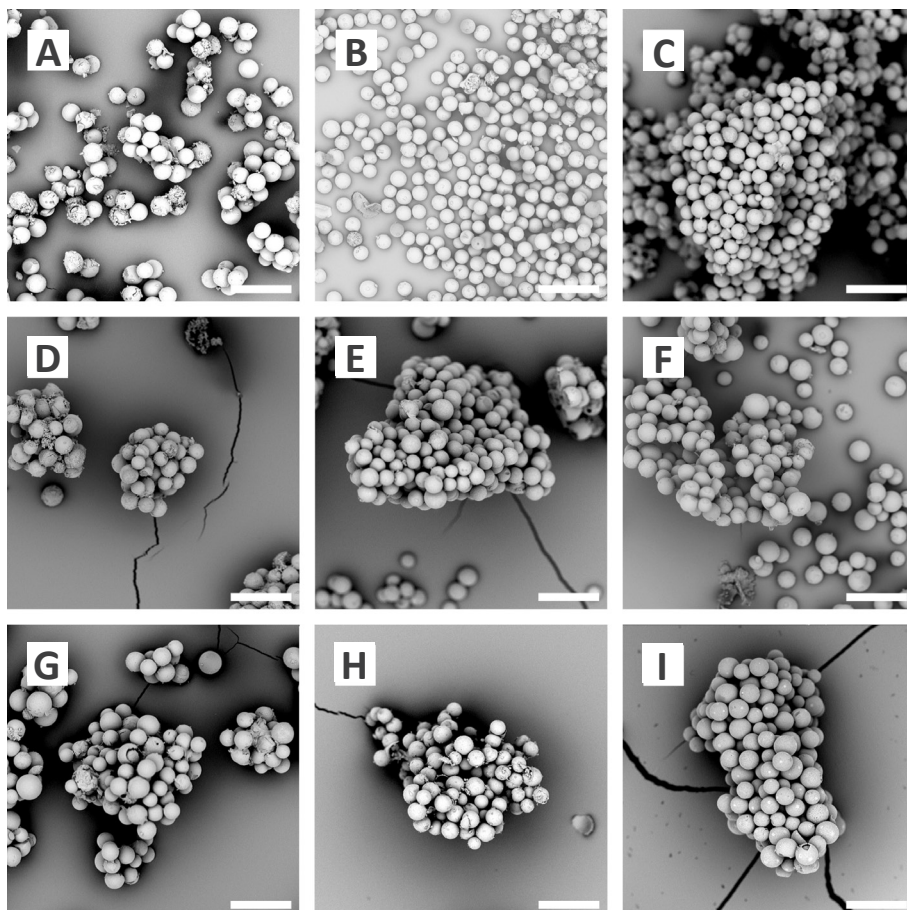


**Figure 2.** Scanning electron micrographs of HoAcAcMS and  $^{166}\text{HoAcAcMS}$  after incubation for different times in phosphate buffer. A-C HoAcAcMS, (A) after one month, (B) after three months and (C) after six months of incubation. D-F  $^{166}\text{HoAcAcMS}$  neutron irradiated for 3 hours at a neutron flux of  $5 \times 10^{12} \text{ n cm}^{-2} \text{ s}^{-1}$  (D) after one month, (E) after three months and (F) after six months of incubation. G-I  $^{166}\text{HoAcAcMS}$  neutron irradiated for 6 hours at a neutron flux of  $5 \times 10^{12} \text{ n cm}^{-2} \text{ s}^{-1}$  (G) after one month, (H) after three months and (I) after six months of incubation. The magnification in all images is 1000x, the bar represents 50  $\mu\text{m}$ .

HoAcAcMS before incubation in buffer. The negative ions observed in the HoAcAcMS incubated in buffer were oxygen, chlorine, and phosphorous compounds ( $m/z$  31: P;  $m/z$  63:  $\text{PO}_2^-$ ;  $m/z$  79  $\text{PO}_3^-$ ), which were absent in the spectrum of the non incubated microspheres (Fig. 3). All negative ions were distributed evenly through the microspheres, indicating a complete exchange of acetylacetonate by phosphate in the microspheres. Holmium ( $m/z$  165), and holmium-oxygen ( $m/z$  181) was present in both the incubated and non incubated samples. The incubated samples also showed a large peak of sodium ( $m/z$  23) from the buffer salts, which was only present at the particle surface. The HoAcAcMS before incubation in phosphate buffer show additional peaks in the positive secondary ion mode at  $m/z$  74 and  $m/z$

Table I Elemental composition of the HoAcAcMS after incubation in a 116 mM phosphate buffer.

	Day 0 <sup>f</sup>		Day 1		Day 4		Day 7		Day 30		Day 90	
	% <sup>§</sup>	no <sup>†</sup>	%	no	%	no	%	no	%	no	%	no
<b>C</b>	26.4	7.5	15.0	4.4	1.0	0.3	0.6	0.2	0.5	0.1	0.7	0.2
<b>H</b>	4.0	13.5	3.5	12.0	1.5	4.9	2.2	7.5	1.5	4.5	1.6	4.6
<b>O</b>	20.3	4.3	29.0	6.3	35.4	7.2	37.9	8.1	30.9	5.7	30.1	5.6
<b>Ho</b>	48.4	1.0	47.2	1.0	50.8	1.0	48.2	1.0	55.5	1.0	55.8	1.0
<b>P</b>	0.5	0.05	5.2	0.6	10.7	1.1	10.7	1.2	11.3	1.1	11.0	1.0
<b>Composition<sup>‡</sup></b>	Ho <sub>2</sub> (AcAc) <sub>3</sub> * H <sub>2</sub> O	Intermediate	HoPO <sub>4</sub> * 3 H <sub>2</sub> O	HoPO <sub>4</sub> * 3 H <sub>2</sub> O	HoPO <sub>4</sub> * 3 H <sub>2</sub> O	HoPO <sub>4</sub> * 3 H <sub>2</sub> O	HoPO <sub>4</sub> * 3 H <sub>2</sub> O	HoPO <sub>4</sub> * 3 H <sub>2</sub> O	HoPO <sub>4</sub> * 3 H <sub>2</sub> O	HoPO <sub>4</sub> * 3 H <sub>2</sub> O	HoPO <sub>4</sub> * 3 H <sub>2</sub> O	HoPO <sub>4</sub> * 3 H <sub>2</sub> O

<sup>f</sup> data taken from Bult *et al.* (9).

<sup>§</sup> results from elemental analysis are the mean of two values

<sup>†</sup> no: the number of atoms, normalized on holmium.

<sup>‡</sup> Composition: the chemical composition of the particles

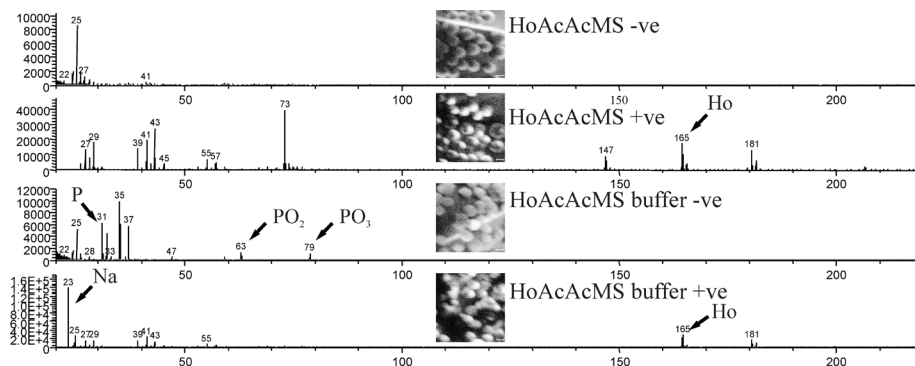


**Figure 3** TOF-SIMS spectra from control HoAcAcMS (HoAcAcMS) and buffer incubated HoAcAcMS (HoAcAcMS buffer). The micrographs show total ion count images in the negative (-ve) and the positive (+ve) secondary ion mode. The peaks of interest are indicated with an arrow.

147, which can be attributed to trimethylsilyl groups from polydimethylsiloxane (18) that is present on the surface the carbon sticker.

The results of IR analysis and TOF-SIMS confirm elemental analysis data that phosphate has replaced acetylacetonate after suspension in buffer. This in turn explains the limited release of holmium from the microspheres, since rare earth metal phosphates are practically insoluble in aqueous media; the solubility product of  $\text{HoPO}_4$  in water is lower than  $10^{-25}$  mole  $\text{L}^{-1}$  (19). The exchange of acetylacetonate by phosphate, without changing the surface morphology, is a so called *chimie douce* reaction (20). *Chimie douce* reactions are topotactic, meaning that the products retain the precursor geometry, and usually take place under mild conditions. Beta diketones, like acetylacetonate, are prone to these types of reactions (21, 22).

The *in vivo* stability study was carried out to determine the *in vivo* implications of the results obtained in the *in vitro* experiment. Radioactive and cold HoAcAcMS were administered intratumorally to VX2 carcinoma-bearing rabbits. All animals recovered from anaesthesia, and the animals received  $40 \pm 10$  MBq  $^{166}\text{HoAcAcMS}$ , corresponding to  $4 \pm 1$  mg microspheres intratumorally. Approximately 80% of the intended dose was administered, which was attributed to the premature settling of the microspheres in the syringes. Nuclear imaging and CT imaging showed a selective administration of microspheres in the tumor (Fig. 4). One animal showed uptake of activity in the lungs (approximately 5% of the injected dose) apart from uptake in the tumor, due to the inadvertent delivery of  $^{166}\text{HoAcAcMS}$  in a blood vessel surrounding the tumor artery. This animal however, completed the experiment in good health. The inadvertent delivery of activity can be avoided in humans by administering the microspheres under ultrasound guidance, making it easier to distinguish tumor tissue from blood vessels and liver tissue (6).

The excretion of holmium after intratumoral administration of HoAcAcMS to the blood, urine and the faeces was below the detection limit in all samples (0.1 ppm for Ho on ICP OES). Suzuki and co-workers found that release of free holmium ( $\text{Ho}^{3+}$ ) to

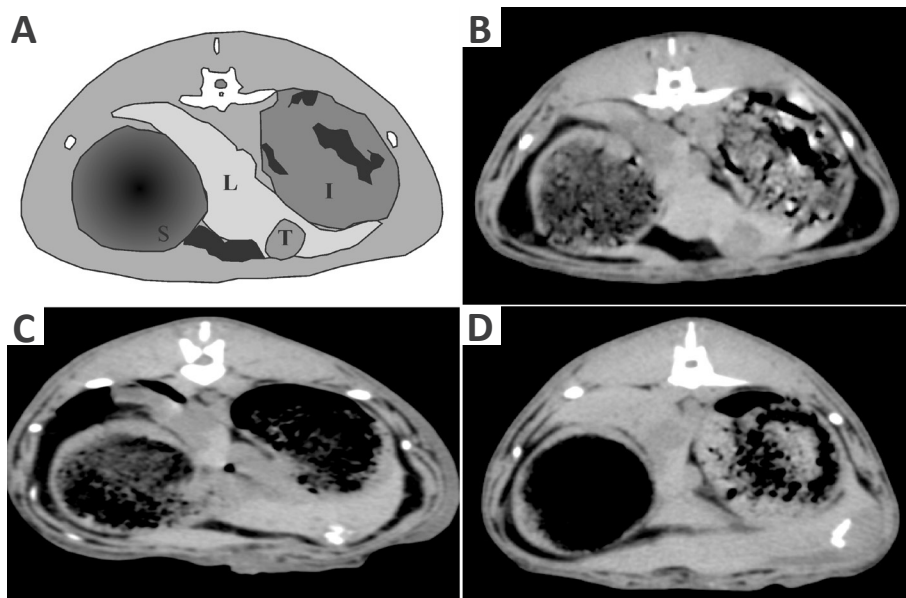


**Figure 4.** A) Schematic outline of rabbit anatomy on X-ray CT image (L = liver, T = tumor, S = stomach, I = intestine). B) X-ray CT image of rabbit before intratumoral administration of  $^{166}\text{HoAcAcMS}$  showing the tumor, C) X-ray CT image of rabbit after intratumoral administration of  $^{166}\text{HoAcAcMS}$  showing the selective deposition in the tumor as white artifacts, D) X-ray CT image four weeks after administration, before termination, the white area in the tumor is still present as a cluster, although the shape has changed.

the urine and faeces occurred rapidly after local intrahepatic administration of the in-situ gel forming complex holmium-166-chitosan (23). Therefore it can be concluded that  $\text{Ho}^{3+}$  was not released from the HoAcAcMS, and that the microspheres retained their integrity as confirmed by histology.

Although the results from the *in vitro* and the *in vivo* stability study show a minimal to no release of holmium from the HoAcAcMS, the *in vivo* data cannot be related to the chimie douce reaction found *in vitro*. The phosphate concentration (116 mM) used for the *in vitro* experiment is substantially higher than the phosphate concentration in human serum (around 1.5 mM (24)). The high phosphate concentration *in vitro* was required to keep the pH stable throughout the experiment, which, however, might accelerate the exchange of acetylacetonate by phosphate. The exchange of acetylacetonate by phosphate could not be established *in vivo* since paraffin interfered with the TOF-SIMS measurements, nonetheless, the presence of intact microspheres and the absence of holmium in urine, faeces and blood show that the HoAcAcMS are stable *in vivo*. The identification of the chemical structure of the HoAcAcMS after intratumoral administration requires further research.

A transient rise in ASAT was observed after the administration of the radioactive microspheres, which can be attributed to the subxiphoid manipulation of liver tissue, and radiation effects of the  $^{166}\text{HoAcAcMS}$ . No other elevations from baseline levels or differences in serum enzyme levels were found between the radioactive

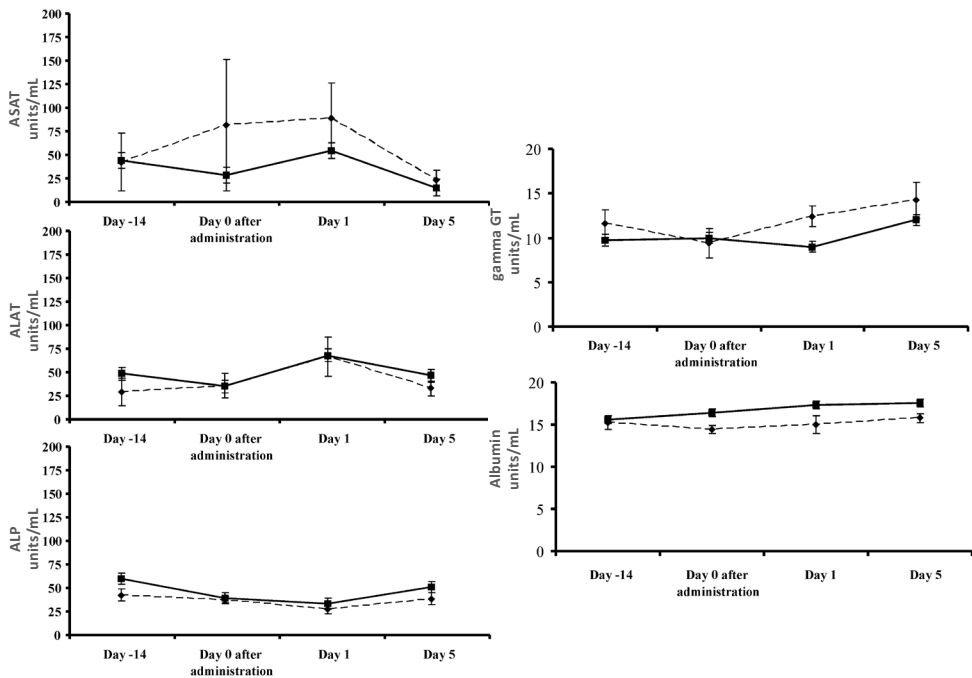
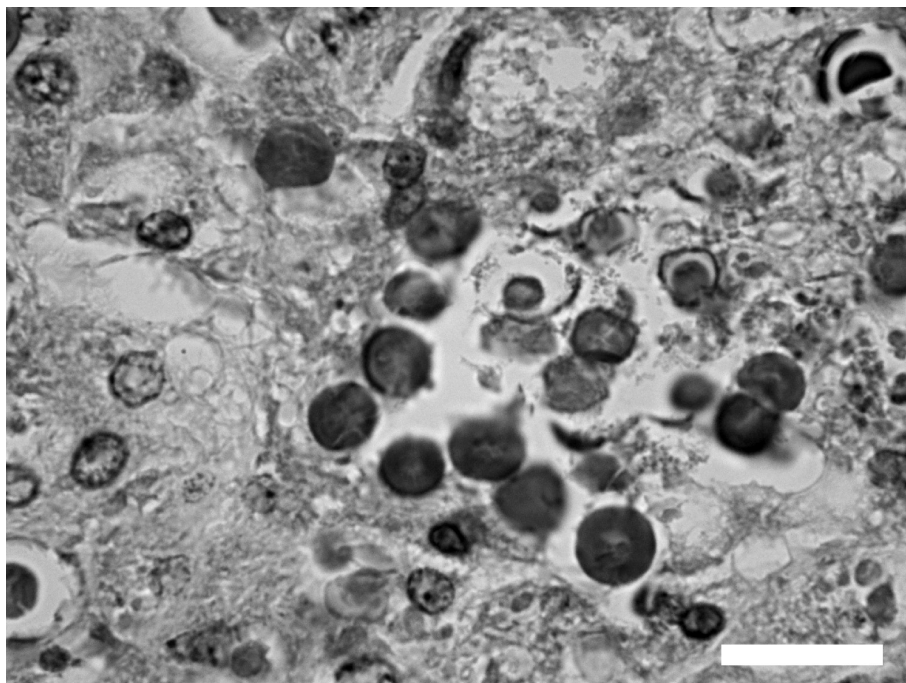


Figure 5. Serum enzyme levels (ASAT, ALAT,  $\gamma$ -GT, ALP and albumin) of rabbits that received non-radioactive HoAcAcMS (solid line) and radioactive <sup>166</sup>HoAcAcMS (dotted line) in time. Bars represent SD.

and non-radioactive group (see Fig. 5). A similar transient rise in ASAT was previously observed after transcatheter radioembolization of liver tissue with HoPLLAMS, which was attributed to the manipulation of liver tissue and radiation effects of the microspheres (25). No changes in albumin levels were observed in the present study, an indication that the liver function was not impaired by intratumoral administration of either HoAcAcMS or <sup>166</sup>HoAcAcMS.

Histological evaluation of liver sections showed intact microspheres amidst necrotic tissue (Fig. 6), which is in agreement with the results from the *in vitro* stability study showing intact HoAcAcMS after 6 months incubation in buffer (Fig. 2).

Possible release of holmium from the HoAcAcMS was determined by measuring the holmium content in bone. Holmium is a bone seeking element, and it has been shown that within 4 days after intravenous administration of holmium nitrate, approximately 55% of the injected dose accumulates in bone (26). Therefore, if holmium ( $\text{Ho}^{3+}$ ) would be released from the HoAcAcMS *in vivo*, the holmium levels in bone would be elevated. In accordance with the holmium levels in urine and faeces, the holmium levels in all bone samples were below the detection limit and it can be concluded that no release of holmium from the HoAcAcMS has occurred.



**Figure 6.** Light micrograph at 400x magnification of a H&E stained section of liver tissue. The microspheres in red are clustered amidst necrotic tissue. The bar represents 20  $\mu\text{m}$ .

## Conclusion

This paper demonstrates the stability of HoAcAcMS, both *in vitro* and *in vivo*. The *in vitro* release was approximately 0.5% after six months of incubation in buffer. The microspheres remained spherical, and a holmium phosphate complex was formed while the surface morphology was retained. No release of holmium was observed after the intratumoral injection of HoAcAcMS in VX2 tumor-bearing rabbits, and the microspheres remained intact in tumor tissue for one month. The results confirm the potential of these microspheres as a novel intratumoral radioablation device.

## Acknowledgements

Financial support by the Dutch Technology Foundation STW, under grant 06069 is gratefully acknowledged. Dr. G.C. Krijger and ms. M.J.J. Koster-Ammerlaan are acknowledged for performing the neutron irradiations. Ms. H.M. de Bruin, Mr. N.J.M. Attevelt and Mr. H.W.G. Vosmeer are gratefully acknowledged for biotechnical assistance. The authors would like to thank prof. dr. K.P. de Jong for valuable discussions. Dr. W.H. Müller and Mr. C.T.W.M. Schneijdenberg are acknowledged for their assistance with the SEM measurements.

## References

1. A. Jemal, R. Siegel, E. Ward, Y. Hao, J. Xu, and M.J. Thun. Cancer statistics, 2009. *Ca Cancer J Clin.* 59:225-249 (2009).
2. D.M. Parkin, F. Bray, J. Ferlay, and P. Pisani. Global cancer statistics, 2002. *Ca Cancer J Clin.* 55:74-108 (2005).
3. J.E. Kennedy. High-intensity focused ultrasound in the treatment of solid tumours. *Nat Rev Cancer.* 5:321-327 (2005).
4. J.P. McGahan, P.D. Browning, J.M. Brock, and H. Tesluk. Hepatic ablation using radiofrequency electrocautery. *Invest Radiol.* 25:267-270 (1990).
5. G. ter Haar, D. Sinnett, and I. Rivens. High intensity focused ultrasound--a surgical technique for the treatment of discrete liver tumours. *Phys Med Biol.* 34:1743-1750 (1989).
6. J.H. Tian, B.X. Xu, J.M. Zhang, B.W. Dong, P. Liang, and X.D. Wang. Ultrasound-guided internal radiotherapy using yttrium-90-glass microspheres for liver malignancies. *J Nucl Med.* 37:958-963 (1996).
7. E. Liapi and J.F. Geschwind. Transcatheter and ablative therapeutic approaches for solid malignancies. *J Clin Oncol.* 25:978-986 (2007).
8. J.K. Kim, K.H. Han, J.T. Lee, Y.H. Paik, S.H. Ahn, J.D. Lee, K.S. Lee, C.Y. Chon, and Y.M. Moon. Long-term clinical outcome of phase IIb clinical trial of percutaneous injection with holmium-166/chitosan complex (Milican) for the treatment of small hepatocellular carcinoma. *Clin Cancer Res.* 12:543-548 (2006).
9. W. Bult, P.R. Seevinck, G.C. Krijger, T. Visser, L.M. Kroon-Batenburg, C.J. Bakker, W.E. Hennink, A.D. van het Schip, and J.F. Nijsen. Microspheres with ultrahigh holmium content for radioablation of malignancies. *Pharm Res.* 26:1371-1378 (2009).
10. W. Bult, S.G.C. Kroeze, M. Elschot, P.R. Seevinck, F.J. Beekman, P.R. Luijten, W.E. Hennink, A.D. van het Schip, J.L.H.R. Bosch, J.F.W. Nijsen, and J.J.M. Jans. Intratumoral administration of holmium-166 acetylacetonate microspheres as a novel minimally-invasive treatment for small kidney tumors. Submitted.
11. M.A.D. Vente, J.F. Nijsen, R. de Roos, M.J. van Steenberg, C.N. Kaaijk, M.J. Koster-Ammerlaan, P.F. de Leege, W.E. Hennink, A.D. van het Schip, and G.C. Krijger. Neutron activation of holmium poly(L-lactic acid) microspheres for hepatic arterial radio-embolization: a validation study. *Biomed Microdevices.* 11:763-772 (2009).
12. S.W. Zielhuis, J.F.W. Nijsen, G.C. Krijger, A.D. van het Schip, and W.E. Hennink. Holmium-loaded poly(L-lactic acid) microspheres: In vitro degradation study. *Biomacromolecules.* 7:2217-2223 (2006).
13. K. Chughtai and R.M. Heeren. Mass spectrometric imaging for biomedical tissue analysis. *Chem Rev.* 110:3237-3277 (2010).
14. R.J. van Es, O. Franssen, H.F. Dullens, M.R. Bernsen, F. Bosman, W.E. Hennink, and P.J. Slootweg. The VX2 carcinoma in the rabbit auricle as an experimental model for intra-arterial embolization of head and neck squamous cell carcinoma with dextran microspheres. *Lab Anim.* 33:175-184 (1999).
15. J.F.W. Nijsen. Radioactive holmium poly(L-lactic acid) microspheres for treatment of hepatic malignancies: efficacy in rabbits. Thesis Utrecht University 2001, pp. 109-122.
16. M.L. Smits, J.F. Nijsen, M.A. van den Bosch, M.G. Lam, M.A.D. Vente, J.E. Huijbregts, A.D. van het Schip, M. Elschot, W. Bult, H.W. de Jong, P.C. Meulenhoff, and B.A. Zonnenberg. Holmium-166 radioembolization for the treatment of patients with liver metastases: design of the phase I HEPAR trial. *J Exp Clin Cancer Res.* 29:70 (2010).
17. D.R. Lide, ed., *CRC Handbook of Chemistry and Physics*, 89th Edition (Internet Version 2009), CRC Press/Taylor and Francis, Boca Raton, FL.
18. X. Dong, A. Gusev, and D.M. Hercules. Characterization of polysiloxanes with different functional groups by time-of-flight secondary ion mass spectrometry. *Journal of the American Society for Mass Spectrometry.* 9:292-298 (1998).
19. R. Kijkowska and R.Z. LeGeros. Preparation and properties of lanthanide phosphates. *Key Engineering Materials.* 246/248:79-82 (2005).
20. J. Rouxel and M. Tournoux. Chimie douce with solid precursors, past and present. *Solid State Ionics.* 84:141-149 (1996).

## Chapter 4

21. C.J. Harlan, A. Kareiva, D.B. MacQueen, R. Cook, and A.R. Barron. Yttrium-doped aluminates: A chimie douce route to Y<sub>3</sub>Al<sub>5</sub>O<sub>12</sub> (YAG) and Y<sub>4</sub>Al<sub>2</sub>O<sub>9</sub> (YAM). *Advanced Materials*. 9:68-71 (1997).
22. C. Lu, Z.F. Ding, and R.H. Lipson. A new chimie douce approach to crystalline vanadium pentoxide nanobelts. *Journal of Materials Chemistry*. 19:6512-6515 (2009).
23. Y.S. Suzuki, Y. Momose, N. Higashi, A. Shigematsu, K.B. Park, Y.M. Kim, J.R. Kim, and J.M. Ryu. Biodistribution and kinetics of holmium-166-chitosan complex (DW-166HC) in rats and mice. *J Nucl Med*. 39:2161-2166 (1998).
24. T.J. Sinton, D.M. Cowley, and S.J. Bryant. Reference intervals for calcium, phosphate, and alkaline phosphatase as derived on the basis of multichannel-analyzer profiles. *Clin Chem*. 32:76-79 (1986).
25. M.A.D. Vente, J.F.W. Nijssen, T.C. de Wit, J.H. Seppenwoolde, G.C. Krijger, P.R. Seevinck, A. Huisman, B.A. Zonnenberg, T.S.G.A.M. Van den Ingh, and A.D. van het Schip. Clinical effects of transcatheter hepatic arterial embolization with holmium-166 poly(L: -lactic acid) microspheres in healthy pigs. *Eur J Nucl Med Mol Imaging*. 35:1259-1271 (2008).
26. P.W. Durbin. Metabolic characteristics within a chemical family. *Health Phys*. 2:225-238 (1960).







## Chapter 5

# Interstitial microbrachytherapy using holmium-166 acetylacetonate microspheres: a feasibility study in feline liver cancer patients

W. Bult, M.A.D. Vente, E. Vandermeulen, I. Gielen, P.R. Seevinck,  
J. Saunders, A.D. van het Schip, C.J.G. Bakker, G.C. Krijger,  
K. Peremans and J.F.W. Nijsen

Submitted

## Abstract

**Purpose:** Holmium-166 acetylacetonate microspheres ( $^{166}\text{HoAcAcMS}$ ) are proposed as a novel intratumoral radioablation device. This paper presents a study in feline patients with unresectable liver cancer in which the feasibility of intratumoral administrations of  $^{166}\text{HoAcAcMS}$  was investigated.

**Methods and Materials:** Three European Shorthair cats with unresectable liver tumors of different histotype were selected and treated with  $^{166}\text{HoAcAcMS}$ . One cat had a biopsy-confirmed hepatocellular carcinoma (HCC), one had a cholangiocarcinoma (CC), and one cat had a malignant epithelial liver tumor (MELT) of unspecified histotype. The  $^{166}\text{HoAcAcMS}$  were injected percutaneously under ultrasound guidance into the tumor. Follow-up consisted of regular physical examinations and hematological and biochemical analyses.

**Results:**  $^{166}\text{HoAcAcMS}$  were technically successfully administered to three liver tumor-bearing cats with palliative intent. The treatment was well tolerated in all cases and the clinical condition of the animals improved markedly. Most biochemical and hematological parameters normalized shortly after treatment. The life of all cats was extended and associated with a good quality of life. The HCC cat was euthanized six months after the first administration due to disease progression, the CC cat succumbed four months after the first treatment due to the formation of a pulmonary embolism. The MELT cat developed bacterial meningitis and was euthanized three months post treatment.

**Conclusions:** Percutaneous intratumoral injection of radioactive  $^{166}\text{HoAcAcMS}$  is feasible in liver tumor-bearing cats. This radioablation technique appears to be efficacious and not associated with adverse side effects.

**Keywords:** holmium, liver, tumor, intratumoral, radioablation, microsphere

## Introduction

The intratumoral administration by means of direct injection of radionuclide containing devices has been clinically explored as a treatment option for solid tumors, not amenable for surgical resection. Glass microspheres incorporated with the high-energy beta emitter yttrium-90 ( $^{90}\text{Y}$ ) as well as colloids tagged with the beta emitter phosphor-32 ( $^{32}\text{P}$ ) incorporated in a chromic matrix have been intratumorally injected in patients with intrahepatic malignancies (1, 2). Signs of toxicity were absent and tumor response was high (tumor size reduction in 90 % of the lesions for  $^{90}\text{Y}$  and partial remission or complete remission in 12/17 patients for  $^{32}\text{P}$ ), although the patient numbers were low. Only patients with a limited number of lesions (maximally three) were included in these studies. Another device that has been clinically applied is holmium-166 ( $^{166}\text{Ho}$ ) labeled chitosan, a gel-forming natural polymer (3). Again response rates were very high, 31/40 (77%) patients showed complete tumor necrosis, but due to leakage of  $^{166}\text{Ho}$  to the systemic circulation in 11/40 patients (25%), suppression of the hematopoietic system was observed.

$^{166}\text{Ho}$  indeed can be considered an ideally suited radioisotope for intratumoral radioablation, since  $^{166}\text{Ho}$  not only emits high-energy beta particles but low-energy gamma rays as well, and has a favorable half-life of 26.8 h (4). The beta particles have a maximum tissue range of 8.7 mm allowing for radioablation and the gamma-emission permits nuclear imaging which is useful for dosimetric calculations. Moreover, holmium can be visualized by magnetic resonance imaging (MRI) and X-ray computed tomography (CT) due to the paramagnetic properties and the high attenuation coefficient of holmium, respectively (5).  $^{166}\text{Ho}$  acetylacetonate microspheres ( $^{166}\text{HoAcAcMS}$ ) have been developed and characterized (6) at our institution and its suitability as a radioablation device has already been investigated in renal cell carcinoma-bearing mice (7). Microsphere treated mice did not show tumor growth ( $141 \pm 99 \text{ mm}^3$  at time of treatment versus  $104 \pm 95 \text{ mm}^3$  after two weeks), whereas the tumor size in the saline treated control group increased dramatically (from  $122 \pm 33 \text{ mm}^3$  to  $4150 \pm 300 \text{ mm}^3$  two weeks post-injection).

In this paper, we present the clinical results of radioablation with  $^{166}\text{HoAcAcMS}$  of liver malignancies in a spontaneous liver tumor-bearing model, specifically, in three house cats with liver cancer of different tumor histotypes. The aim was to evaluate both the toxicity and efficacy.

## Materials and Methods

### Microsphere preparation

$\text{HoAcAcMS}$  were prepared as previously described (6). The microspheres (200 mg) were packed in high-density poly-ethylene vials (type A; Posthumus Plastics, Beverwijk, The Netherlands) and neutron activated via the  $^{165}\text{Ho} [n,\gamma] ^{166}\text{Ho}$  reaction in a nuclear reactor with a nominal thermal neutron flux of  $5 \times 10^{12} \text{ cm}^{-2} \text{ s}^{-1}$  (Delft University of Technology, Delft, The Netherlands) (8). After neutron activation,  $^{166}\text{HoAcAcMS}$  were suspended in 1.1 mL of sterile water containing 2% Pluronic® F-68 (Sigma-Aldrich Chemie B.V., Zwijndrecht, The Netherlands) and 10% ethanol abs. (Merck B.V., Amsterdam, The Netherlands). The  $^{166}\text{HoAcAcMS}$  were suspended by

gentle agitation and repeatedly drawing up and down with a syringe. Subsequently, aliquots were drawn up in 1-mL Luer Taper syringes prefilled with the Pluronic solution. The amount of radioactivity present in each syringe was measured in a dose calibrator (VDC-404, Veenstra Instrumenten B.V., Joure, The Netherlands), and approximately 0.1 mL air was drawn up. Each syringe was placed into an acrylic glass cylinder (inner and outer diameter 9 and 25 mm, respectively), to limit the radiation dose, especially to the hands, both during dose preparation and administration.

### **Patient selection**

Eligible feline patients should have unresectable, biopsy-proven malignant primary liver cancer, and no apparent (extrahepatic) metastases, as assessed on CT. Life expectancy should at least be three months and the general condition should be adequate. A comorbidity with a grave prognosis or a severely debilitating disease was an exclusion criteria. All owners were required to give informed consent prior to treatment.

### **Patient characteristics**

Three European Shorthair cats with liver cancer were included; one hepatocellular carcinoma (HCC) (14 y), one unclassified malignant epithelial liver tumor (MELT) (12 y), and one cholangiocarcinoma (CC) (14 y) patient. Findings during physical examination included impaired alertness, emaciation and muscle weakness, a dull coat, and in the cat with HCC, a very large palpable mass in the epigastric and mesogastric regions. The clinical condition of these animals was poor, and the only alternative to euthanasia for these animals was decided to be an experimental treatment, in this case intratumoral injections of  $^{166}\text{HoAcAcMS}$ .

### **Anesthesia and analgesia**

General anesthesia was induced by i.v. administration of propofol and maintained by inhalation of isoflurane (1.5-2.0%  $\text{O}_2$ /air (1:1)). Peri- and postoperative analgesia consisted of buprenorphine (4dd 0.06 mg i.v. or i.m.), and antibacterial prophylaxis was provided by amoxicillin/clavulanic acid (4dd 0.5 ml i.v. or, after discharge, 2dd 37.5 mg p.o.). Additional medication consisted of prednisolone (2dd 2.5 mg p.o.) and for the cat with HCC metoclopramid (4dd 0.1 mg i.v. or, after discharge, 4dd 0.15 mg p.o.).

### **Imaging and treatment planning**

Pretreatment CT was performed to determine tumor localization and size, using a single row detector spiral CT (Prospeed, GE Medical Systems, Milwaukee, WI). On the transaxial CT slices the tumors were segmented and the volume of each tumor was estimated. A dose escalation scheme of 30, 100, and 300 Gy on the tumor tissue was followed. The dosage of  $^{166}\text{HoAcAcMS}$  was divided into several aliquots, the number depending on the tumor volume. The dosage was distributed evenly over the tumorous parts of the liver, based on the pretreatment CT analysis.

Prior to administration of  $^{166}\text{HoAcAcMS}$ , an ultrasound examination was

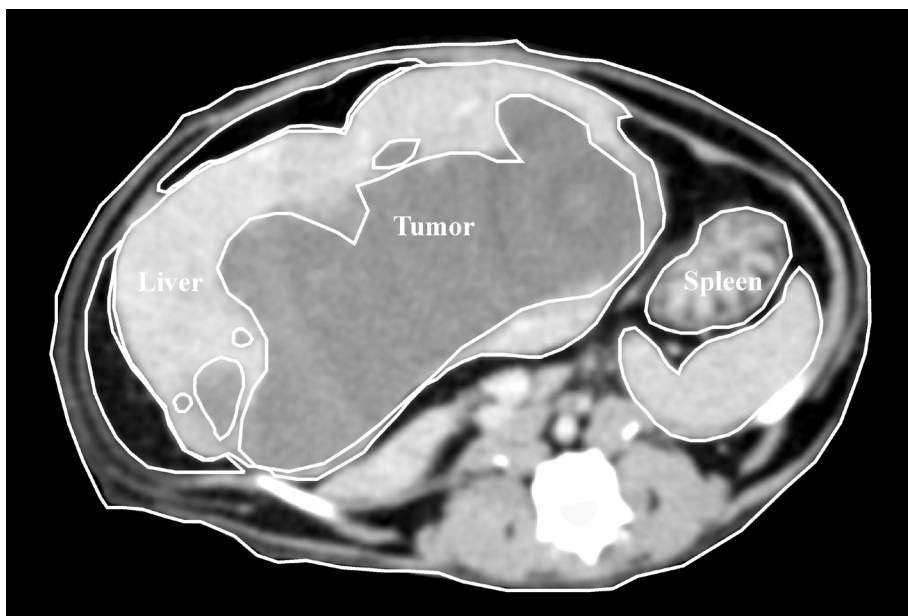


Figure 1. Segmented CT image for dose planning of the MELT patient

performed, including microbubble-enhanced (SonoVue<sup>®</sup>, Bracco International, Inc., Switzerland) ultrasound, to help in distinguishing between liver parenchyma, (viable) tumors, and necrotic tissue. These images were compared with the CT images, to verify the localization of the tumors of interest.

Directly post administration, the distribution of the  $^{166}\text{HoAcAcMS}$  in the tumors was qualitatively assessed by planar nuclear imaging and single photon emission computed tomography (SPECT), using a three-headed gamma camera (Triad<sup>®</sup>, Trionix Research Laboratory, Twinsburg, USA), equipped with a low-energy, ultrahigh resolution parallel hole collimator. SPECT was performed to ascertain the selective deposition of  $^{166}\text{HoAcAcMS}$ , and to confirm the absence of activity in the lungs.

#### Administration procedure

The  $^{166}\text{HoAcAcMS}$  suspensions were vigorously mixed immediately prior to administration, to ensure that a homogeneous suspension was obtained, and to mix the air with the suspension. The  $^{166}\text{HoAcAcMS}$  were injected intratumorally under ultrasound guidance to discriminate between tumorous tissue and non-tumorous liver parenchyma and to visualize large blood vessels in the liver. The  $^{166}\text{HoAcAcMS}$  were injected through 22G x 1.5'' and 22G x 2.0'' needles under slow retraction. For larger tumors the injection positions were separated by 1.5 cm. The activity that remained in the syringes was measured immediately after injection. The tumor absorbed dose (in Gy ( $\text{J kg}^{-1}$ )) was calculated using the formula: activity (MBq) x 15.87 ( $\text{mJ MBq}^{-1}$ ) / tumor weight (g) (9). Assumed tumor tissue density was  $1.1 \text{ g cm}^{-3}$ .

### Patient follow-up

The animals were discharged when the exposure rate was below  $20 \mu\text{Sv h}^{-1}$  at one meter. The follow-up consisted of regular physical examinations and hematological and biochemical analyses. CT and MRI were refrained from since the risks associated with anesthesia outweighed the benefits.

### Histological evaluation and *ex vivo* imaging

After euthanasia the owner of the HCC cat donated the cat's remains for further analysis. Prior to processing for histological examination and *ex vivo* imaging, the liver was flushed with a formaldehyde solution (4%) and stored in the same solution. CT and MR imaging and histological analysis of the HCC liver was performed *ex vivo* to gain insight in the *in vivo* stability of the HoAcAcMS. A 64-slice CT scanner (Brilliance<sup>®</sup>, Philips Medical Systems, Best, The Netherlands) was used; the tube voltage was set at 120 kV and the tube current was 269 mAs. MR imaging of the *ex vivo* liver was performed using a 1.5-Tesla clinical MRI system (Achieva<sup>®</sup>, Philips Medical Systems, Best, The Netherlands). The MR images were acquired according to previously described protocols (5). For histological analysis, tissue portions of approximately one  $\text{cm}^3$  were embedded in paraffin, and cut in sections of  $4 \mu\text{m}$  and stained using haematoxylin and eosin. In addition, a piece of femur was excised and subjected to neutron activation analysis to determine the holmium content in the bone. These values were compared to the holmium content in a femur of a non-holmium treated cat.

**Table I.** Tumor volume, injected dosage, absorbed dose, and survival

Cat	Tumor volume ( $\text{cm}^3$ )	Dosage injected (MBq)	Absorbed dose (Gy)	Survival* (days)
HCC	648	550	12	
		950	21	181 days
MELT	139	950	99	93 days
CC	94	2170	333	122 days

\* post treatment

## Results

Three cats were included in this feasibility study. Tumor volume was determined by CT to assess the required amount of activity (Fig. 1). The injected activity dosage varied from 550 to 2170 MBq (Table I). The biodistribution of the  $^{166}\text{HoAcAcMS}$  was qualitatively assessed by nuclear imaging (planar and SPECT) (Fig. 2). The deposits of  $^{166}\text{HoAcAcMS}$  were confined to the liver at the injection sites, viz. in the tumors. Not later than four days post treatment, the exposure rate was  $< 20 \mu\text{Sv h}^{-1}$  at 1 meter, and the cats were taken home with guidelines for safe handling of the animals.





**Figure 2.** Gamma scintigraph (maximum intensity projection), acquired after treatment of the MELT patient.

The clinical condition of the cats gradually improved and weight gain, improved alertness, mobility and condition of the coat were observed within one week after treatment. The biochemical and most hematological parameters normalized within one week (Table II).

At the time of initial presentation, the condition of the HCC cat was very poor. The tumor volume was  $648\text{ cm}^3$ , and the intended tumor dose was 30 Gy. However, due to premature settling of  $^{166}\text{HoAcAcMS}$  in the syringe, the cat only received 550 MBq, which corresponds to 12 Gy. Upon treatment its clinical condition improved rapidly. After 100 days the cat showed signs of tumor relapse and a second treatment with 950 MBq  $^{166}\text{HoAcAcMS}$  was given (day 112), corresponding to a tumor absorbed dose of 21 Gy. Although the animal's clinical condition and its relevant blood parameters (Table II) improved, 69 days after the second treatment the presence of a very large intra-abdominal mass, i.e., the partially necrotic, partially hypertrophic and still tumor-bearing liver, was presenting a source of persistent and aggravating discomfort. For this reason it was decided, six months after the first procedure, to euthanize the animal.

Upon presentation, the cat with MELT was cachectic, and CT (Fig. 1) showed a large solitary mass in the liver ( $139\text{ cm}^3$ ). This cat was injected with 950 MBq  $^{166}\text{HoAcAcMS}$  corresponding to a tumor absorbed dose of 99 Gy and was taken home after three days. Its clinical condition improved and remained constant for 76 days, after which the animal developed sopor and paraparesis. It was decided to euthanize the animal 93 days after the treatment. Necropsy revealed, apart from lesions in the liver, lesions in the kidneys, and bacterial meningitis.

The cat with CC had a tumor volume of  $94\text{ cm}^3$ . Since this animal was planned to receive the highest dose, it was decided to administer the  $^{166}\text{HoAcAcMS}$  in two

**Table II** Relevant hematological and biochemical parameters of the hepatocellular carcinoma (HCC)

Day	0 <sup>†</sup>		4		40		56	
	HCC	CC	HCC	CC	HCC	CC	HCC	CC
Leukocyte count (5000 – 15000 $\mu\text{L}^{-1}$ ) <sup>§</sup>	n.d.*	9980	28150	14200	29650	9170	15650	11260
Hemoglobin (8 – 15 g dL <sup>-1</sup> )	n.d.	7.8	4.2	6.3	8.4	8.3	9.8	7.5
Prothrombin time (5 - 11 s) <sup>§</sup>	21.3	40	7.6	40	n.d.	10.4	9.8	11
Albumin (2.5 - 4.5 g dL <sup>-1</sup> ) <sup>§</sup>	2.45	3.17	2.36	3.18	3.11	3.1	3.36	3.24
Bilirubin (total) (< 0.4 mg dL <sup>-1</sup> ) <sup>§</sup>	0.42	0.14	0.37	0.14	0.21	0.15	0.23	0.16

<sup>†</sup> Due to lack of owner compliance no data presented of MELT cat

<sup>‡</sup> Days after first treatment

<sup>§</sup> (reference value)

\* n.d. = not determined

sessions with 44 days in between in order to retain sufficient liver function. In the right hemiliver, 1500 MBq and in the left side 670 MBq <sup>166</sup>HoAcAcMS was injected. The total tumor absorbed dose was 333 Gy. The hematological and biochemical parameters of this cat remained normalized throughout the entire follow-up period (Table II). At day 122 after the first treatment, the cat was euthanized owing to the formation of a pulmonary embolism.

The HCC cat was subjected to a complete necropsy, which revealed an emaciated physical condition, a very large liver with a very heterogeneous, nodular outer surface. Neither signs of metastatic disease were observed in any of the other organs, nor any other macroscopic abnormalities. On both the CT and the MR images, the depots of <sup>166</sup>HoAcAcMS were clearly visualized (Fig. 3). Histological examination showed clusters of intact HoAcAcMS, surrounded by necrotic tissue (Fig. 4). In both the bone sample of the treated cat (the one with HCC) and that of a control animal the holmium concentration was below the detection limit (10 ppm).

## Discussion

Intratumoral radioablation offers perspectives in patients with unresectable malignancies e.g. brain, kidney, head and neck tumors (7, 10, 11). In this pilot study this concept was investigated in a spontaneous animal model, namely the domestic cat with primary liver cancer.

The number of subjects is limited yet the results are encouraging in that treatment through intratumorally injected <sup>166</sup>HoAcAcMS undoubtedly was beneficial, i.e.,

and cholangiocarcinoma (CC) cats<sup>†</sup>.

100		112		116		139	181
HCC	CC	HCC	CC	HCC	CC	HCC	HCC
n.d.	n.d.	19410	n.d.	19410	n.d.	15320	16800
n.d.	n.d.	8.7	n.d.	8.5	n.d.	8.7	5.7
n.d.	9.7	8.8	n.d.	8.2	n.d.	n.d.	n.d.
n.d.	3.2	3.5	n.d.	2.8	n.d.	3.19	3.34
n.d.	0.12	0.34	n.d.	0.34	n.d.	0.34	0.34

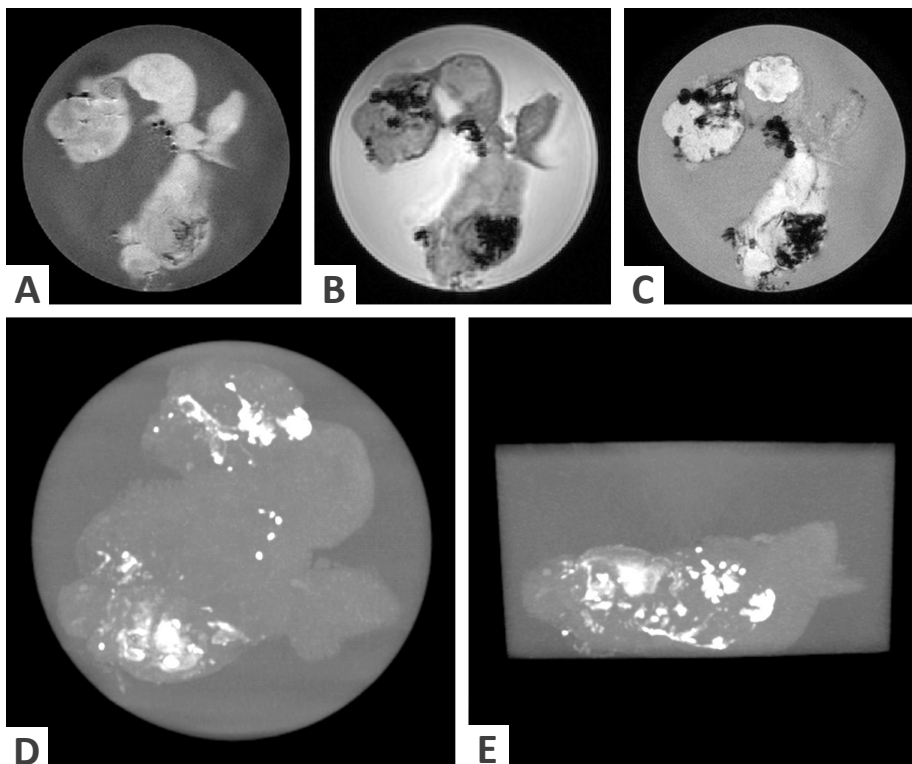


**Figure 3.** MR and CT images of the *ex vivo* HCC liver in a plastic bucket.  $T_1$ -weighted TSE, insensitive for holmium (a). 3D FFE (b), and  $T_2$ -weighted mFFE (c), on which the holmium cluster of HoAcAcMS are visible as black artifacts. CT images (maximum-intensity projections) of the *ex vivo* HCC liver; top view (d) and side view (e). The radiopaque structures correspond with the HoAcAcMS depots.

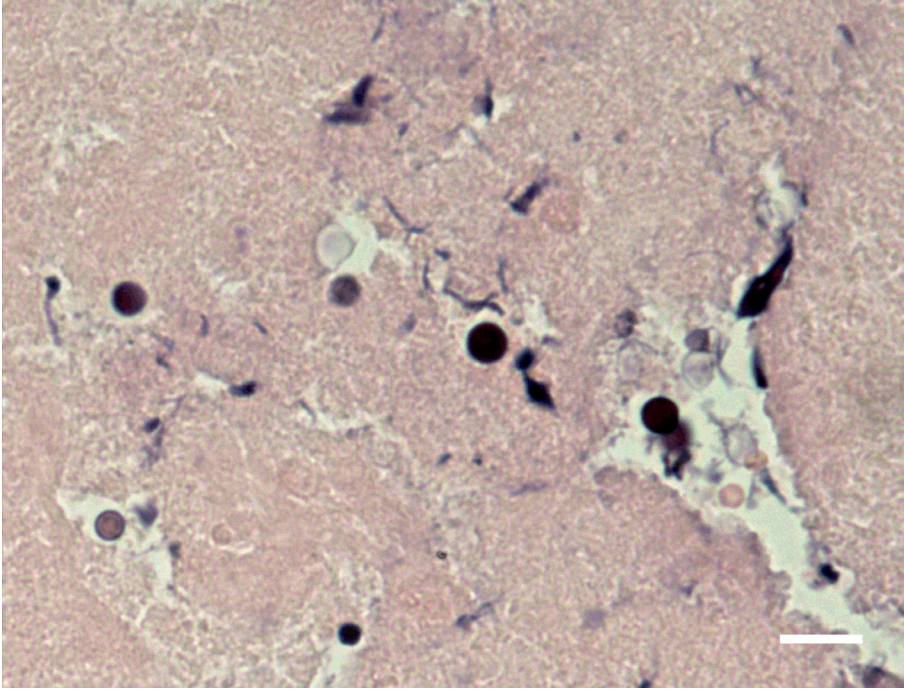


**Figure 4.** Histological (haematoxylin eosin stained) section of the liver of the HCC cat. Intact HoAcAcMS (dark spherical structures) are surrounded by necrotic tissue. Bar represents 20  $\mu$ m.

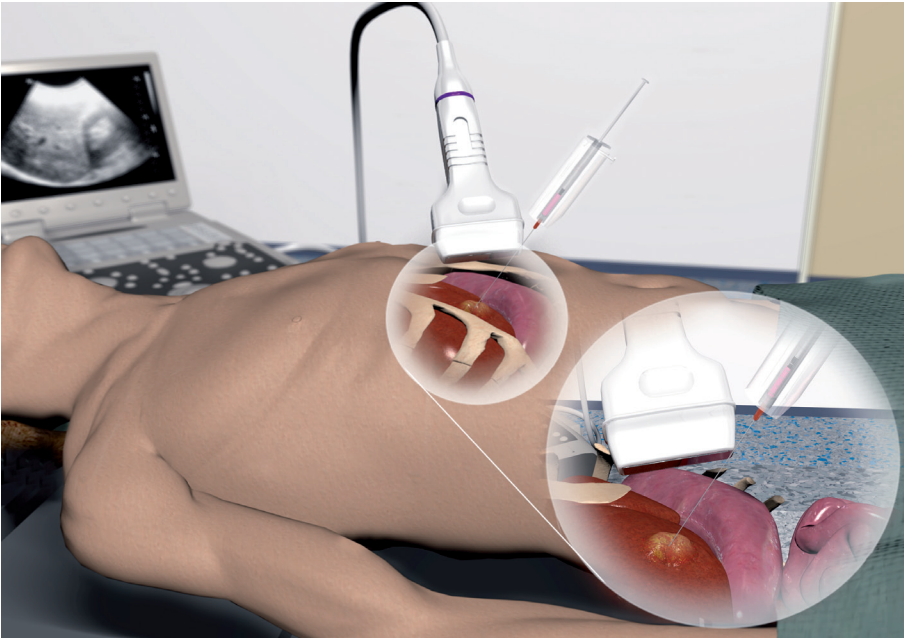


**Figure 5.** Artist impression of the percutaneous  $^{166}\text{HoAcAcMS}$  injection procedure in a patient. The needle is placed in the tumor in the liver, and the microspheres are injected under ultrasound guidance.

clinically all animals rapidly improved. Only in the HCC cat a high leukocyte count was observed, probably caused by the large intra-abdominal tumor mass that was partly necrotic. The treatments were well tolerated, and the life of all cats was extended and associated with a good quality of life.

Recently, Ricke *et al.* reported on the local response after intratumoral administration of iridium brachytherapy catheters in liver metastases of colorectal carcinoma. The authors observed already substantial tumor response at a tumor absorbed dose of 15 Gy (12). In our study, the tumor absorbed dose ranged widely (12-333 Gy), and there was no obvious dose-response relation observed. Remarkably, the higher doses were not associated with an increase in toxicity. Both issues need to be investigated in larger studies.

In the present study, the intended tumor dose was calculated assuming a homogeneous distribution of the  $^{166}\text{HoAcAcMS}$  in the tumor. In fact the microspheres were injected into the viable tumor tissue and not in the necrotic center of the tumor which results in a considerably higher absorbed dose on the vital tumor cells. This probably explains the observed effect of the  $^{166}\text{HoAcAcMS}$  treatment even in the cat with HCC tumor that received only 12 Gy in the first treatment.

Settling of the microspheres in the syringe was one of the practical problems encountered during the injection procedure and resulted in the delivery of only part (mean  $56 \pm 20\%$ ) of the intended dose. After the first treatment this problem was circumvented by preparing double the amount of activity. In order to achieve a standardized, reproducible procedure, several aspects may be addressed.

First, the particles can be suspended in a more viscous medium, like iodinated poppy seed oil (2). Second, particle size reduction might enhance the homogeneity and decrease the settling of particles in the suspension. In concordance with Stokes' law, the sedimentation velocity of particles in suspension is reduced by substantially decreasing the particle diameter (13, 14). Finally, a dedicated administration device needs to be developed with a limited dead volume for accurate delivery of the  $^{166}\text{HoAcAcMS}$  suspension.

CT and MRI showed depots of  $\text{HoAcAcMS}$  in the *ex vivo* liver and histological analysis revealed that the microspheres retained their structural integrity for at least two months. Furthermore, the *in vivo* release of holmium from the  $^{166}\text{HoAcAcMS}$  was investigated by neutron activation analysis of a piece of femur since holmium is a bone-seeking element (15). Holmium levels in bone were below the detection limit, which is an indication that no holmium had released. The aforementioned findings demonstrate that  $^{166}\text{HoAcAcMS}$  constitute a safe radioablation device.

The injection procedure of  $^{166}\text{HoAcAcMS}$  (Fig. 5) can be considered a minimally invasive technique like percutaneous radiofrequency ablation. The  $^{166}\text{HoAcAcMS}$  may be a useful device for the radioablation of not easily accessible malignancies in delicate organs.

## Conclusion

The present study demonstrates the feasibility of radioablation of malignancies with  $^{166}\text{HoAcAcMS}$ . Treatment was well tolerated by three animals with extensive liver

cancer, and resulted in an increase in lifespan, with a good quality of life. This study showed that the  $^{166}\text{HoAcAcMS}$  remain intact for at least two months post treatment.

The  $^{166}\text{HoAcAcMS}$  may also be useful for radioablation of other inoperable and not easily accessible tumors but more preclinical studies are warranted before a phase I patient study can be initiated.

## Acknowledgements

A grant from the Dutch Technology foundation STW, under no. 06069, is gratefully acknowledged. The authors would like to thank Mr. Hendrik Haers, DVM for ultrasound assistance and Mrs. Anneke Koster-Ammerlaan for performing the neutron irradiations of the microspheres.

## References

1. N. Firusian and W. Dempke. An early phase II study of intratumoral P-32 chromic phosphate injection therapy for patients with refractory solid tumors and solitary metastases. *Cancer*. 85:980-987 (1999).
2. J.H. Tian, B.X. Xu, J.M. Zhang, B.W. Dong, P. Liang, and X.D. Wang. Ultrasound-guided internal radiotherapy using yttrium-90-glass microspheres for liver malignancies. *J Nucl Med*. 37:958-963 (1996).
3. J.K. Kim, K.H. Han, J.T. Lee, Y.H. Paik, S.H. Ahn, J.D. Lee, K.S. Lee, C.Y. Chon, and Y.M. Moon. Long-term clinical outcome of phase IIb clinical trial of percutaneous injection with holmium-166/chitosan complex (Milican) for the treatment of small hepatocellular carcinoma. *Clin Cancer Res*. 12:543-548 (2006).
4. D.R. Lide (ed.), *CRC Handbook of Chemistry and Physics*, 89th Edition (Internet Version 2009), CRC Press/Taylor and Francis, Boca Raton, FL.
5. P.R. Seevinck, J.H. Seppenwoolde, T.C. de Wit, J.F. Nijsen, F.J. Beekman, A.D. van het Schip, and C.J. Bakker. Factors affecting the sensitivity and detection limits of MRI, CT, and SPECT for multimodal diagnostic and therapeutic agents. *Anticancer Agents Med Chem*. 7:317-334 (2007).
6. W. Bult, P.R. Seevinck, G.C. Krijger, T. Visser, L.M. Kroon-Batenburg, C.J. Bakker, W.E. Hennink, A.D. van het Schip, and J.F. Nijsen. Microspheres with ultrahigh holmium content for radioablation of malignancies. *Pharm Res*. 26:1371-1378 (2009).
7. W. Bult, S.G.C. Kroeze, M. Elschot, P.R. Seevinck, F.J. Beekman, P.R. Luijten, W.E. Hennink, A.D. van het Schip, J.L.H.R. Bosch, J.F.W. Nijsen, and J.J.M. Jans. Intratumoral administration of holmium-166 acetylacetonate microspheres as a novel minimally-invasive treatment for small kidney tumors. In preparation (2010).
8. M.A.D. Vente, J.F. Nijsen, R. de Roos, M.J. van Steenberghe, C.N. Kaaijk, M.J. Koster-Ammerlaan, P.F. de Leege, W.E. Hennink, A.D. van het Schip, and G.C. Krijger. Neutron activation of holmium poly(L-lactic acid) microspheres for hepatic arterial radio-embolization: a validation study. *Biomed Microdevices*. 11:763-772 (2009).
9. M.A.D. Vente, J.F.W. Nijsen, T.C. de Wit, J.H. Seppenwoolde, G.C. Krijger, P.R. Seevinck, A. Huisman, B.A. Zonnenberg, T.S.G.A.M. Van den Ingh, and A.D. van het Schip. Clinical effects of transcatheter hepatic arterial embolization with holmium-166 poly(L: -lactic acid) microspheres in healthy pigs. *Eur J Nucl Med Mol Imaging*. 35:1259-1271 (2008).
10. T.W. Vitaz, P.C. Warnke, V. Tabar, and P.H. Gutin. Brachytherapy for brain tumors. *J Neurooncol*. 73:71-86 (2005).
11. L. Do, A. Puthawala, and N. Syed. Interstitial brachytherapy as boost for locally advanced T4 head and neck cancer. *Brachytherapy*. 8:385-391 (2009).
12. J. Ricke, K. Mohnike, M. Pech, M. Seidensticker, R. Ruhl, G. Wieners, G. Gaffke, S. Kropf, R. Felix, and P. Wust. Local Response and Impact on Survival After Local Ablation of Liver Metastases from Colorectal Carcinoma by Computed Tomography-Guided High-Dose-Rate Brachytherapy. *Int J Radiat Oncol Biol Phys* (2010).
13. A.N. Martin. Coarse Dispersions. In Martin A.N. (ed.), *Physical Pharmacy*, Lea & Febiger, Philadelphia, 1993, pp. 477-511.
14. W. Bult, R. Varkevisser, F. Soulimani, P.R. Seevinck, H. de Leeuw, C.J. Bakker, P.R. Luijten, A.D. van het Schip, W.E. Hennink, and J.F. Nijsen. Holmium nanoparticles: preparation and in vitro characterization of a new device for radioablation of solid malignancies. *Pharm Res*. 27:2205-2212 (2010).
15. P.W. Durbin. Metabolic characteristics within a chemical family. *Health Phys*. 2:225-238 (1960).





## Chapter 6

# Intratumoral administration of holmium-166 acetylacetonate microspheres as a novel minimally-invasive treatment for small kidney tumors

W. Bult, S.G.C. Kroeze, M. Elschot, P.R. Seevinck, F.J. Beekman,  
H.W.A.M. de Jong, P.R. Luijten, W.E. Hennink, A.D. van het Schip,  
J.L.H.R. Bosch, J.F.W. Nijsen, J.J.M. Jans

in preparation

## Abstract

The widespread use of cross-sectional imaging techniques has resulted in a dramatic increase of incidentally detected small kidney tumors. Minimally invasive treatments need to be developed to eradicate these potentially lethal masses. In this paper a novel local ablation technique employing intratumoral administration of small (12  $\mu\text{m}$ ) holmium-166 acetylacetonate microspheres ( $^{166}\text{HoAcAcMS}$ ) is presented.  $^{166}\text{Ho}$  emits high-energy beta particles suitable for anticancer therapy and the simultaneously emitted gamma rays allow for nuclear imaging. Moreover, non-radioactive holmium-165 can be visualized by both CT and MRI, due to its high mass attenuation coefficient and paramagnetic properties, respectively. These imaging opportunities offer many advantages such as imaging the distribution of HoAcAcMS post-treatment for direct therapy evaluation and follow-up. In the present study, the potential of  $^{166}\text{HoAcAcMS}$  as a local treatment for small renal masses was successfully demonstrated. Moreover, the unique multimodality imaging opportunities are investigated making this a novel minimally invasive approach to eradicate small renal masses.

**Keywords:** holmium, kidney cancer, imaging, local ablation, radiotherapy

## Introduction

Kidney cancer accounts for approximately 3% of all cancers. With a world-wide incidence of 208,000 new cases and a mortality of 102,000 patients each year, it is one of the most lethal genitourinary malignancies (1). In recent years a dramatic increase of the number of incidentally detected renal tumors has occurred, largely due to the more widespread use of noninvasive imaging techniques such as x-ray computed tomography (CT), ultrasound and magnetic resonance imaging (MRI). These tumors currently account for up to 60% of kidney cancers (2) and are generally small (<4cm) and low grade (3-5). Although most of these small renal masses are relatively slow-growing, they are by no means harmless. Eleven to eighteen percent of these small masses will develop into a higher grade tumor and 4-6% will eventually metastasize within the following 10 years (6, 7). Once the kidney cancer has metastasized, patients have a median survival of 20 months (8).

Radical nephrectomy of the tumor-bearing kidney has long been the gold standard treatment for individual localized lesions (9). The steady rise in the number of patients with small renal tumors and the morbidity associated with nephrectomy has led to the development of less invasive treatments. Recently, nephron-sparing surgery was shown to be effective in cancer control and preservation of renal function (10).

At present, minimally invasive techniques most commonly applied for treatment of small renal tumors are cryoablation and radiofrequency ablation (RFA). These thermoablative techniques employ either freezing or heat to eradicate tumorous tissue, and can be applied either percutaneously or by laparoscopy (11). Both methods have been successfully used to treat tumors present in breast, liver, kidney and bone. Despite the promising results of these techniques in treatment of small renal tumors, the clinic is presented with their respective limitations. Recurrence or persistence of the tumor is more often present after cryoablation and RFA compared to partial nephrectomy (12). As a consequence, multiple sessions are often necessary (13) and both techniques are restricted to treatment of tumors smaller than 4 cm. Tumor persistence is frequently observed after RFA of larger tumors (14, 15). Larger tumors are associated with the risk of fracturing the ice-ball after cryoablation, resulting in bleeding and potential consequent kidney loss. External beam radiotherapy, another locoregional ablation technique, has not been effective against kidney cancer due to breathing-related movement of the kidneys and the radiosensitivity of adjacent tissue. In contrast to external beam radiotherapy, local administration of radioactive sources is not as limited by the radiosensitivity of the healthy tissue due to selective deposition of radioactivity in the tumor.

In this paper, a novel local ablation technique is presented using small (10 - 15  $\mu\text{m}$ ) holmium-166 acetylacetonate microspheres (<sup>166</sup>HoAcAcMS) with a high holmium load (16). <sup>166</sup>Ho emits both high-energy beta particles ( $E_{\beta\text{max}}$  1.77 and 1.85 MeV, maximum tissue penetration 8 mm, mean tissue penetration 2.5 mm) and gamma rays (0.081 MeV) that allow for nuclear imaging and has a half-life of 26.8 h (17). Moreover, non-radioactive holmium-165 can be visualized by CT and

MRI, due to its high mass attenuation coefficient and its paramagnetic properties, respectively (18). These imaging opportunities offer many advantages such as visualizing the distribution of holmium microspheres peri and post-treatment for direct therapy evaluation and follow-up. This study provides a proof of principle for intratumoral administration of  $^{166}\text{HoAcAcMS}$  as novel treatment strategy for kidney cancer and demonstrates the elegant *in vivo* multimodality imaging necessary for treatment guidance and monitoring.

## Materials and Methods

### Cell culture

The Balb/C renal carcinoma cell line Renca, kindly provided by the National Cancer Institute (Frederick, USA), was maintained at 37°C and 5% CO<sub>2</sub> in Dulbecco's Modified Eagle's Medium (DMEM) (Lonza, Breda, the Netherlands) supplemented with 10% fetal bovine serum (Lonza, Basel, Switzerland), 1% Penicillin/Streptomycin and 1% glutamine. This cell line originates from Balb/C mice and its pattern of growth mimics that of human renal cell carcinoma in terms of growth of a solid tumor, good vascularisation and the spontaneous metastatic spread to lung and liver. To prepare for *in vivo* transplantation, cells were trypsinized and centrifuged at 1500 rpm for 5 minutes, washed with PBS and counted. Finally, cells were resuspended in PBS and kept on ice until transplantation.

### Animal experiments

All experimental protocols were conducted in agreement with the Netherlands Experiments on Animals Act and the European convention guidelines. Animals were housed under standard laboratory conditions. Male Balb/C mice (Charles River, Maastricht, the Netherlands) aged 9-11 weeks were used for experiments. All surgical procedures were performed under general anesthesia (Isoflurane USP 1.5-4.0% (IsoFlo, Abbott Animal Health, Hoofddorp, The Netherlands), nitrous oxide 0.5%, oxygen 0.5%). To provide sufficient analgesia each mouse received 100 µL buprenorfine subcutaneously (Buprecare, AST Pharma, Oudewater, The Netherlands) 0.03 mg mL<sup>-1</sup>, diluted in NaCl 0.9% prior to surgery and 24 h post surgery. After all procedures the abdominal muscles and skin were closed in separate layers with vicryl 5.0 (Johnson&Johnson Intl., St-Stevens-Woluwe, Belgium).

### Renal tumor model

One million Renca cells in 100 µL PBS were injected subcutaneously in both flanks of 6 mice. Subcutaneous tumors were allowed to grow for 3 weeks, after which tumors were harvested, cut in small cubes and placed in 0.9% NaCl until transplantation. Access to the kidney was obtained by a dorsal incision at the midline of the back followed by a transversal incision of the abdominal muscles. The left kidney was mobilized and held with a non-traumatic forceps. A small incision was made in the renal capsule and a tumor cube of 8 mm<sup>3</sup> was transplanted under the renal capsule. The abdominal muscles and skin were closed. Renal tumors were allowed to grow

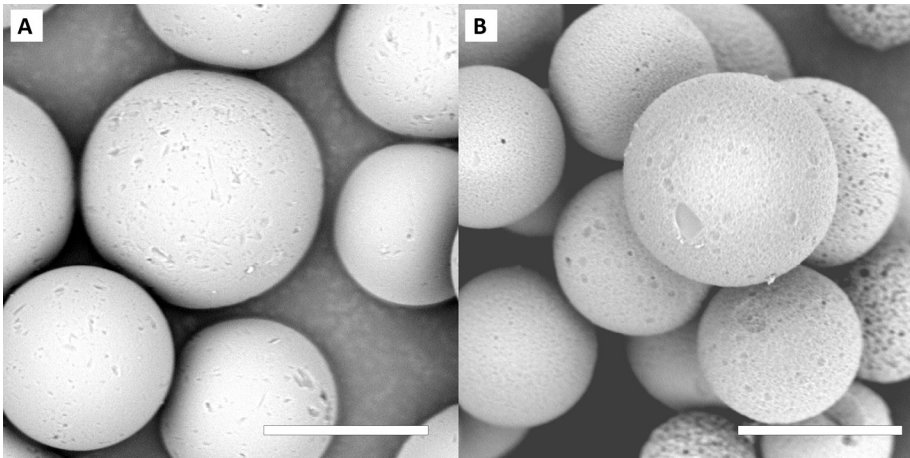


**Figure 1.** Scanning electron micrographs of HoAcAcMS. **(A)** HoAcAcMS before neutron irradiation, **(B)** <sup>166</sup>HoAcAcMS after neutron irradiation for 1 h at a thermal neutron flux of  $5 \times 10^{12} \text{ cm}^{-2} \times \text{s}^{-1}$ . Magnification of both samples was 10,000x, the bar represents 10  $\mu\text{m}$ .

for 1 week, while wellbeing of mice was followed by measuring body weight and scoring physical appearance.

### Holmium acetylacetonate microspheres

Holmium acetylacetonate microspheres (HoAcAcMS) were prepared as described by Bult *et al.* (16). In short, the lipophilic holmium complex holmium acetylacetonate (HoAcAc) is dissolved in chloroform (5.5% w/w) and emulsified in an aqueous polyvinylalcohol solution (2% w/w). This emulsion is stirred at 500 rpm for 40 hours at 25 °C under a continuous flow of nitrogen, to evaporate the chloroform. Thereafter, the microspheres are washed and sieved followed by drying at 50°C. Approximately 60 mg holmium acetylacetonate microspheres is then transferred to a high-density poly-ethylene (HDPE) vial (Posthumus Plastics, Beverwijk, the Netherlands). The HDPE vial with microspheres is neutron irradiated in a nuclear reactor with a nominal thermal neutron flux of  $5 \times 10^{12} \text{ cm}^{-2} \text{ s}^{-1}$  (Reactor Institute Delft, The Netherlands) to render the microspheres radioactive. Quality control was performed to assess the microsphere integrity after neutron irradiation by determining the particle size using a coulter counter (Multisizer 3, Beckman Coulter, Mijdrecht, The Netherlands), performing light microscopy (Nikon Eclipse, Nikon, Amstelveen, The Netherlands) and electron microscopy (Phenom, Phenom-World B.V., Eindhoven, The Netherlands). For electron microscopy, samples were mounted on an aluminum stub, and coated with a Pt layer of 6 nm. Images were acquired at an operating voltage of 5 kV.

The radioactive <sup>166</sup>Ho microspheres (<sup>166</sup>HoAcAcMS; 600 MBq) were suspended in 1.2 mL of an aqueous Pluronic solution (2% w/v). Approximately 50  $\mu\text{L}$  was taken up in 29 G insulin syringes (Becton Dickinson Ultra Fine, Breda, the Netherlands), and the activity was measured using a dose calibrator (VDC-404, Veenstra Instruments,

Joure, The Netherlands). Prior to administration, the syringes were placed in an acrylic glass cylinder to limit the dose on the hands and the syringe was agitated vigorously to obtain a homogenous suspension.

### Administration of microspheres

Access to the left kidney was obtained as described in the methods section (renal tumor model). While holding the kidney with a non-traumatic forceps, 10  $\mu\text{L}$  of the  $^{166}\text{HoAcAcMS}$  (approximately 5 MBq or 500  $\mu\text{g}$  microspheres) suspension was administered intratumorally with a 29G needle. After administration the syringes were measured in a dose calibrator to determine the dose administered to the tumors. Under comparable conditions control mice received either 10  $\mu\text{L}$  0.9% NaCl or 500  $\mu\text{g}$  non-radioactive microspheres. At 2 hours, 1, 2, 3, 7 and 14 days after the administration of microspheres ( $n=4/\text{group}$ ) or NaCl ( $n=5/\text{group}$ ) mice were sacrificed by cervical dislocation.

### Imaging

Immediately following administration of HoAcAcMS, the mice remained anesthetized and were placed in a dedicated small animal CT (U-CT, MILabs, Utrecht, The Netherlands). Images were acquired at a tube voltage of 45 kV, a tube current of 350 mAs and a voxel size of 83  $\mu\text{m}$  (isotropic). Two mice were sacrificed after administration of  $^{166}\text{HoAcAcMS}$  for multimodality imaging. Single photon emission tomography imaging was performed on a U-SPECT system (MILabs, Utrecht, The Netherlands) with a general purpose mouse collimator (75 focussing 0.6 mm diameter pinholes) to assess the  $^{166}\text{HoAcAcMS}$  distribution on a sub-half-millimeter resolution (19). Images were reconstructed using eight iterations Pixel-based Ordered Subset Expectation Maximization with 16 subsets (20). Compensation for distance dependent sensitivity and blurring of pinholes during reconstruction was applied through point source based system calibration (21). From the SPECT images, the dose distribution could be calculated as described by the MIRD S-voxel method (22). The MCNPX 2.5.0 Monte Carlo Code (23) was used to estimate the  $^{166}\text{Ho}$  dose convolution kernel. For each voxel in a  $15.375 \times 15.375 \times 15.375 \text{ mm}^3$  cube of tissue material ( $\rho = 1.06 \text{ g cm}^{-3}$ ) the absorbed dose was calculated as a result of the  $^{166}\text{Ho}$  source uniformly distributed in the center voxel of the cube. The voxel size chosen was 375  $\mu\text{m}$  (isotropic), equal to the voxel size of the reconstructed SPECT images. Dose maps were calculated by convolution of the SPECT images with the simulated  $^{166}\text{Ho}$  dose kernel. MRI was performed on a 4.7 T horizontal bore small animal scanner (Varian, Oxford, UK). Images were acquired using a multi-slice gradient echo MR sequence with an echo time of 3.0 msec and repetition time of 242 msec, a field of view (FOV) of  $64 \times 32 \text{ mm}^2$ , a scan matrix of  $256 \times 128$  with 38 slices resulting in a voxel size of  $0.25 \times 0.25 \times 0.5 \text{ mm}^3$ , eight signal averages and a  $25^\circ$  flip angle.

### Histopathologic analysis

Tumor-bearing and contralateral kidney, liver, spleen and heart/lung were weighed and radioactivity was measured in a dose calibrator. Tumor size was measured using

digital callipers. Tumor volumes were calculated using the following equation  $V = (A \times 0.5) \times B^2$ , where A is the largest diameter and B the smallest. Tumor-bearing kidneys were placed in 4% formaldehyde before embedding in paraffin. Paraffin embedded tissue was cut in sections of 5  $\mu\text{m}$  and processed using haematoxylin and eosin (H&E).

### Inductively coupled plasma mass spectrometry

Inductively coupled plasma mass spectrometry (ICP MS) was performed to determine the holmium content in mouse femurs, both in the NaCl and HoAcAcMS groups. Approximately 50 mg bone was accurately weighed and destructed in a 1 mL *aqua regia* (a mixture of three parts concentrated hydrochloric acid and one part concentrated nitric acid). After destruction, the samples were evaporated to dryness, and dissolved in 4 mL 2% nitric acid (*w/w*). Samples were measured on a Varian 820 MS (Varian, Middelburg, The Netherlands), which allows for accurate detection of 0.5 ng holmium per mL sample.

## Results

### Microsphere administration

Holmium acetylacetonate microspheres with a narrow size distribution (10 – 15  $\mu\text{m}$ , mean diameter 12.5  $\mu\text{m}$ ) were prepared using a previously described method (16). The microspheres had a smooth surface, both before and after neutron irradiation (Fig. 1). The size distribution was not affected by neutron irradiation, and the specific activity of the <sup>166</sup>HoAcAcMS was 10 MBq  $\text{mg}^{-1}$  at the time of delivery.

<sup>166</sup>HoAcAcMS were successfully administered to 24 Renca tumor-bearing Balb/C mice. As a control, 36 tumor-bearing animals received 10  $\mu\text{L}$  of saline and 2 mice received non-radioactive HoAcAcMS. The mean tumor diameter at the time of treatment was 5.6 mm  $\pm$  1.6 mm. All mice recovered from anesthesia and animal welfare was monitored daily. The intended dose to be administered to the tumor was 5 MBq (or 500  $\mu\text{g}$ ) of <sup>166</sup>HoAcAcMS. The average administered dose was 2.7 MBq  $\pm$  1.2 MBq, (corresponding to 270  $\pm$  120  $\mu\text{g}$  of microspheres). It should be mentioned that half of the intended 5 MBq radiation dose was administered due to premature settling of <sup>166</sup>HoAcAcMS in the needle and adsorption of <sup>166</sup>HoAcAcMS onto the syringe wall. Nevertheless, all animals received a calculated tumor absorbed dose sufficient to fully eradicate the tumor.

Holmium is a bone seeking element, and it was shown that 55% of the injected dose was absorbed in bone within 96 hours after administration of holmium nitrate (24). ICP MS was performed to determine to holmium content in bone. The background holmium content in femurs of mice in the NaCl group was 2.36  $\pm$  2.1 ng per mg (mean  $\pm$  sd) bone. The holmium content in femurs of mice in the holmium group was 5.90  $\pm$  3.8 ng per mg (mean  $\pm$  sd) bone. When expressed as a percentage of injected dose the leakage of holmium from the injection site was 0.12  $\pm$  0.2%.

### Efficacy

The tumor size was 62  $\pm$  47  $\text{mm}^3$  at the day of treatment. The tumor volume remained comparable in treatment and the control group for up to three days after

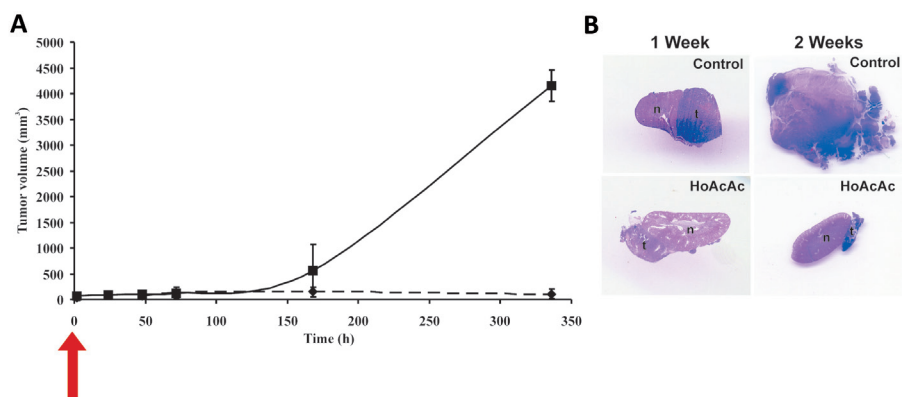


**Figure 2.** (A) Tumor volume at different time points after treatment. The solid line represents the tumor weights of the saline group. The dashed line represents the tumor weights of the  $^{166}\text{HoAcAcMS}$  treated group. The red arrow indicates the time of treatment. (B) Haematoxylin and eosin staining of kidney and tumor tissue 1 and 2 weeks after  $^{166}\text{HoAcAcMS}$  or control treatment. No normal kidney tissue is visible in control treated tumors after two weeks. (n indicates normal kidney, t indicates tumor.)

administration. The tumor volume in the saline group showed a dramatic increase from  $122 \pm 33 \text{ mm}^3$  at three days post-injection, to  $4150 \pm 300 \text{ mm}^3$  two weeks post-injection. The administration of non-radioactive microspheres resulted in tumors that were of similar size as the tumors in the control group one week after treatment (average  $590 \text{ mm}^3$ ). Importantly, the tumor volume in the  $^{166}\text{HoAcAc}$  treated group remained constant from  $141 \pm 99 \text{ mm}^3$  at three days post-injection to  $104 \pm 95 \text{ mm}^3$  after two weeks (Fig. 2). In the mice treated with radioactive microspheres the activity was retained in the tumors up to 48 h. This is the last time point at which accurate measurements of these low amounts of activity can be performed with a dose calibrator. Four mice showed a slightly increased activity in the lungs (average activity measured  $0.150 \text{ MBq}$ ), most likely due to the inadvertent delivery of  $^{166}\text{HoAcAcMS}$  in a blood vessel in or around the tumor. No activity was detected in other organs. No discomfort or toxic effects were observed in these mice. Furthermore, the physical appearance and the bodyweight of mice in the  $^{166}\text{HoAcAcMS}$  ( $22.2 \pm 1.8 \text{ g}$ ), saline ( $22.1 \pm 1.2 \text{ g}$ ) and cold microsphere group ( $22.1 \pm 1.3 \text{ g}$ ) remained constant throughout the experiment. No aberrant behaviour was observed.

Histopathologic analysis of tumor bearing kidney in the saline group showed a large tumorous mass on the kidney after one week. Two weeks after the administration of the NaCl, the kidneys were completely engulfed by the tumor, and no kidney tissue could be seen (see Fig. 2B). Conversely, histopathologic analysis of the tumor bearing kidneys in the  $^{166}\text{HoAcAcMS}$  group showed a small tumor at one week and two weeks post administration (Fig. 2B).



## Imaging

After administration of microspheres the mice underwent (micro) CT imaging, which revealed deposits of HoAcAcMS in the kidney area. On CT the skeleton and approximately 300  $\mu\text{g}$  <sup>166</sup>HoAcAcMS (corresponding with 3 MBq <sup>166</sup>Ho) were clearly visible. Substantial accumulation of particles was seen at the site of injection. No microspheres were detected outside the kidney area (Fig. 3 B).

SPECT and MRI offer advantages over CT imaging with respect to sensitivity (SPECT and MRI) and visualization of soft tissue (MRI). The powerful multimodality imaging characteristics of holmium were demonstrated with these two modalities in mice that were terminated immediately following administration of microspheres to the tumor. CT, SPECT and MRI images were acquired on dedicated animal scanners (Fig. 3 A to D). HoAcAcMS were clearly visualized using SPECT imaging and the SPECT images served as a template for the construction of a dose map (Fig. 3 E). The dose map shows a selective deposition of therapeutic beta particles at the site of injection, leading to a tumor absorbed dose in excess of 2200 Gy. For a more detailed anatomical depiction of the soft tissue, MR images were acquired. On  $T_2^*$  weighted MRI scans, holmium causes a rapid signal decay due to the paramagnetic nature of this element. Consequently, holmium appears as blackening on  $T_2^*$  weighted images. As can be seen in Figure 3, holmium is clearly visible as a dark spot in the upper side of the kidney, where it was administered in the tumor. By combining the sensitivity, and high quantitative accuracy of SPECT imaging (25-27) with the soft tissue imaging of MRI, the <sup>166</sup>HoAcAcMS treatment can accurately be evaluated to ensure complete tumor ablation.

## Discussion

In our study, the feasibility and efficacy of <sup>166</sup>HoAcAcMS as a minimally invasive treatment was assessed in a mouse model for kidney cancer. Importantly, the intratumoral administration of 2.7 MBq <sup>166</sup>HoAcAcMS arrested tumor growth. The effect on tumor volume is apparent one week post-administration when approximately 95% of the ionizing radiation dose has been delivered. Assuming all beta energy is deposited in the tumor, the calculated tumor absorbed dose was around 2200 Gy (Fig. 3 E). This value is approximately 25-fold higher than the 60 - 80 Gy absorbed dose used in external beam radiotherapy as a value sufficient for complete tumor kill. Despite the high calculated absorbed dose, the localized nature of the radiation dose considerably reduces unwanted toxicity. The radiation dose to the healthy tissue was below 23 Gy (28) in the largest part of the kidney and the surrounding organs, as shown in the dose map (Fig. 3 F). Given the maximum penetration depth of the emitted beta particles (8 mm), the radiation dose to healthy parenchyma is expected to be negligible when translating to the human situation. The amount of microspheres to be administered is below this limit; therefore little to no long term toxicity is expected when the radioactive holmium has decayed. Moreover, ICP MS measurements showed that there was little release of holmium from the injection site; 0.12% of the injected dose was detected in bone.

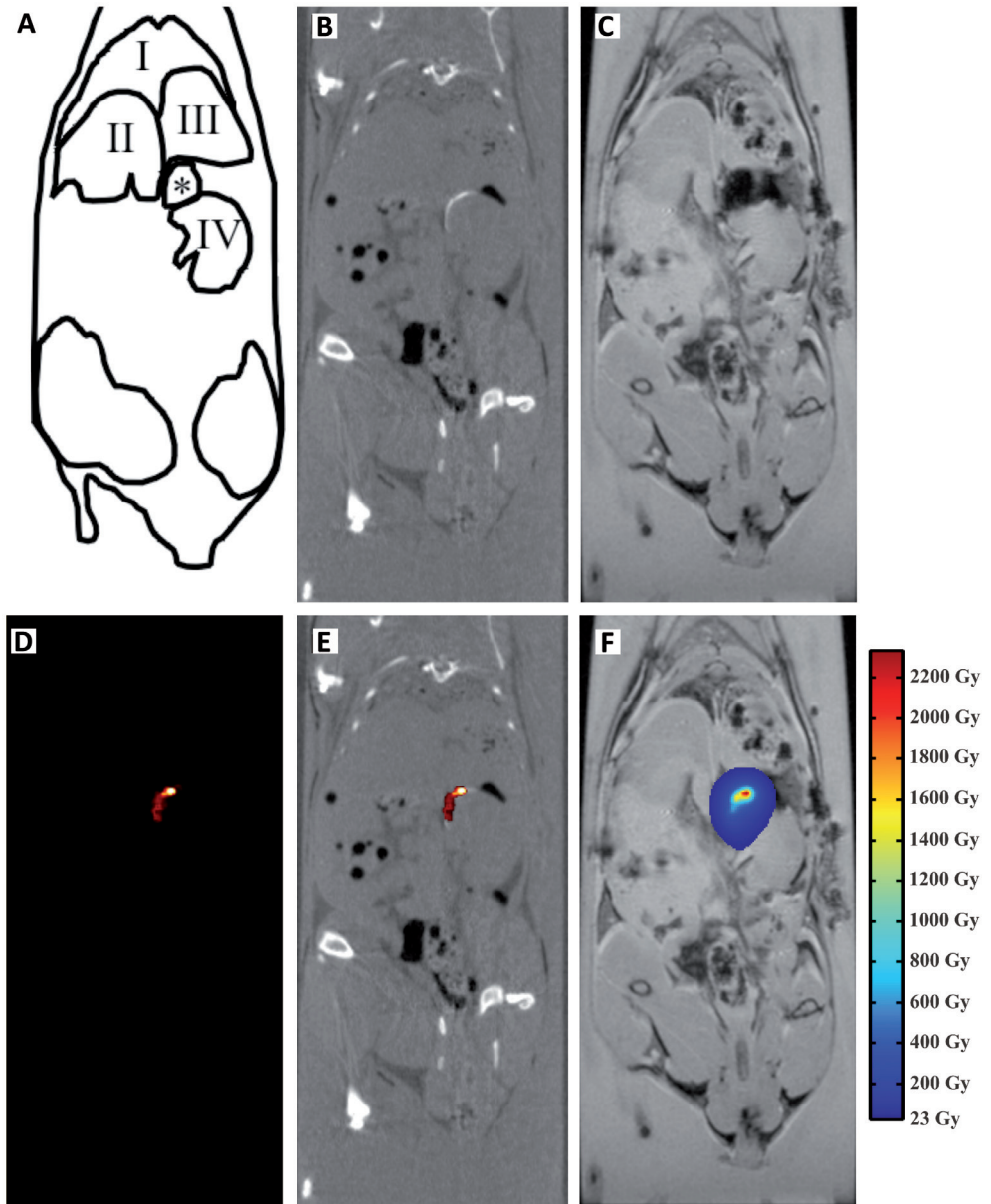


**Figure 3.** An example of the multimodality imaging characteristics of intratumorally administered HoAcAcMS. Images are acquired immediately following administration of the microspheres. **(A)** A schematic representation of the mouse anatomy (I: Lungs; II: Liver; III: Stomach; IV: Kidney; \*: Artefact caused by holmium on MRI image) **(B)** CT image, depicting the HoAcAcMS in the kidney area as white dots. **(C)** MR image showing the soft tissue detail of this imaging modality and the deposition of HoAcAcMS as a dark spot. **(D)** SPECT image, showing a selective visualisation of radioactive microspheres in the kidney area. **(E)** Fused SPECT and CT image. **(F)** MRI image fused with the dose map, showing the absorbed dose distribution in the kidney area.

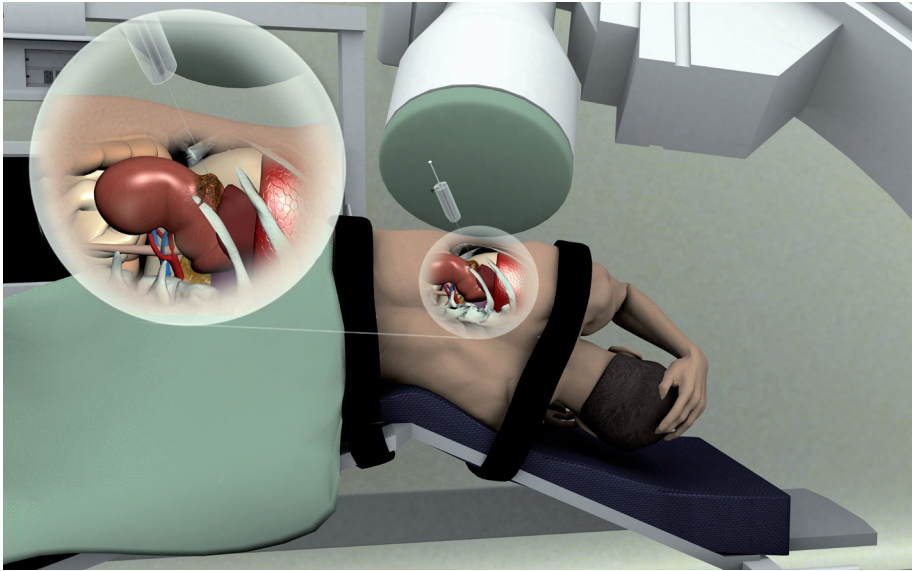


**Figure 4.** Schematic drawing of a percutaneous approach to  $^{166}\text{HoAcAcMS}$  application. The  $^{166}\text{HoAcAcMS}$  are administered intratumorally by a shielded syringe under real-time CT guidance.

In addition to the efficacy, the multimodality imaging characteristics of  $^{166}\text{HoAcAcMS}$  were investigated. Deposits of approximately 270 micrograms of  $\text{HoAcAcMS}$  were clearly visible on SPECT, CT and MRI images (Fig. 3 B-D). The  $^{166}\text{HoAcAcMS}$  can therefore be regarded as a true multimodality imaging agent. The specificity of SPECT was superior to that of both CT and MRI. In this study CT imaging was used to determine the distribution of  $^{166}\text{HoAcAcMS}$ , since the low amounts of activity administered result in a long acquisition time with SPECT (6 minutes for CT versus 45 minutes SPECT). In patients the amount of activity will be 20- to 100-fold higher, allowing for faster SPECT image acquisition.

The use of radioactive microspheres in the treatment of an experimental tumor model was successful, and results are very promising. Although the orthotopic mouse model resembles the human situation in many aspects, a number of points need to be addressed before intratumoral administration of  $^{166}\text{HoAcAcMS}$  can be routinely applied in humans. First of all, toxicity studies should be performed in humans. Radioactive holmium poly(L-lactic acid) particles of 20-50  $\mu\text{m}$  for intra-arterial application have been evaluated for biodistribution, efficacy and toxicity in rats, rabbits and pigs, and have shown their stability and safety (29, 30), and a phase I study in patients with liver metastases has recently been initiated (31). Similar toxicity experiments will need to be performed for the  $^{166}\text{HoAcAcMS}$  described here prior to initiating a clinical trial.

The tumors in study ranged from 4 to 8 mm at the time of treatment, which is the maximum penetration range of the beta particles in tissue. Consequently, the ionizing radiation reached the complete tumor. In patients eligible for nephron

sparing surgery, tumors are approximately 2 to 4 cm at the time of diagnosis. It is expected that 4 to 8 injections with  $^{166}\text{HoAcAcMS}$  would be required to effectively eradicate tumors from 2 – 4 cm. This is feasible since more conventional treatments including RFA need multiple RFA probes to achieve complete tumor kill (14). Using multiple deposits of  $^{166}\text{HoAcAcMS}$ , an accurate delivery of the dose can be given independent of shape and size of the tumor.

A technical problem we encountered was the delivery of approximately 50% of the intended dose (5 MBq), due to adsorption of radioactive microspheres onto the syringe wall and due to the small volume that was injected. When treating patients, the volume to be administered is higher resulting in a smaller difference between aimed and actual administered dose. However, the adsorption of microspheres onto the syringe wall needs to be further investigated to obtain a delivery device that allows for safe and reproducible administration of microspheres.

In this study, the  $^{166}\text{HoAcAcMS}$  were administered at laparotomy. In patients, the procedure can be performed laparoscopically or preferably percutaneously under CT or ultrasound guidance. Image guidance will ensure proper administration and prevent the inadvertent delivery of radioactive microspheres to blood vessels. An illustration of the percutaneous approach under CT guidance is shown in Figure 4. This minimally invasive approach would initially make the administration of  $^{166}\text{HoAcAcMS}$  particularly suitable for treatment of patients with comorbidities or multiple tumors, situations frequently encountered in kidney cancer patients.

In conclusion, the present study demonstrates that intratumoral administration of  $^{166}\text{HoAcAcMS}$  is a promising novel minimally invasive treatment of small renal masses. The tumor growth was arrested and no holmium-related toxicity was observed. Importantly, multimodality imaging including CT, SPECT and MRI of small amounts of  $^{166}\text{HoAcAcMS}$  was feasible. This will lead to an improved therapy evaluation and follow-up and provides a fundamental advantage over current therapies.

### Acknowledgements

The authors would like to thank M.J.J. Koster-Ammerlaan for the neutron irradiations, R. de Roos for preparing the microsphere suspensions, L. Hubens for technical assistance, Prof. dr. D.R.A. Uges and J. IJmker for ICP MS measurements, R.M. Ramakers for his help with the U-CT and U-SPECT image acquisition and R. Giles for critically reading the manuscript. Financial support from the Dutch technology foundation STW, under grant 06069 is gratefully acknowledged.

## References

1. D.M. Parkin, F. Bray, J. Ferlay, and P. Pisani. Global cancer statistics, 2002, *Ca Cancer J Clin.* 55:74-108 (2005).
2. L.G. Luciani, R. Cestari, and C. Tallarigo. Incidental renal cell carcinoma-age and stage characterization and clinical implications: study of 1092 patients (1982-1997), *Urology.* 56:58-62 (2000).
3. M. Kato, T. Suzuki, Y. Suzuki, Y. Terasawa, H. Sasano, and Y. Arai. Natural history of small renal cell carcinoma: evaluation of growth rate, histological grade, cell proliferation and apoptosis, *J Urol.* 172:863-866 (2004).
4. J.J. Patard, A. Rodriguez, N. Rioux-Leclercq, F. Guille, and B. Lobel. Prognostic significance of the mode of detection in renal tumours, *BJU Int.* 90:358-363 (2002).
5. K.H. Tsui, O. Shvarts, R.B. Smith, R. Figlin, J.B. de Kernion, and A. Belldegrun. Renal cell carcinoma: prognostic significance of incidentally detected tumors, *J Urol.* 163:426-430 (2000).
6. S.N. Chawla, P.L. Crispin, A.L. Hanlon, R.E. Greenberg, D.Y. Chen, and R.G. Uzzo. The natural history of observed enhancing renal masses: meta-analysis and review of the world literature, *J Urol.* 175:425-431 (2006).
7. T. Klatté, J.J. Patard, M.M. de, K. Bensalah, G. Verhoest, T.A. de la, C.C. Abbou, E.P. Allhoff, G. Carrieri, S.B. Riggs, F.F. Kabbinafar, A.S. Belldegrun, and A.J. Pantuck. Tumor size does not predict risk of metastatic disease or prognosis of small renal cell carcinomas, *J Urol.* 179:1719-1726 (2008).
8. R.J. Motzer, T.E. Hutson, P. Tomczak, M.D. Michaelson, R.M. Bukowski, S. Oudard, S. Negrier, C. Szczylik, R. Pili, G.A. Bjarnason, X. Garcia-del-Muro, J.A. Sosman, E. Solska, G. Wilding, J.A. Thompson, S.T. Kim, I. Chen, X. Huang, and R.A. Figlin. Overall survival and updated results for sunitinib compared with interferon alfa in patients with metastatic renal cell carcinoma, *J Clin Oncol.* 27:3584-3590 (2009).
9. B. Ljungberg, D.C. Hanbury, M.A. Kuczyk, A.S. Merseburger, P.F. Mulders, J.J. Patard, and I.C. Sinescu. Renal cell carcinoma guideline, *Eur Urol.* 51:1502-1510 (2007).
10. S.M. Lucas, J.M. Stern, M. Adibi, I.S. Zeltser, J.A. Cadeddu, and G.V. Raj. Renal function outcomes in patients treated for renal masses smaller than 4 cm by ablative and extirpative techniques, *J Urol.* 179:75-79 (2008).
11. I.S. Gill, M. Aron, D.A. Gervais, and M.A. Jewett. Clinical practice. Small renal mass, *N Engl J Med.* 362:624-634 (2010).
12. D.A. Kunkle, B.L. Egleston, and R.G. Uzzo. Excise, ablate or observe: the small renal mass dilemma--a meta-analysis and review, *J Urol.* 179:1227-1233 (2008).
13. D.A. Kunkle and R.G. Uzzo. Cryoablation or radiofrequency ablation of the small renal mass : a meta-analysis, *Cancer.* 113:2671-2680 (2008).
14. D.A. Gervais, F.J. McGovern, R.S. Arellano, W.S. McDougal, and P.R. Mueller. Radiofrequency ablation of renal cell carcinoma: part 1, Indications, results, and role in patient management over a 6-year period and ablation of 100 tumors, *AJR Am J Roentgenol.* 185:64-71 (2005).
15. R.J. Zagoria, M.A. Traver, D.M. Werle, M. Perini, S. Hayasaka, and P.E. Clark. Oncologic efficacy of CT-guided percutaneous radiofrequency ablation of renal cell carcinomas, *AJR Am J Roentgenol.* 189:429-436 (2007).
16. W. Bult, P.R. Seevinck, G.C. Krijger, T. Visser, L.M. Kroon-Batenburg, C.J. Bakker, W.E. Hennink, A.D. van het Schip, and J.F.W. Nijsen. Microspheres with ultrahigh holmium content for radioablation of malignancies, *Pharm Res.* 26:1371-1378 (2009).
17. J.F.W. Nijsen, B.A. Zonnenberg, J.R. Woittiez, D.W. Rook, I.A. Swildens-van Woudenberg, P.P. van Rijk, and A.D. van het Schip. Holmium-166 poly lactic acid microspheres applicable for intra-arterial radionuclide therapy of hepatic malignancies: effects of preparation and neutron activation techniques, *Eur J Nucl Med.* 26:699-704 (1999).
18. P.R. Seevinck, J.H. Seppenwoolde, T.C. de Wit, J.F.W. Nijsen, F.J. Beekman, A.D. van het Schip, and C.J. Bakker. Factors affecting the sensitivity and detection limits of MRI, CT, and SPECT for multimodal diagnostic and therapeutic agents, *Anticancer Agents Med Chem.* 7:317-334 (2007).
19. F. van der Have, B. Vastenhouw, R.M. Ramakers, W. Branderhorst, J.O. Krah, C. Ji, S.G. Staelens, and F.J. Beekman. U-SPECT-II: An Ultra-High-Resolution Device for Molecular Small-Animal Imaging, *J Nucl Med.* 50:599-605 (2009).

20. W. Branderhorst, B. Vastenhouw, and F.J. Beekman. Pixel-based subsets for rapid multi-pinhole SPECT reconstruction, *Phys Med Biol.* 55:2023-2034 (2010).
21. F. van der Have, B. Vastenhouw, M. Rentmeester, and F.J. Beekman. System calibration and statistical image reconstruction for ultra-high resolution stationary pinhole SPECT, *Ieee Transactions on Medical Imaging.* 27:960-971 (2008).
22. W.E. Bolch, L.G. Bouchet, J.S. Robertson, B.W. Wessels, J.A. Siegel, R.W. Howell, A.K. Erdi, B. Aydogan, S. Costes, E.E. Watson, A.B. Brill, N.D. Charkes, D.R. Fisher, M.T. Hays, and S.R. Thomas. MIRD pamphlet No. 17: the dosimetry of nonuniform activity distributions--radionuclide S values at the voxel level. Medical Internal Radiation Dose Committee, *J Nucl Med.* 40:11S-36S (1999).
23. J.S.M. Hendricks, L.S. Waters, T.L. Roberts, H.W. Egdorf, J.P. Finch, H.R. Trellue, E.J. Pitcher, D.R. Mayo, M.T. Swinhoe, S.J. Tobin, and J.W. Durkee. MCNP Extension, Version 2.5.0. LA-UR-05-2675. 2005. Los Alamos: Los Alamos National Laboratory Report.
24. P.W. Durbin. Metabolic characteristics within a chemical family, *Health Phys.* 2:225-238 (1960).
25. T.C. de Wit, J. Xiao, J.F. Nijsen, A.D. van het Schip, S.G. Staelens, P.P. van Rijk, and F.J. Beekman. Hybrid scatter correction applied to quantitative holmium-166 SPECT, *Phys Med Biol.* 51:4773-4787 (2006).
26. Y. D'Asseler. Advances in SPECT imaging with respect to radionuclide therapy, *Q J Nucl Med Mol Imaging.* 53:343-347 (2009).
27. C. Vanhove, M. Defrise, A. Bossuyt, and T. Lahoutte. Improved quantification in single-pinhole and multiple-pinhole SPECT using micro-CT information, *Eur J Nucl Med Mol Imaging.* 36:1049-1063 (2009).
28. J. O'Donoghue. Relevance of external beam dose-response relationships to kidney toxicity associated with radionuclide therapy, *Cancer Biother Radiopharm.* 19:378-387 (2004).
29. M.A.D. Vente, J.F.W. Nijsen, T.C. de Wit, J.H. Seppenwoolde, G.C. Krijger, P.R. Seevinck, A. Huisman, B.A. Zonnenberg, T.S.G.A.M. Van den Ingh, and A.D. van het Schip. Clinical effects of transcatheter hepatic arterial embolization with holmium-166 poly(L-lactic acid) microspheres in healthy pigs, *Eur J Nucl Med Mol Imaging.* 35:1259-1271 (2008).
30. S.W. Zielhuis, J.F.W. Nijsen, J.H. Seppenwoolde, C.J.G. Bakker, G.C. Krijger, H.F. Dullens, B.A. Zonnenberg, P.P. van Rijk, W.E. Hennink, and A.D. van het Schip. Long-term toxicity of holmium-loaded poly(L-lactic acid) microspheres in rats, *Biomaterials.* 28:4591-4599 (2007).
31. M.L. Smits, J.F.W. Nijsen, M.A. van den Bosch, M.G. Lam, M.A.D. Vente, J.E. Huijbregts, A.D. van het Schip, M. Elschot, W. Bult, H.W. de Jong, P.C. Meulenhoff, and B.A. Zonnenberg. Holmium-166 radioembolization for the treatment of patients with liver metastases: design of the phase I HEPAR trial, *J Exp Clin Cancer Res.* 29:70 (2010).







## Chapter 7

# Holmium Nanoparticles: preparation and *in vitro* characterization of a new device for Radioablation of Solid Malignancies

W. Bult, R. Varkevisser, F. Soulimani, P.R. Seevinck, H. de Leeuw,  
C.J.G. Bakker, P.R. Luijten, A.D. van het Schip, W.E. Hennink, J.F.W. Nijsen

## Abstract

**Purpose:** The present study introduces the preparation and *in vitro* characterization of a nanoparticle device comprising holmium acetylacetonate for radioablation of unresectable solid malignancies.

**Methods:** Holmium acetylacetonate nanoparticles (HoAcAcNP) were prepared by dissolving holmium acetylacetonate in chloroform, followed by emulsification in an aqueous solution of a surfactant and evaporation of the solvent. The diameter, surface morphology, holmium content, and zeta potential were measured, and thermal behavior of the resulting particles was investigated. The stability of the particles was tested in HEPES buffer. The  $r_2^*$  relaxivity of protons and mass attenuation coefficient of the nanoparticles were determined. The particle diameter and surface morphology were studied after neutron activation.

**Results:** Spherical particles with a smooth surface and diameter of  $78 \pm 10$  nm were obtained, and the particles were stable in buffer. Neutron irradiation did not damage the particles, and adequate amounts of activity were produced for nuclear imaging and radioablation of malignancies through intratumoral injections.

**Conclusions:** The present study demonstrates that HoAcAcNP were prepared using a solvent evaporation process. The particle diameter can easily be adapted and can be optimized for specific therapeutic applications and tumor types.

**Keywords:** holmium, nanoparticles, characterization, ablation, tumor

## Introduction

Solid tumors represent the majority of all diagnosed cancer cases in 2009, accounting for more than 1.3 million new cases in the USA and approximately 90% of the cancer related deaths (1). Treatment options of solid tumors with a limited number of metastases include surgical resection, external beam radiotherapy, chemotherapy, and locoregional ablation. Surgery is the preferred treatment option, since this can be regarded as a curative treatment (2). For patients not amenable for surgical resection, external beam radiotherapy is often used curatively. However, due to radiation sensitivity of the adjacent tissue or motion artifacts, not all tumors can be considered for this therapy. In most cases, chemotherapy is applied as palliative treatment. Percutaneous locoregional thermoablative techniques (e.g. radiofrequency ablation and high intensity focused ultrasound) are increasingly applied with promising results in a number of different tumor types, including tumors in the liver, lungs, and kidneys (2, 3). One of the drawbacks associated with these thermoablative therapies is the transport of heat from the tumors by blood vessels, leading to incomplete tumor eradication (3).

The intratumoral administration of beta-emitting radionuclides is an alternative to overcome the drawbacks associated with thermoablative techniques, whilst retaining the specificity of local ablation. The intratumoral administration of high energy beta emitting microspheres has been successfully tested in patients suffering from liver tumors. Yttrium-90 loaded glass microspheres showed a significant tumor response in 24 of 27 patients (4) whereas phosphorous-32 containing nanocolloids (5) showed a significant tumor response in 12 of 17 patients. However, direct visualization of beta particles with a gamma camera is not possible, making these isotopes unsuitable for accurate dosimetric calculations. These drawbacks can be overcome by intratumoral administration of combined beta and gamma emitters. Holmium-166 ( $^{166}\text{Ho}$ ) is a very attractive candidate, since this radionuclide emits gamma rays in addition to high-energy beta particles, allowing for both nuclear imaging and radioablation, respectively. Moreover, holmium can be visualized by CT and MRI due to its high attenuation coefficient and paramagnetic properties (6). The intratumoral injection of  $^{166}\text{Ho}$  nitrate ( $^{166}\text{Ho}(\text{NO}_3)_3$ ) has shown promising results in a rat model of malignant melanoma. A single injection of holmium nitrate distributed throughout the tumor, leading to a significant tumor size reduction (7). A clinically applied  $^{166}\text{Ho}(\text{NO}_3)_3$  loaded device for intratumoral injections is  $^{166}\text{Ho}(\text{NO}_3)_3$  labelled chitosan (8). Response rates were high in patients with hepatocellular carcinoma (31/40), but due to leakage of  $^{166}\text{Ho}$  to the systemic circulation in more than 25% of patients (11/40) hematopoietic suppression was observed. Microspheres with an ultra high holmium content for intratumoral administration were developed to overcome these side effects (9) and were successfully evaluated in a murine renal cell carcinoma model (10). Tumor growth was arrested, and no holmium was observed outside the tumor on SPECT, CT and MRI. Although the treatment showed promising results, only half of the intended dose was administered, due to premature settling of particles in the syringe and the formation of aggregates. After administration the microspheres remained at the site of injection due to their size. The aim of this study is to develop and characterize a holmium containing device

that takes advantage of the favorable properties of micro-sized particles, and circumvents their aforementioned downsides. In this paper we present the development and characterization of nano-sized holmium acetylacetonate particles (HoAcAcNP) as a potential radioablation device for solid malignancies.

## Materials and Methods

All chemicals were commercially available and used as obtained. Acetylacetone, 2,4-pentanedione (AcAc; >99.9%), chloroform (HPLC-grade), didodecyldimethylammonium bromide (DMAB; >98%), 4-(2-Hydroxyethyl)piperazine-1-ethanesulfonic acid (HEPES; >99%), polyvinyl alcohol (PVA, average MW 30,000–70,000) and sodium hydroxide (NaOH; 99%) were purchased from Sigma Aldrich (Steinheim, Germany). Seakem LE Agarose was purchased from Lonza (Basel, Switzerland). Holmium (III) chloride hexahydrate ( $\text{HoCl}_3 \cdot 6\text{H}_2\text{O}$ ; 99.95%) was purchased from Metall Rare Earth Ltd. (Shenzhen, China).

### Particle preparation

Holmium acetylacetonate was prepared as described earlier (11). HoAcAcNP were prepared by solvent evaporation after emulsification. HoAcAc crystals were dissolved in chloroform (5.5% (w/w)), and subsequently recrystallized by rapid evaporation of the chloroform under a continuous flow of nitrogen. The recrystallized HoAcAc was dissolved in chloroform (5.5%, (w/w)) which was emulsified in an aqueous phase containing a stabilizer (PVA or DMAB, both 2% w/v) using an Ultra-turrax homogenizer (Ultra-turrax T25 basic, IKA, Staufen, Germany) at a stirrer speed of 9,500; 13,500; 20,500 rpm or 24,000 rpm for 5 minutes. After emulsification, the organic solvent was evaporated using a rotator evaporator and the nanoparticles were collected by centrifugation (25,000 rpm for 25 minutes at 4°C) and washed 6 times with water. The particles were lyophilized overnight using a Christ “Alpha 1-2” freeze dryer.

### Particle characterization

Nanoparticle diameter was measured by dynamic light scattering (DLS) using a Malvern ALV CGS-3 (Malvern Instruments, Malvern, UK) equipped with a JDS Uniphase 22mW He-Ne laser operating at 632.8 nm at a 90° angle. Autocorrelation functions were analyzed by the cumulants method by fitting a single exponential to the correlation function to obtain the mean size and the PDI, using the ALV-60 × 0 software V.3.X provided by Malvern. DLS results were recorded as the number weighted mean diameter and Z-average diameter, both in nm.

Scanning electron microscopy (SEM) was performed on samples that were mounted on an aluminum stub, and coated with a 6 nm layer of platinum. SEM micrographs were collected on a FEI FEG-SEM XL30 (FEI Company, Eindhoven, The Netherlands), at a voltage of 5 kV.

Elemental analysis of carbon, hydrogen, oxygen, bromine and holmium of HoAcAcNP, HoAcAc crystals, and recrystallized HoAcAc after evaporation of chloroform was performed by H. Kolbe, Mülheim an der Ruhr, Germany.

Fourier Transform Infrared Spectroscopy of freeze dried HoAcAcNP, holmium acetylacetonate crystals, and recrystallized crystals was performed using a Perkin Elmer SpectrumOne FT-IR spectrometer (PerkinElmer, Groningen, The Netherlands). The spectra were recorded using KBr pellets, by accumulating 256 scans per spectrum. A DSC Q1000 (TA instruments Inc., Etten-Leur, The Netherlands) was used for performing modulated differential scanning calorimetry. Scans were recorded from 25 – 220°C at a heating rate of 2°C min<sup>-1</sup>, and a modulation temperature of 1°C min<sup>-1</sup>.

Zeta potentials of the HoAcAcNP were measured using a Zetasizer Nano (Malvern Instruments, Malvern, UK). Samples of lyophilized nanoparticles were suspended in 10 mM HEPES at pH 7.4 at a concentration of 5 mg mL<sup>-1</sup> and sonicated for 10 min, thereafter the zeta potential was measured. Reported values are the mean of 3 measurements.

The stability of the HoAcAcNP prepared using DMAB and PVA was studied by dispersing them in a HEPES buffer at pH 7.4 (10 mM). At different time points (t = 0, 1, 2, 4, 8, 24, 48 and 72 hours), the particle diameter was measured using DLS at 25°C, as described before. The release of holmium from the HoAcAcNP was determined by transferring one mL of a 50 mg mL<sup>-1</sup> suspension of HoAcAcNP (either prepared in PVA or DMAB) in 10 mM HEPES (pH 7.4) to a Slide-a-Lyzer Dialysis Cassette (Thermo Scientific, Etten-Leur, The Netherlands) with a 10,000 MWCO membrane. All release samples were prepared in triplicate. The cassettes were dialyzed against 500 mL HEPES buffer (10 mM, pH 7.4). At different timepoints (t = 0, 1, 2, 4, 8, 24, 48 and 72 hours), one mL of sample was taken. Four mL HNO<sub>3</sub> 5% (v/v) was added and the holmium content of the resulting solutions was measured using inductively coupled plasma optical emission spectroscopy (ICP OES). Samples were measured at three different wavelengths (339.898, 345.600 and 347.426 nm) in an Optima 4300 CV (PerkinElmer; Norwalk, USA).

### Multimodality imaging

To determine the sensitivity of MRI and X-ray CT for the HoAcAcNP, phantom experiments were carried out on MRI and CT. The phantom used to determine MRI and CT sensitivity consisted of agarose (2% (w/w)) gel samples in which HoAcAcNP were homogeneously dispersed (loadings ranged from 0 to 8 mg nanoparticles per mL agarose) in glass tubes (diameter 10 mm, length 75 mm). Sample tubes were positioned parallel to the B<sub>0</sub> field in the MR scanner. MR imaging was performed using a 1.5 and a 3 Tesla clinical MR scanner (Intera, Achieva, respectively, Philips Healthcare, Best, The Netherlands). The sensitivity of gradient echo MRI for a paramagnetic contrast agent can be expressed in terms of its r<sub>2</sub>\* relaxivity (in [sec<sup>-1</sup> mg<sup>-1</sup> mL]) which represents the change in the effective proton transverse relaxation rate (R<sub>2</sub>\* in [sec<sup>-1</sup>]) per unit concentration (in mg mL<sup>-1</sup>). The R<sub>2</sub>\* relaxation rate characterizes the rate of monoexponential signal decay due to transverse relaxation. To determine the r<sub>2</sub>\* relaxivity of HoAcAcNP, the R<sub>2</sub>\* relaxation rates of the HoAcAcNP dilution series were determined with a multiple gradient echo MR sequence, acquiring 15 echos with an echo spacing of 1.39 msec, a repetition time of 500 msec, a field of view (FOV) of 128x128x20 mm, a voxel size of 1x1x5 mm,

two signal averages and a 60° flip angle. Linear regression of the  $R_2^*$  values and the HoAcAc NP concentrations provided the  $r_2^*$  relaxivity (6). For qualitative purposes, a second agarose phantom was constructed, with depots of HoAcAcNP in decreasing concentrations by serial dilution (ranging from 100  $\mu\text{g}$  to 1.5  $\mu\text{g}$  nanoparticles). To obtain cavities of a reproducible size in this gel, 2 mL pipette tips were positioned in the gel prior to setting of the gel. After setting of the gel the pipette tips were removed and 50  $\mu\text{L}$  of a homogeneous HoAcAcNP suspension was pipetted into the cavities thus obtained. The particles were left to settle, followed by filling with agarose gel. This phantom was positioned coaxially in a 3 Tesla clinical MR scanner, and used to determine the minimal amount of HoAcAcNP that can be visualized using MR imaging. Imaging parameters were similar for this phantom setup, apart from the 15° flip angle.

Quantitative X-ray CT imaging was performed on a clinical 64 slice CT scanner (Brilliance, Philips Medical Systems, Best, The Netherlands). The sample tubes were positioned co-axially to the main axis of the scanner. Using the methods described by Seevinck *et al.*, a linear regression curve was constructed to determine the sensitivity of X-ray CT for HoAcAcNP (6).

Neutron irradiations were performed in the pneumatic rabbit system operational in a nuclear research reactor (Department of Radiation, Radionuclides and Reactors, Delft University of Technology, Delft, The Netherlands) (12). Approximately 50 mg HoAcAcNP was accurately weighed and transferred into a high-density polyethylene vial (Posthumus plastics, Beverwijk, the Netherlands) and irradiated for 30 or 60 minutes in a facility with a thermal neutron flux of  $5 \times 10^{12} \text{ n cm}^{-2} \text{ s}^{-1}$ . After neutron irradiation the radioactivity was measured. To ensure safe handling of the nanoparticles for SEM image acquisition and DLS measurements, the  $^{166}\text{HoAcAcNP}$  were left to decay for one month.

## Results and Discussion

HoAcAcNP were prepared using solvent evaporation technology. In short, recrystallized HoAcAc was dissolved in chloroform, and the resulting solution was emulsified in an aqueous solution with 2% (w/w) PVA followed by evaporation of the solvent. Particles with a number weighted mean diameter ranging from  $1708 \pm 276$  to  $799 \pm 147$  nm were obtained when increasing the stirrer speed from 9500 to 24000 rpm (see Table I and Fig 1). The yield for all batches was  $51 \pm 2\%$ . Scanning electron microscopy (SEM) revealed spherical particles with a rugged surface (Fig. 1 A), with a similar particle diameter as the number weighted particle diameter observed with dynamic light scattering (DLS). A larger z-average particle diameter was measured owing to the presence of a few large particles (13) (Table I).

To decrease the particle diameter, the cationic surfactant didodecyldimethylammonium bromide (DMAB) was used as an emulsifier (14). With increasing stirrer speed from 9500 to 24000 rpm, the number weighted mean particle diameter substantially decreased from  $1168 \pm 252$  to  $78 \pm 10$  nm (Table I). The yield for all batches was  $47 \pm 5\%$ . Spherical particles with a smooth surface were observed with SEM (Fig. 1 B). The smaller diameter of the particles using DMAB instead of PVA can

**Table I.** Effects of preparation variables on the particle size and polydispersity index ( $n=3$ ) of HoAcAcNP.

Stirrer speed (rpm)	Emulsifier	Particle diameter Number weighted mean <sup>‡</sup>	Particle diameter Z-average <sup>‡</sup>	PDI*
9500	2% PVA	1708 ± 276	2143 ± 687	0.26
13500	2% PVA	1153 ± 259	1685 ± 29	0.28
20500	2% PVA	1002 ± 161	1414 ± 128	0.24
24000	2% PVA	799 ± 147	1175 ± 149	0.25
9500	2% DMAB	1168 ± 252	1677 ± 789	0.25
13500	2% DMAB	653 ± 166	997 ± 509	0.27
20500	2% DMAB	311 ± 123	659 ± 68	0.35
24000	2% DMAB	78 ± 10	462 ± 265	0.21

<sup>‡</sup> results displayed as particle diameter ± standard deviation in nm

\* PDI = Polydispersity Index; a measure to determine the heterogeneity of the particle size. 1 being completely heterodisperse, 0 being completely monodisperse.

be explained by the lower critical micelle concentration for DMAB compared to PVA (14). Consequently, DMAB more readily stabilizes chloroform droplets in emulsion, promoting the formation of small chloroform droplets. Particle characterization was performed on the particles with a mean diameter of around 78 nm prepared with DMAB at a stirrer speed of 24,000 rpm. When PVA particles were used as a comparison, the particles prepared at 24,000 rpm in PVA were used.

Table II shows that the holmium content of the HoAcAcNP, as determined by elemental analysis, was 43.7% (*w/w*), which is higher than the holmium content of the HoAcAc crystals (31.9% (*w/w*)) used as the starting material. An increase in holmium content was also observed in a previous study on the preparation of HoAcAc microspheres (HoAcAcMS), which was attributed to a loss of acetylacetonate during reorganization of acetylacetonate around Ho(III) ions during the gradual evaporation of the solvent (9). Interestingly, HoAcAc crystals also showed an increase in holmium content from 31.9% (*w/w*) to 38.3% (*w/w*) after dissolution of the HoAcAc crystals in chloroform followed by recrystallization. The holmium content in the HoAcAcNP was further increased to 43.7%. The bromine content was also determined in the HoAcAcNP prepared in DMAB, to determine the amount of emulsifier present after washing. The amount of bromine present was 0.8% (*w/w*), after washing 6 times with water, which is representative of 0.8% of DMAB. Infrared spectroscopy, elemental analysis and differential scanning calorimetry (DSC) were performed to investigate the HoAcAcNP and the HoAcAc crystals. The infrared spectra of the original HoAcAc crystals, recrystallized HoAcAc and the HoAcAcNP, irrespective of the preparation characteristics, show characteristic peaks for acetylacetonate at 1517 and 1610  $\text{cm}^{-1}$  representing the C=C and the C=O stretching bands of acetylacetonate, respectively

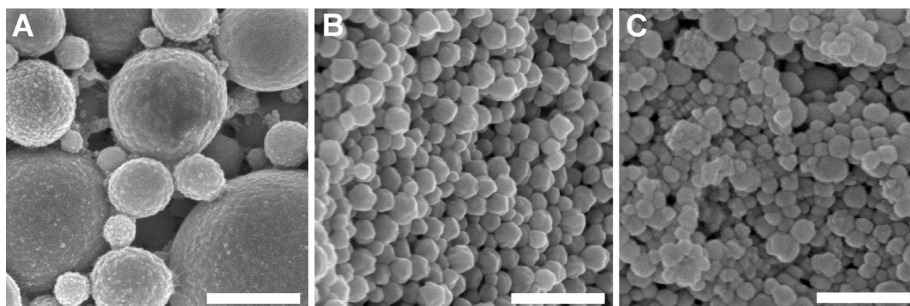


**Figure 1.** Scanning electron micrographs of HoAcAcNP showing the effect of emulsifier on particle diameter and surface **A)** particles prepared using PVA as emulsifier **B)** particles prepared using DMAB as emulsifier. Stirrer speed was 24,000 rpm for both formulations. **C)** particles prepared using DMAB as emulsifier after neutron irradiation (1 h at a neutron flux of  $5 \times 10^{12} \text{ n cm}^{-2} \text{ s}^{-1}$ ). The magnification was 100,000x for all samples, bar represents 500 nm.

(15) (Fig. 2). This is a confirmation that acetylacetonate is present in both the recrystallized HoAcAc and the HoAcAcNP. The presence of small but sharp peaks in the dark grey spectrum (HoAcAc crystals) at around  $3600 \text{ cm}^{-1}$  is an indication that crystal water is present in the HoAcAc crystals (16). These peaks are less pronounced in the black and grey spectrum, indicating that the structure of HoAcAc crystals has changed during particle preparation and water was lost from the complex. The more pronounced peaks in the grey spectrum (HoAcAcNP) around  $2800 - 3000 \text{ cm}^{-1}$  can be explained by the presence of surfactant in the sample. These peaks are characteristic for aliphatic alkyl chains originating from DMAB, the presence of which was determined by elemental analysis.

Based on results from elemental analysis in combination with the finding from IR spectroscopy that all forms contain acetylacetonate, HoAcAc crystals consist of

**Table II.** Elemental analysis of HoAcAc crystals, recrystallized HoAcAc and HoAcAcNP.

Element	HoAcAc crystals ( $\text{HoAcAc}_3 \cdot 3 \text{ H}_2\text{O}$ )		HoAcAc recrystallized ( $\text{Ho}_2\text{AcAc}_5 \cdot 2 \text{ H}_2\text{O}$ )		HoAcAcNP ( $\text{Ho}_2\text{AcAc}_4 \cdot \text{H}_2\text{O}$ )	
	Calculated (%)	Measured <sup>1</sup> (%)	Proposed (%)	Measured (%)	Proposed (%)	Measured (%)
C	34.9	35.6	34.9	34.1	31.5	31.6
H	5.3	5.3	4.6	4.4	4.2	4.4
O	27.9	26.3	22.3	21.8	21.0	19.9
Ho	31.9	32.6	38.3	37.6	43.3	43.7
Br	-	-	-	-	<1%	0.8

<sup>1</sup> Measured values are presented as the mean of duplicate analyses.



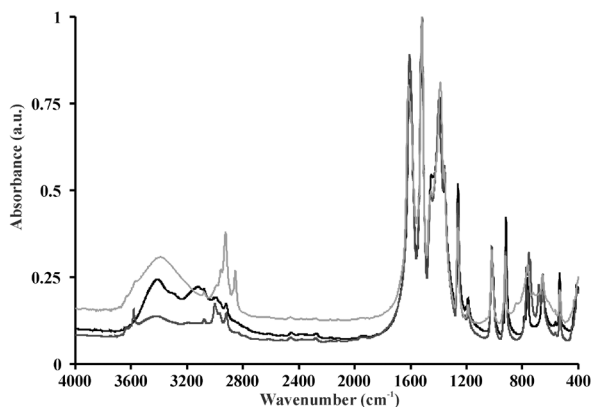


**Figure 2.** IR absorbance spectra of HoAcAc crystals (dark grey), recrystallized HoAcAc (in black) and HoAcAcNP prepared at 24000 rpm in DMAB (in grey). The spectra were normalized to the peak at  $1517\text{ cm}^{-1}$ .

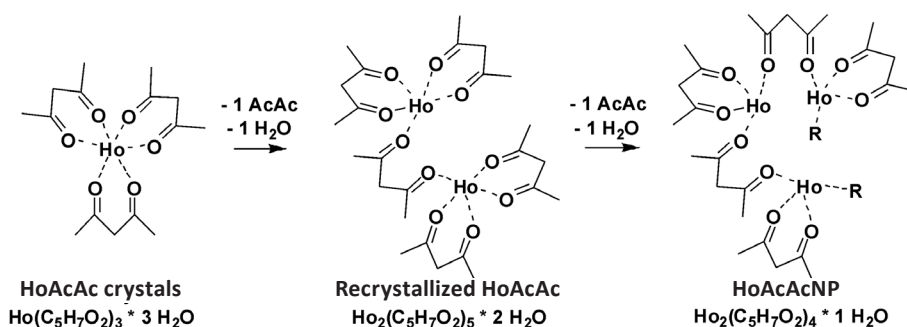


**Figure 3.** Schematic representation of the proposed different forms of HoAcAc complexes. In each subsequent step, acetylacetonate and one water molecule is lost. The remaining acetylacetonate molecules act as bridges between Ho(III) ions. (AcAc and R = acetylacetonate)

**Table III.** Summary of DSC results from HoAcAc crystals, before and after recrystallization, and HoAcAcNP ( $n= 4-6$ )

	Onset $T_{\text{max}}$ ( $^{\circ}\text{C}$ )	$T_{\text{max}}$ ( $^{\circ}\text{C}$ )	$\Delta H$ ( $\text{J g}^{-1}$ )
HoAcAc crystals	$120 \pm 17$	$126 \pm 11$	$113 \pm 12$
HoAcAc recrystallized	$98 \pm 12$	$112 \pm 8$	$43 \pm 9$
	$147 \pm 9$	$154 \pm 7$	$12 \pm 5$
HoAcAcNP	$187 \pm 4$	$198 \pm 3$	$14 \pm 7$

three acetylacetonate ligands and three water molecules complexed with the Ho(III) ion, as reported previously (16). Elemental analysis of recrystallized HoAcAc gives evidence that 2.5 acetylacetonate molecules and one water molecule surround each Ho(III) ion, while in HoAcAcNP each Ho(III) is expected to be surrounded by two acetylacetonate molecules and one water molecule (Fig. 3, Table II).

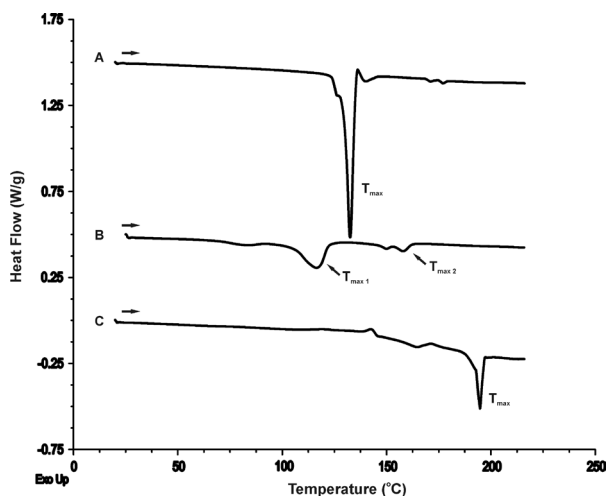


**Figure 4.** mDSC thermograms of (A) HoAcAc crystals, (B) recrystallized HoAcAc and (C) HoAcAcNP.  $T_{\max}$  is the peak maximum of the endotherm.

Differential scanning calorimetry of HoAcAc crystals showed an endotherm at  $126 \pm 11^\circ\text{C}$  (Fig. 4 A, Table III), which can be attributed to loss of water from the complex (15). Interestingly, the thermograms of recrystallized HoAcAc show endotherms at  $126^\circ\text{C}$  and  $156^\circ\text{C}$  (Fig. 4 B, Table III), indicating the presence of a reorganized HoAcAc structure after recrystallization from chloroform (Fig. 3). The HoAcAcNP showed an endotherm at  $198 \pm 3^\circ\text{C}$  (Fig. 4 C, Table III), likely associated with a loss of water. The higher temperature needed to expel one water molecule is an indication that the HoAcAc in the nanoparticles is reorganized in a network-like structure. A schematic representation of the proposed reorganization process is shown in Figure 3. Definite clarification of the structural rearrangement requires extensive further research.

The use of recrystallized HoAcAc was a prerequisite for the formation of nanoparticles. When HoAcAc crystals were used small needle-like structures were formed instead of nanoparticles. In HoAcAc crystals, three acetylacetonate molecules are complexed with one Ho(III) ion. After recrystallization of HoAcAc, the Ho(III) ion loses half an acetylacetonate molecule, resulting in one acetylacetonate molecule that bridges between two Ho(III) ions. When dissolving the recrystallized HoAcAc in chloroform, followed by rapid evaporation of the chloroform, another half acetylacetonate is lost per Ho(III) ion. We expect this to lead to the formation of another acetylacetonate bridge between two Ho(III) ions. The gradual removal of solvent is imperative in this particle preparation method, allowing acetylacetonate to exert a bridging effect between Ho(III) ions (17).

A positive zeta potential of  $26.1 \pm 5.4$  mV was recorded for nanoparticles prepared with the cationic surfactant DMAB. The use of PVA as the stabilizer resulted in particles with a slightly positive zeta potential value of  $3.4 \pm 5.0$  mV. The stability of the particles was investigated by measuring the particle diameter over time. Particles prepared with DMAB as emulsifier did not show aggregation after 72 hours in 10 mM HEPES buffer pH 7.4, at  $25^\circ\text{C}$ . The positive zeta potential

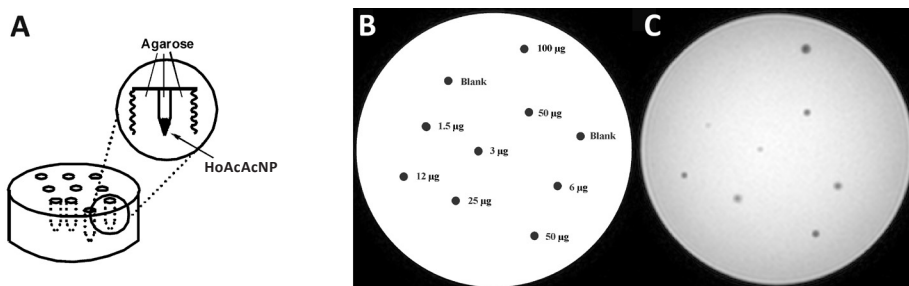


**Figure 5.** Agarose MRI phantom setup for the determination of the minimally visible amount of nanoparticles. **A)** shows how the phantom was constructed, **B)** shows a schematic representation of the phantom layout and the amounts of nanoparticles in  $\mu\text{g}$  **C)** shows the actual image at 3T.

of particles prepared in DMAB creates repulsive forces between the particles, thereby preventing particle aggregation (18). Obviously, the zeta potential of particles prepared in PVA is insufficient to create these repulsive forces, leading to particle aggregation. Additionally, the stability of the HoAcAcNP was investigated by measuring the release of holmium from the particles after suspension for 72 h in 10 mM HEPES buffer pH 7.4 at 25°C. The release of holmium from the nanoparticles prepared in DMAB was  $1.9 \pm 0.1\%$  after 72 hours. The release from the particles prepared in PVA was  $7.6 \pm 4.7\%$  after 72 hours. The particles prepared in DMAB are more stable and thus seem more suitable for intratumoral radioablation. However, mid- and long-term stability experiments in different media (i.e. serum, lactates, citrates) are required prior to *in vivo* efficacy experiments.

The MR imaging characteristics were assessed on clinical 1.5 and 3 Tesla MR systems using agarose phantoms with manganese to mimic the susceptibility of liver tissue (19). The paramagnetic nature of holmium causes an enhanced transverse relaxation rate, which results in signal loss seen as blackening on  $T_2^*$  weighted images (20). The MRI sensitivity of HoAcAcNP is described by the  $r_2^*$ , and was calculated from transverse images using the method described by Seevinck *et al.* (6). The  $r_2^*$  is  $110 \text{ s}^{-1} \text{ mg}^{-1} \text{ mL}$  (1.5 Tesla) and  $295 \text{ s}^{-1} \text{ mg}^{-1} \text{ mL}$  (3 Tesla), which was lower than expected, when compared to HoAcAcMS ( $15 \mu\text{m}$ ;  $r_2^* 264 \text{ s}^{-1} \text{ mg}^{-1} \text{ mL}$  at 1.5 Tesla (9)) with a similar holmium content (45% w/w). This lower  $r_2^*$  is likely caused by the particle size of the HoAcAcNP. The dephasing of spins for the HoAcAcMS of around  $15 \mu\text{m}$  follows a static regimen where field inhomogeneities caused by holmium are dephased before molecular diffusion can average out this signal. In nanoparticle dispersions however, molecular diffusion of protons averages out the local field inhomogeneities, thereby reducing the  $r_2^*$  of HoAcAcNP compared to HoAcAcMS (21, 22).

An MRI phantom setup was used to determine the minimum detectable amount of HoAcAcNP at 3 Tesla using a typical  $T_2^*$  weighted scan technique (Fig. 5). The observed minimum detectable amount was  $1.5 \mu\text{g}$  and equals that of HoAcAcMS (9) which is explained by the deposits in which the HoAcAcNP are packed together in the phantom mimicking larger particles (21, 23).

Holmium is a more potent CT contrast agent than the routinely used iodine-based agents (6). The effect of holmium on CT is related to its mass attenuation coefficient  $\mu$ . The  $\mu$  value was determined by constructing a linear curve as described by Seevinck *et al.* (6). The  $\mu$  value is 16 HU mg<sup>-1</sup> for the HoAcAcNP, which is similar to that of HoAcAcMS (9). This was expected, since the  $\mu$  value is not dependent on the particle size, but only dependent on the holmium concentration in the phantom (6). Neither significant changes in the size distribution nor in particle surface were observed after neutron irradiation of 50 mg HoAcAcNP (1 hour irradiation time and a neutron flux of  $5 \times 10^{12}$  n cm<sup>-2</sup> s<sup>-1</sup> (Fig. 1C)) and resulted in 600 MBq of holmium-166. This activity is sufficient for treatment of a single solitary, inoperable tumor (<3 cm) by intratumoral injection (9). Additionally, the gamma rays emitted by holmium-166 can be visualized by gamma scintigraphy, the results of which can be used for tumor absorbed dose quantification (24).

A limiting factor in intratumoral injection of a microsphere suspension is the aggregation and settling of the microspheres in the syringe prior to administration. In a renal cell carcinoma mouse model this resulted in the administration of only half of the intended dose of HoAcAcMS (10). According to Stokes' law, the sedimentation velocity of a particle in a dispersion medium is proportional to  $d^2$ , which is the particle diameter in centimeter (25). The HoAcAcNP described in the present study have an approximately 200 fold lower diameter compared to the HoAcAcMS, which reduces the sedimentation velocity by a factor 40,000. Also, the positive zeta potential of the HoAcAcNP contributes to prevent aggregation. In this way a suspension of HoAcAcNP prepared in DMAB can be obtained, which seems ideally suited for intratumoral injections. In large tumors multisite injections of micro-sized holmium particles are required to obtain a homogeneous tumor irradiation. In tumors in or near delicate structures only single injections can be administered. One might even speculate that the use of nano-sized particles results in a homogeneous particle distribution throughout the tumor following a single injection, but this is subject of further investigation.

## Conclusion

In conclusion, the present study demonstrates that HoAcAcNP can be prepared using a solvent evaporation process. The particle diameter can easily be adapted and can be optimized for specific therapeutic applications and tumor types. The element holmium is very suitable as a contrast agent, since it is one of the only true multimodality (radio)nuclides, allowing for MR imaging, CT imaging and gamma scintigraphy. Moreover, holmium can be made sufficiently radioactive to exert a therapeutic effect when injected intratumorally.

## Acknowledgements

Financial support by the Dutch Technology Foundation under grant 06069 is gratefully acknowledged. The authors would like to thank miss A.H.L. Lie for help with preparing the particles, dr. W.H. Müller, Mr. C.T.W.M. Schneijdenberg and

Mr. J.D. Meeldijk for their assistance with SEM image acquisition. The valuable discussions with Dr. T. Visser and Dr. M. van de Weert are gratefully acknowledged. Miss M.J.J. Koster-Ammerlaan is acknowledged for her help with the neutron irradiation experiments.

## References

1. A. Jemal, R. Siegel, E. Ward, Y. Hao, J. Xu, and M.J. Thun. Cancer statistics, 2009, *Ca Cancer J Clin.* 59:225-249 (2009).
2. J.E. Kennedy. High-intensity focused ultrasound in the treatment of solid tumours, *Nat Rev Cancer.* 5:321-327 (2005).
3. E. Liapi and J.F. Geschwind. Transcatheter and ablative therapeutic approaches for solid malignancies, *J Clin Oncol.* 25:978-986 (2007).
4. J.H. Tian, B.X. Xu, J.M. Zhang, B.W. Dong, P. Liang, and X.D. Wang. Ultrasound-guided internal radiotherapy using yttrium-90-glass microspheres for liver malignancies, *J Nucl Med.* 37:958-963 (1996).
5. N. Firusian and W. Dempke. An early phase II study of intratumoral P-32 chromic phosphate injection therapy for patients with refractory solid tumors and solitary metastases, *Cancer.* 85:980-987 (1999).
6. P.R. Seevinck, J.H. Seppenwoolde, T.C. de Wit, J.F. Nijsen, F.J. Beekman, A.D. van het Schip, and C.J. Bakker. Factors affecting the sensitivity and detection limits of MRI, CT, and SPECT for multimodal diagnostic and therapeutic agents, *Anticancer Agents Med Chem.* 7:317-334 (2007).
7. J.D. Lee, W.I. Yang, M.G. Lee, Y.H. Ryu, J.H. Park, K.H. Shin, G.E. Kim, C.O. Suh, J.S. Seong, B.H. Han, C.W. Choi, E.H. Kim, K.H. Kim, and K.B. Park. Effective local control of malignant melanoma by intratumoural injection of a beta-emitting radionuclide, *Eur J Nucl Med Mol Imaging.* 29:221-230 (2002).
8. J.K. Kim, K.H. Han, J.T. Lee, Y.H. Paik, S.H. Ahn, J.D. Lee, K.S. Lee, C.Y. Chon, and Y.M. Moon. Long-term clinical outcome of phase IIb clinical trial of percutaneous injection with holmium-166/chitosan complex (Milican) for the treatment of small hepatocellular carcinoma, *Clin Cancer Res.* 12:543-548 (2006).
9. W. Bult, P.R. Seevinck, G.C. Krijger, T. Visser, L.M. Kroon-Batenburg, C.J. Bakker, W.E. Hennink, A.D. van het Schip, and J.F. Nijsen. Microspheres with ultrahigh holmium content for radioablation of malignancies, *Pharm Res.* 26:1371-1378 (2009).
10. W. Bult, S.G.C. Kroeze, M. Elschoot, P.R. Seevinck, F.J. Beekman, P.R. Luijten, W.E. Hennink, A.D. van het Schip, J.L.H.R. Bosch, J.F.W. Nijsen, and J.J.M. Jans. Intratumoral administration of holmium-166 acetylacetonate microspheres as a novel minimally-invasive treatment for small kidney tumors, In preparation.
11. J.F.W. Nijsen, B.A. Zonnenberg, J.R. Woittiez, D.W. Rook, I.A. Swildens-van Woudenberg, P.P. van Rijk, and A.D. van het Schip. Holmium-166 poly lactic acid microspheres applicable for intra-arterial radionuclide therapy of hepatic malignancies: effects of preparation and neutron activation techniques, *Eur J Nucl Med.* 26:699-704 (1999).
12. M.A. Vente, J.F. Nijsen, R.R. de, M.J. van Steenberg, C.N. Kaaijk, M.J. Koster-Ammerlaan, P.F. de Leege, W.E. Hennink, A.D. van het Schip, and G.C. Krijger. Neutron activation of holmium poly(L-lactic acid) microspheres for hepatic arterial radio-embolization: a validation study, *Biomed Microdevices.* 11:763-772 (2009).
13. V. Filipe, A. Hawe, and W. Jiskoot. Critical Evaluation of Nanoparticle Tracking Analysis (NTA) by NanoSight for the Measurement of Nanoparticles and Protein Aggregates, *Pharm Res.* 27:796-810 (2010).
14. H.Y. Kwon, J.Y. Lee, S.W. Choi, Y.S. Jang, and J.H. Kim. Preparation of PLGA nanoparticles containing estrogen by emulsification-diffusion method, *Colloids and Surfaces A-Physicochemical and Engineering Aspects.* 182:123-130 (2001).
15. J.F.W. Nijsen, M.J. van Steenberg, H. Kooijman, H. Talsma, L.M. Kroon-Batenburg, M. van de Weert, P.P. van Rijk, A. De Witte, A.D. van het Schip, and W.E. Hennink. Characterization of poly(L-lactic acid) microspheres loaded with holmium acetylacetonate, *Biomaterials.* 22:3073-3081 (2001).
16. H. Kooijman, F. Nijsen, A.L. Spek, and A.D. van het Schip. Diaquatris(pentane-2,4-dionato-O,O')holmium(III) monohydrate and diaquatris(pentane-2,4-dionato-O,O')holmium(III) 4-hydroxypentan-2-one solvate dihydrate, *Acta Crystallogr C.* 56:156-158 (2000).
17. A.J. Dillen, R.J.A.M. Terode, D.J. Lensveld, J.W. Geus, and K.P. de Jong. Synthesis of supported catalysts by impregnation and drying using aqueous chelated metal complexes, *J Catal.* 216:257-264 (2003).

18. S. Feng and G. Huang. Effects of emulsifiers on the controlled release of paclitaxel (Taxol) from nanospheres of biodegradable polymers, *J Control Release*. 71:53-69 (2001).
19. J.H. Seppenwoolde, J.F.W. Nijsen, L.W. Bartels, S.W. Zielhuis, A.D. van het Schip, and C.J. Bakker. Internal radiation therapy of liver tumors: Qualitative and quantitative magnetic resonance imaging of the biodistribution of holmium-loaded microspheres in animal models, *Magn Reson Med*. 53:76-84 (2004).
20. S. Fossheim, C. Johansson, A.K. Fahlvik, D. Grace, and J. Klaveness. Lanthanide-based susceptibility contrast agents: assessment of the magnetic properties, *Magn Reson Med*. 35:201-206 (1996).
21. P.R. Seevinck, J.H. Seppenwoolde, J.J.M. Zwanenburg, J.F.W. Nijsen, and C.J.G. Bakker. FID Sampling Superior to Spin-Echo Sampling for T-2\*-Based Quantification of Holmium-Loaded Microspheres: Theory and Experiment, *Magnetic Resonance in Medicine*. 60:1466-1476 (2008).
22. K.T. Yung. Empirical models of transverse relaxation for spherical magnetic perturbers, *Magn Reson Imaging*. 21:451-463 (2003).
23. R. Kuhlper, H. Dahnke, L. Matuszewski, T. Persigehl, W.A. von, T. Allkemper, W.L. Heindel, T. Schaeffter, and C. Bremer. R2 and R2\* mapping for sensing cell-bound superparamagnetic nanoparticles: in vitro and murine in vivo testing, *Radiology*. 245:449-457 (2007).
24. T.C. de Wit, J. Xiao, J.F. Nijsen, F.D. van Het Schip, S.G. Staelens, P.P. van Rijk, and F.J. Beekman. Hybrid scatter correction applied to quantitative holmium-166 SPECT, *Phys Med Biol*. 51:4773-4787 (2006).
25. A.N. Martin. Coarse Dispersions. In Martin A.N. (ed), *Physical Pharmacy*, Lea & Febiger, Philadelphia, 1993, pp. 477-511.







## **Chapter 8**

# **Summary and future perspectives**

## Summary

Since the mid-nineties, research has been carried out at the Nuclear Medicine Department of the University Medical Center Utrecht on holmium-166 poly(L-lactic acid) microspheres ( $^{166}\text{HoPLLAMS}$ ). These microspheres are intended as an intra-arterial microdevice for internal radiation therapy of patients with unresectable liver malignancies, and are currently under clinical investigation. For certain localized tumors, such as kidney and brain tumors, direct injection of radioactive microspheres into the tumor is the preferred approach. However, to date no  $^{166}\text{Ho}$  containing device specifically tailored to this application has been proposed yet. The aim of this dissertation is to describe the preparation and characterization of such a holmium-loaded radioablation device, followed by *in vitro* and *in vivo* stability studies, and *in vivo* efficacy experiments. In addition to the development of holmium-loaded microspheres, the preparation of holmium loaded nanoparticles is investigated.

**Chapter 2** reviews the currently available literature on microsphere based radioembolization techniques for treatment of patients with chemorefractory, unresectable liver tumors. These microspheres are administered through a catheter which is selectively placed in the hepatic artery. The predominant arterial blood supply to hepatic malignancies is exploited to achieve a high tumor targeting. The use of yttrium-90 ( $^{90}\text{Y}$ ) labeled glass and resin microspheres for treatment of unresectable liver malignancies has shown very promising results. Almost 90% of patients show a response (stable disease, partial remission, or complete remission) to  $^{90}\text{Y}$  radioembolization of hepatic malignancies. The selective administration procedure is laborious, and physicians are forced to use surrogate particles to predict the biodistribution, due to the lack of quantitative imaging possibilities associated with the use of the pure beta emitter  $^{90}\text{Y}$ . This can be overcome by using a combined beta and gamma emitter, like rhenium-186, rhenium-188 or holmium-166.  $^{166}\text{HoPLLAMS}$  were proposed as a further improvement of this radioembolization technique, and, in preclinical studies, this microdevice's stability, safety and efficacy were extensively investigated. Holmium is ideally suited for radioembolization, since it can be visualized *in vivo* using both nuclear imaging, X-ray computed tomography (CT) and magnetic resonance imaging (MRI). Currently, these  $^{166}\text{HoPLLAMS}$  are under clinical evaluation in patients with chemorefractory, unresectable liver tumors. Unfortunately, not all patients are amenable for intra-arterial radioembolization and these patients might benefit from intratumoral radioablation with radioactive sources, so called interstitial microbrachytherapy.  $^{166}\text{HoAcAcMS}$  were proposed as a microbrachytherapy device. In addition, the intratumoral administration of radioactive microspheres is not limited to liver tumors, but can be used in solid tumors in other organs as well.

**Chapter 3** describes the preparation and characterization of holmium acetylacetonate microspheres (HoAcAcMS): microspheres dedicated for intratumoral radioablation. Since the injection volume is limited in solid tumors, the activity per sphere

should be as high as possible. Compared to the  $^{166}\text{HoPLLAMS}$ , the holmium content of the  $\text{HoAcAcMS}$  was 130% higher (44% w/w versus 19% w/w for the  $\text{HoPLLAMS}$ ) which is considered sufficient for intratumoral radioablation. Chemical characterization of these  $\text{HoAcAcMS}$  revealed a structural rearrangement of acetylacetonate around holmium during particle formation. Neither changes in the particle size nor in the particle surface were observed after neutron irradiation for up to six hours at a neutron flux of  $5 \times 10^{12} \text{ n cm}^{-2} \text{ s}^{-1}$ . Additionally, it was found that the sensitivity on MRI and CT also increased due to the 2.5 fold holmium increase, which is expected to facilitate image-guided delivery of the  $\text{HoAcAcMS}$  in patients.

**Chapter 4** presents the results of an *in vitro* and *in vivo* stability study of the  $\text{HoAcAcMS}$ . For the *in vitro* study, non-neutron irradiated and neutron irradiated  $\text{HoAcAcMS}$  were suspended in phosphate buffer, and the holmium content in buffer was determined at different timepoints. After incubation for 180 days in phosphate buffer, the release of holmium (3+) from the microspheres was  $0.5 \pm 0.2\%$ . The microspheres were analyzed using elemental analysis, infrared spectroscopy (IR spectroscopy), time of flight secondary ion mass spectrometry (TOF-SIMS), and scanning electron microscopy. Elemental analysis, IR spectroscopy and TOF-SIMS showed that the acetylacetonate in the microspheres was replaced by phosphate within four days, creating a very stable complex. Interestingly, SEM showed that the particles retained their size and shape, irrespective of the incubation time. The *in vivo* stability was assessed after intratumoral administration of  $^{166}\text{HoAcAcMS}$  to VX-2 tumor-bearing rabbits. The holmium content in urine, faeces and blood was determined to assess leakage of holmium from the microspheres. The holmium content in all these samples was below the detection limit. The rabbits were terminated one month after administration of  $^{166}\text{HoAcAcMS}$  and histological analysis of the tumor tissue revealed intact microspheres amidst necrotic tissue. The holmium content in bone (piece of femur) was below the detection limit of 0.1 ppm indicating no holmium had released from the microspheres. Altogether, it is concluded that  $^{166}\text{HoAcAcMS}$  are highly stable *in vivo* and therefore can be safely used for radioablation of liver malignancies.

**Chapter 5** reports on a case series of three cats with inoperable liver tumors of different histotype (hepatocellular carcinoma (HCC), cholangiocarcinoma (CC) and malignant epithelial liver tumors (MELT) of unknown origin) which underwent treatment with  $^{166}\text{HoAcAcMS}$ , administered percutaneously under ultrasound guidance. Follow-up consisted of regular physical examinations and hematological and biochemical analyses. The  $^{166}\text{HoAcAcMS}$  were successfully administered, and the treatment was well tolerated by all animals. The clinical condition of the cats improved markedly, as did most biochemical and hematological parameters shortly after treatment resulting in the extension of life in good quality of all animals. The HCC cat was euthanized six months after the first administration due to disease progression, the CC cat succumbed four months after the first treatment due to the formation of a pulmonary embolism, whereas the MELT cat developed bacterial meningitis and was euthanized three months post treatment. This radioablation

technique appears to be efficacious and not associated with adverse side effects and therefore it is concluded that percutaneous intratumoral administration of radioactive  $^{166}\text{HoAcAcMS}$  is feasible in cats suffering from liver tumors.

**Chapter 6** describes the use of intratumorally administered  $^{166}\text{HoAcAcMS}$  as a novel minimally-invasive treatment for kidney tumors. The efficacy of  $^{166}\text{HoAcAcMS}$  was compared to the intratumoral administration of saline in a renal cell carcinoma mouse model. Either five MBq  $^{166}\text{HoAcAcMS}$  in 10  $\mu\text{L}$  or 10  $\mu\text{L}$  saline was injected when the tumors were approximately 6 mm in size. After administration of  $^{166}\text{HoAcAcMS}$ , CT images were acquired on a dedicated small animal CT. At predefined time points post administration, the mice were sacrificed and the tumor, kidneys and liver, lungs, heart and spleen were excised. The tumor size was determined by measurement with digital calipers and the organs were measured using a dose calibrator, to determine the amount of radioactivity in the organs. The mice of the  $^{166}\text{HoAcAcMS}$  group showed an arrest in the tumor growth, whereas the tumors in the control group showed an exponential increase in tumor volume. Additionally, the multimodality imaging characteristics were exploited by performing micro CT, microSPECT and MR imaging on dedicated animal scanners. All imaging modalities showed a similar distribution of  $^{166}\text{HoAcAcMS}$ . The biodistribution of the  $^{166}\text{HoAcAcMS}$  as shown on the SPECT images was used to calculate a realistic dose distribution. Quantitative analysis of SPECT images, and the possibility to use these images for dosimetry is a fundamental advantage of the  $^{166}\text{HoAcAcMS}$  over other ablative techniques. This will improve the clinical application of this therapy, in terms of safety and efficacy.

**Chapter 7** is dedicated to the preparation of another holmium containing radioablation device: HoAcAc nanoparticles (HoAcAcNP). From the previous *in vivo* experiments described in chapters 4, 5 and 6, it was concluded that intratumoral injections with  $^{166}\text{HoAcAcMS}$  (approximately 8  $\mu\text{m}$ ) are effective, yet premature settling of the  $^{166}\text{HoAcAcMS}$  in the syringe posed a problem. By substantially reducing the particle size, the sedimentation rate of particle suspension is reduced, which may contribute to a standardized, reproducible injection procedure. A second (theoretical) advantage of a particle size reduction is an improved intratumoral distribution, leading to a better dose delivery. Spherical nanoparticles with a smooth surface and a diameter of  $0.08 \pm 0.01 \mu\text{m}$  were obtained with a holmium content of 44% (w/w) using a solvent evaporation technique. The nanoparticles were stable and showed a holmium release of less than 2% after 72 h in HEPES 10 mM. Neutron irradiation for one hour at a neutron flux of  $5 \times 10^{12} \text{ n cm}^{-2} \text{ s}^{-1}$  neither affected the particle size nor particle surface morphology. Additionally, the sensitivity of the HoAcAcNP on MRI and CT was assessed and it was observed that the sensitivity on CT was similar to the sensitivity of the HoAcAcMS. The sensitivity on MRI decreased due to the substantially reduced particle size, yet was similar to the MR sensitivity of HoAcAcMS when the particles are clustered. This led to the visualization of as little as 1.5  $\mu\text{g}$  of HoAcAcNP on MRI.

## Future perspectives

The main focus of this thesis was on HoAcAcMS which have been investigated in detail, and more insights into their formation, *in vitro* and *in vivo* stability, and efficacy have been obtained. However, a number of issues need to be addressed prior to the start of a phase I study in man. This thesis presents the work of a relatively short-term (one month) *in vivo* toxicity study, yet a longer *in vivo* toxicity study is required to evaluate the long-term effects of HoAcAcMS in tissue.

Treatment of solid tumors by direct injection of  $^{166}\text{HoAcAcMS}$  should be accurate and safe, irrespective of the tumor location. To this end, an injection system that enables accurate, reproducible administration of  $^{166}\text{HoAcAcMS}$  has to be developed.

In addition, this system has to shield both the beta particles and gamma rays to protect the physician from ionizing radiation in compliance with the as-low-as-reasonably-achievable (ALARA) principle.

Another issue to be addressed is the number of injections per target volume. The maximum tissue range of the  $^{166}\text{Ho}$  beta particles is 8.7 mm, and consequently tumors larger than 2 cm require multiple injections to achieve >100 Gy dose throughout the tumor. Therefore, the number and positions of injections to obtain complete tumor kill in larger (>2 cm) tumors needs to be investigated and standardized.

Apart from intratumoral injection HoAcAcMS may be used for transarterial hepatic radioembolization. For this modality, the particle size of HoAcAcMS needs to be increased from 15  $\mu\text{m}$  to 25 – 30  $\mu\text{m}$ , in order to obtain a particle size similar to the HoPLLAMS already in use. Potential advantages of the HoAcAcMS compared to HoPLLAMS rely on the higher holmium load per microsphere. Owing to the higher holmium content per sphere, similar amounts of activity can be administered in a lesser number of particles, thus reducing the risk of retrograde flow or stasis due to macro-embolization of hepatic vessels. Also, patient eligibility would be extended because patients suffering from portal vein thrombosis, which occurs in a high percentage of patients suffering from (primary) liver cancer, will then be allowed to receive holmium radioembolization treatment. The high holmium content of the HoAcAcMS allows for visualization on MRI of the relatively small amount of spheres used for the pretreatment scout dose. This might further pave the way for MR guided transcatheter radioembolization. The CT sensitivity of the HoAcAcMS might even allow for visualization of non-radioactive microspheres on the latest generation fluoroscopy systems currently used in angiography suites. This will further improve the image-guided transcatheter radioembolization treatment with holmium microspheres.

HoAcAc nanoparticles have also been prepared and characterized, and are proposed as a radioablation device that could be theorized to better penetrate tumorous tissue upon injection, but this has to be established. This can be investigated by comparing the intratumoral distribution of HoAcAc nanoparticles and HoAcAcMS following intratumoral injection.

Apart from this therapeutic application, the HoAcAc nanoparticles might be suitable as an MR contrast agent since their size is in the range of iron oxide particles (so-called superparamagnetic iron oxide (SPIO) particles 70 – 150 nm), which are

used for the detection of liver lesions. This requires a number of studies including cell uptake and toxicity studies to evaluate the feasibility of HoAcAc nanoparticles for this purpose.

A number of yet unexplored research possibilities in the field of holmium containing (micro)devices for potential diagnostic as well as therapeutic applications exist, and promises a bright future for these systems tagged with this fascinating element of the lanthanide group.









# Nederlandse Samenvatting

Sinds halverwege de jaren '90 van de vorige eeuw is er op de afdeling Nucleaire Geneeskunde van het Universitair Medisch Centrum Utrecht onderzoek verricht aan holmium beladen poly(melkzuur) microsferen ( $^{166}\text{Ho}$ PLLAMS). Deze microsferen zijn beoogd als een intra-arterieel 'microdevice' voor de behandeling van patiënten met niet-reseceerbare levermaligniteiten, en worden thans getest in een fase I studie bij patiënten met niet-reseceerbare levermetastasen. Voor sommige niet-reseceerbare tumoren, in bijvoorbeeld de hersenen en de nieren, zou directe intratumorale injectie van radioactieve microsferen een goede behandeltechniek zijn. Er is echter nog geen holmium-166 bevattend microdevice beschikbaar speciaal voor de ablatie van anderszins onbehandelbare tumoren met behulp van intratumorale injecties. Het doel van dit promotieonderzoek is het ontwikkelen en karakteriseren van een dergelijk holmium microsfeerpreparaat, het uitvoeren van *in vitro* en *in vivo* stabiliteitsonderzoek aan dit device, en de werkzaamheid *in vivo* hiervan te onderzoeken. Naast de ontwikkeling van holmium microsferen wordt ook onderzocht of het mogelijk is om holmiumbeladen nanodeeltjes te maken.

**Hoofdstuk 2** omvat een overzicht van microsfeer gebaseerde radioembolisatie-technieken, welke zijn ontwikkeld voor de behandeling van patiënten met levermaligniteiten die niet (voldoende) reageren op chemotherapie en niet-reseceerbaar zijn. Deze microsferen worden toegediend via een catheter die selectief in de leverslagader is geplaatst. Op deze manier wordt gebruikgemaakt van de vrijwel exclusief arteriële bloedtoevoer van levermaligniteiten om een hoge mate van tumor targeting te bewerkstelligen. Het gebruik van yttrium-90 ( $^{90}\text{Y}$ ) beladen hars- en glas-microsferen voor de behandeling van niet-reseceerbare levertumoren heeft goede klinische resultaten laten zien. In ongeveer 90% van de patiënten wordt er een gunstig effect op de tumoren gezien, variërend van stabiele ziekte tot complete remissie na radioembolisatie met deze  $^{90}\text{Y}$  microsferen. De selectieve catheterisatieprocedure is echter dikwijls complex en tijdrovend, en de klinici zijn genooddaakt om surrogaatdeeltjes te gebruiken om de biodistributie te voorspellen, aangezien kwantitatieve beeldvorming onmogelijk is met  $^{90}\text{Y}$ , omdat dit radio-isotoop uitsluitend bètadeeltjes uitzendt. Door een isotoop te gebruiken dat zowel bètadeeltjes als gammafotonen uitzendt, zoals rhenium-186, rhenium-188 en holmium-166, kan dit nadeel worden opgelost.

De klinische introductie van  $^{166}\text{Ho}$ PLLAMS zal naar verwachting voor een verdere verfijning van de microsfeergebaseerde radioembolisatietechnieken zorgen, en in preklinische studies is de veiligheid en werkzaamheid van dit radioembolisatie device inmiddels grondig onderzocht. Het isotoop  $^{166}\text{Ho}$  is uitermate geschikt voor radioembolisatie, aangezien de  $^{166}\text{Ho}$ PLLAMS *in vivo* kunnen worden afgebeeld met behulp van nucleaire beeldvorming, magnetische resonantie beeldvorming (MRI) en computertomografie (CT). Momenteel wordt de veiligheid en de werkzaamheid van deze  $^{166}\text{Ho}$ PLLAMS onderzocht bij patiënten met niet-reseceerbare metastasen in de lever.

Helaas komen niet alle patiënten met niet-reseceerbare maligne levertumoren in aanmerking voor behandeling met intra-arteriële radioembolisatie. Deze patiënten zouden mogelijk profijt hebben van direct intratumoraal ingebrachte

radioactieve bronnen, zogenaamde interstitiële microbrachytherapie. Holmium-166 acetylacetaat microsferen ( $^{166}\text{HoAcAcMS}$ ) zijn speciaal voor deze toepassing ontwikkeld. Bovendien is de intratumorale toediening van radioactieve microsferen niet beperkt tot alleen de lever, maar kunnen ook solide tumoren in andere organen hiermee worden behandeld.

**Hoofdstuk 3** beschrijft de ontwikkeling en karakterisering van de HoAcAcMS, microsferen specifiek bedoeld voor intratumorale toediening. Aangezien het volume dat in een tumor geïnjecteerd kan worden vaak beperkt is, moet de activiteit per microsfeer zo hoog mogelijk zijn. De HoAcAcMS bevatten ten opzichte van de HoPLLAMS ongeveer 130% meer holmium per microsfeer (44% voor de HoAcAcMS t.o.v. 17% voor de HoPLLAMS), wat voldoende wordt geacht voor intratumorale radioablatie. De chemische karakterisering van de microsferen toonde aan dat de deeltjes worden gevormd door het reorganiseren van het acetylacetaat rond de holmium ionen. Neutronenactivering gedurende 6 uur met een thermische neutronenflux van  $5 \times 10^{12} \text{ n cm}^{-2} \text{ s}^{-1}$  had geen invloed op het oppervlak van de HoAcAcMS, noch op de deeltjesgrootte. Verder leidt het hogere holmiumgehalte tot een rechtevenredige toename in sensitiviteit van de beeldvormingsmodaliteiten MRI en CT, wat beeldgeleide toediening van de  $^{166}\text{HoAcAcMS}$  ten goede komt.

In **Hoofdstuk 4** worden de resultaten beschreven van een *in vitro* en *in vivo* stabiliteitsonderzoek van de HoAcAcMS. Voor het *in vitro* stabiliteitsonderzoek werden zowel neutronengeactiveerde als niet-geactiveerde HoAcAcMS in een fosfaat buffer gesuspendeerd. De afgifte van holmium aan de fosfaatbuffer werd onderzocht op verschillende tijdpunten; na 180 dagen incubatie in de buffer was  $0,5 \pm 0,2\%$  vrijgekomen uit de HoAcAcMS. De microsferen zijn geanalyseerd met behulp van element analyse, infraroodspectroscopie (IR spectroscopie), "time of flight" secundaire ionen-massaspectrometrie (TOF-SIMS) en scanning elektronenmicroscopie (SEM). Element analyse, IR spectroscopie en TOF-SIMS toonden aan dat het acetylacetaat in de microsferen binnen 4 dagen volledig is uitgewisseld met fosfaat uit de buffer waardoor een zeer stabiel complex ontstaat. Bovendien bleek uit SEM-beelden dat de morfologie van de microsferen niet veranderd was ongeacht de incubatieduur. De *in vivo* stabiliteit van de microsferen werd onderzocht in tumordragende konijnen waarbij  $^{166}\text{HoAcAcMS}$  intratumoraal werden toegediend. Het holmiumgehalte in urine, feces en bloed werd bepaald om de lekkage van holmium uit de microsferen te bepalen. In alle monsters was het holmiumgehalte beneden de detectielimiet. De konijnen werden een maand na toediening van de  $^{166}\text{HoAcAcMS}$  geëuthanaseerd, waarna histologische analyse aantoonde dat de microsferen intact waren, omringd door necrotisch (tumor) weefsel. Er werd geen holmium gemeten in het bot, wat een aanwijzing is dat er geen holmium uit de microsferen was geëkt. Dit in ogenschouw nemende, kan worden geconcludeerd dat  $^{166}\text{HoAcAcMS}$  stabiel zijn *in vivo*, en daarmee dat ze veilig zijn voor gebruik bij radioablatie van (lever)tumoren.

**Hoofdstuk 5** beschrijft een haalbaarheidsstudie waarbij een drietal katten met niet-reseceerbare levertumoren van verschillende celtypen (hepatocellulair carcinoom

(HCC), cholangiocarcinoom (CC) en een maligne epitheliale levertumor (MELT) van onbekend histotype) echogeleid percutaan  $^{166}\text{HoAcAcMS}$  toegediend kregen. De follow-up van de dieren bestond uit frequente lichamelijk onderzoeken en biochemische en hematologische analyses. De  $^{166}\text{HoAcAcMS}$  werden succesvol toegediend, en de behandeling werd door alle katten goed doorstaan. De klinische status van de katten verbeterde zienderogen, als ook de biochemische en de hematologische parameters. De behandelingen resulteerden in een verlenging van het leven en een verbetering van de kwaliteit van leven. De HCC kat werd zes maanden na de eerste behandeling geëuthanaseerd vanwege ziekteprogressie, de CC kat bezweek 4 maanden na de eerste behandeling aan een longembolie, terwijl de MELT kat een bacteriële meningitis ontwikkelde waarvoor hij 3 maanden na de eerste behandeling werd geëuthanaseerd. De radioablatietechniek lijkt een effectieve behandeling waarbij weinig bijwerkingen voorkomen en derhalve kan er worden geconcludeerd dat de behandeling van levertumoren via percutane intratumorale injecties in katten haalbaar is.

In **hoofdstuk 6** worden resultaten gepresenteerd van een studie naar de effectiviteit van  $^{166}\text{HoAcAcMS}$  als een nieuwe minimaal invasieve techniek voor de behandeling van kleine niertumoren, waarbij de  $^{166}\text{HoAcAcMS}$  intratumoraal werden toegediend. Het diermodel bestond uit de muis met het geïmplanteerde niercelcarcinoom. De  $^{166}\text{HoAcAcMS}$  (5 MBq in 10  $\mu\text{l}$ ) direct geïnjecteerd wanneer de tumoren ongeveer 6 mm in diameter waren. Bij de controlegroep werd uitsluitend 10  $\mu\text{l}$  fysiologisch zout toegediend. Na toediening van de microsferen werden er CT-beelden gemaakt met behulp van een micro-CT-systeem om de verdeling van de microsferen te beoordelen. Op verschillende tijdpunten na toediening van de microsferen werden de muizen geëuthanaseerd en werden de tumor, nieren, lever, milt, hart en de longen uitgenomen. De tumorgrootte werd gemeten en met een dosiscalibrator werd bepaald hoeveel radioactiviteit in de organen was terechtgekomen. Het tumorvolume van de muizen die behandeld waren met  $^{166}\text{HoAcAcMS}$  bleef gelijk, terwijl het tumorvolume van de met fysiologisch zout behandelde muizen een exponentiële groei liet zien. Naast de effectiviteit werden ook de multimodale beeldvormingseigenschappen van de  $^{166}\text{HoAcAcMS}$  onderzocht door CT, SPECT en MRI uit te voeren met behulp van speciale proefdierscanners. Alle beeldvormingsmodaliteiten lieten een identieke distributie van de  $^{166}\text{HoAcAcMS}$  zien. Op basis van de microSPECT-beelden kon de geabsorbeerde-dosisverdeling worden berekend. Kwantitatieve analyse van de SPECT-beelden en daarmee de mogelijkheid van dosimetrie is een fundamenteel voordeel van de  $^{166}\text{HoAcAcMS}$  ten opzichte van andere ablatietechnieken. Deze mogelijkheid zal de toekomstige klinische toepassing van deze therapie verbeteren, zowel qua veiligheid als effectiviteit.

In **hoofdstuk 7** wordt de ontwikkeling van een ander holmium radioablatie device besproken: HoAcAc nanoparticles (HoAcAcNP). Uit de in hoofdstukken 4, 5 en 6 beschreven *in vivo* studies werd mede geconcludeerd dat intratumorale injecties met  $^{166}\text{HoAcAcMS}$  (met een diameter van ongeveer 8  $\mu\text{m}$ ) zeker effectief waren voor de behandeling van solide tumoren, maar dat het vroegtijdig uitzakken van

de microsferensuspensie in de spuit soms een praktisch probleem vormde. Door de deeltjesgrootte substantieel te verkleinen neemt de sedimentatiesnelheid af, waardoor er meer gestandaardiseerd en reproduceerbaar kan worden toegediend. Een tweede (theoretisch) voordeel is dat de afname van de deeltjesgrootte zelfs tot een verbetering van de intratumorale distributie van de deeltjes zou leiden door een betere weefselpenetratie. Er werden nanodeeltjes met een glad oppervlak, een diameter van  $0,08 \pm 0,01 \mu\text{m}$  en een holmiumgehalte van 44% gemaakt via een 'solvent evaporation'-methode. De deeltjes waren stabiel en lieten minder dan 2% holmiumlekkage zien na 72 uur in een HEPES buffer van 10 mM. Eén uur bestralen met een thermische neutronenflux van  $5 \times 10^{12} \text{ n cm}^{-2} \text{ s}^{-1}$  beïnvloedde de deeltjesgrootte en het deeltjesoppervlak niet. Daarnaast werd er onderzoek gedaan naar de sensitiviteit van CT en MRI voor de HoAcAcNP, en het bleek dat de sensitiviteit van CT voor deze deeltjes identiek was aan die voor de HoAcAcMS. De sensitiviteit van MRI nam echter af door de afname in deeltjesgrootte ten opzichte van de HoAcAcMS. Wanneer de deeltjes geclusterd waren, was de sensitiviteit echter gelijk. De kleinste hoeveelheid HoAcAcNP die met MRI kon worden gedetecteerd was 1,5  $\mu\text{g}$ .





# List of Affiliations


## Affiliations

C.J.G. Bakker	Image Sciences Institute, Department of Radiology and Nuclear Medicine, University Medical Centre Utrecht, Utrecht, The Netherlands
F.J. Beekman	Image Sciences Institute, Department of Radiology and Nuclear Medicine, University Medical Centre Utrecht, Utrecht, The Netherlands
W. Bult	Department of Radiology and Nuclear Medicine, University Medical Centre Utrecht, Utrecht, The Netherlands
H.W.A.M. de Jong	Department of Radiology and Nuclear Medicine, University Medical Centre Utrecht, Utrecht, The Netherlands
H. de Leeuw	Image Sciences Institute, Department of Radiology and Nuclear Medicine, University Medical Centre Utrecht, Utrecht, The Netherlands
M. Elschot	Department of Radiology and Nuclear Medicine, University Medical Centre Utrecht, Utrecht, The Netherlands
I. Gielen	Department of Veterinary Medical Imaging and Small Animal Orthopaedics, Faculty of Veterinary Medicine, Ghent University, Merelbeke, Belgium
R.M.A. Heeren	FOM institute for Atomic and Molecular Physics, Amsterdam, The Netherlands
W.E. Hennink	Department of Pharmaceutics, Utrecht Institute for Pharmaceutical Sciences, Utrecht University, Utrecht, The Netherlands
J.J.M. Jans	Department of Urology, University Medical Centre Utrecht, Utrecht, The Netherlands
G.C. Krijger	Department of Radiation, Radionuclides and Reactors, Delft University of Technology, Delft, The Netherlands
S.G.C. Kroeze	Department of Urology, University Medical Centre Utrecht, Utrecht, The Netherlands
L.M.J. Kroon-Batenburg	Department of Crystal and Structural Chemistry, Utrecht University, Utrecht, The Netherlands
P.R. Luijten	Department of Radiology and Nuclear Medicine, University Medical Centre Utrecht, Utrecht, The Netherlands



J.F.W. Nijssen	Department of Radiology and Nuclear Medicine, University Medical Centre Utrecht, Utrecht, The Netherlands
K. Peremans	Department of Veterinary Medical Imaging and Small Animal Orthopaedics, Faculty of Veterinary Medicine, Ghent University, Merelbeke, Belgium
J. Saunders	Department of Veterinary Medical Imaging and Small Animal Orthopaedics, Faculty of Veterinary Medicine, Ghent University, Merelbeke, Belgium
P.R. Seevinck	Image Sciences Institute, Department of Radiology and Nuclear Medicine, University Medical Centre Utrecht, Utrecht, The Netherlands
F. Soulimani	Inorganic Chemistry and Catalysis Group, Department of Chemistry, Faculty of Science, Utrecht University, Utrecht, The Netherlands
O.M. Steinebach	Department of Radiation, Radionuclides and Reactors, Delft University of Technology, Delft, The Netherlands.
A.D. van het Schip	Department of Radiology and Nuclear Medicine, University Medical Centre Utrecht, Utrecht, The Netherlands
E. Vandermeulen	Department of Veterinary Medical Imaging and Small Animal Orthopaedics, Faculty of Veterinary Medicine, Ghent University, Merelbeke, Belgium
R. Varkevisser	Department of Radiology and Nuclear Medicine, University Medical Centre Utrecht, Utrecht, The Netherlands
M.A.D. Vente	Department of Radiology and Nuclear Medicine, University Medical Centre Utrecht, Utrecht, The Netherlands
T. Visser	Inorganic Chemistry and Catalysis Group, Department of Chemistry, Faculty of Science, Utrecht University, Utrecht, The Netherlands
B. Th. Wolterbeek	Department of Radiation, Radionuclides and Reactors, Delft University of Technology, Delft, The Netherlands.
B.A. Zonnenberg	Department of Internal Medicine, University Medical Centre Utrecht, Utrecht, The Netherlands





**Curriculum Vitae  
and  
List of Publications**



Wouter Bult was born on September 4, 1979, in the picturesque little town of Putte, situated at the Dutch-Belgium border. He finished his secondary school in 1997 at the RSG 't Rijks in Bergen op Zoom. In that same year, he commenced the study of pharmaceutical sciences at Utrecht University, the Netherlands. During the master phase, he performed a research project of 6 months at the Victorian College of Pharmacy in Melbourne, Australia. In May 2004, he obtained his pharmacists degree. Wouter subsequently worked as a pharmacist at the Utrecht Veterinary School. In December 2005, Wouter started his PhD project at the Department of Nuclear medicine of the University Medical Center Utrecht, in close cooperation with the Utrecht Institute of Pharmaceutical Sciences, which resulted in this thesis. As of June 1, 2010, he started working as a pharmacist at the Department of Hospital and Clinical Pharmacy of the University Medical Centre Groningen. Wouter is married to Rosemarie Wasmann, and they have a daughter named Sophie.

Wouter Bult is op 4 september 1979 geboren in het kleine pittoreske dorp Putte, gelegen op de grens van Nederland en België. In 1997 rondde hij op RSG 't Rijks te Bergen op Zoom de middelbare school succesvol af, en begon in datzelfde jaar aan de studie Farmacie in Utrecht. Tijdens de doctoraalfase van deze studie heeft hij 6 maanden onderzoek gedaan aan de Victorian College of Pharmacy in Melbourne, Australië. In mei 2004 ontving hij de apothekersbul. Vervolgens trad hij in dienst als apotheker bij de Apotheek Diergeneeskunde, aan de Faculteit der Diergeneeskunde in Utrecht. In december 2005 is hij begonnen aan het promotieonderzoek op de afdeling Nucleaire Geneeskunde in samenwerking met het Utrecht Institute for Pharmaceutical Sciences, wat uiteindelijk geleid heeft tot dit proefschrift. Op 1 juni 2010 is hij gestart met een baan als projectapotheker in het Universitair Medisch Centrum Groningen. Wouter is getrouwd met Rosemarie Wasmann, en ze hebben samen een dochter, Sophie.

### Articles

Boeve M, **Bult W**. Diclofenamide. Tijdschr Diergeneeskd. 2005 Apr 15; 130(8): 256

**Bult W**, Seevinck PR, Krijger GC, Visser T, Kroon-Batenburg LM, Bakker CJ, Hennink WE, van het Schip AD, Nijsen JF. Microspheres with ultrahigh holmium content for radioablation of malignancies. Pharm Res. 2009 Jun;26(6):1371-1378

**Bult W**, Vente MA, Zonnenberg BA, van het Schip AD, Nijsen JF. Microsphere radioembolization of liver malignancies: current developments. Q J Nucl Med Mol Imaging. 2009 Jun; 53(3): 325-335

Vente MA, de Wit TC, van den Bosch MA, **Bult W**, Seevinck PR, Zonnenberg BA, de Jong HW, Krijger GC, Bakker CJ, van het Schip AD, Nijsen JF. Holmium-166 poly(L-lactic acid) microsphere radioembolisation of the liver: technical aspects studied in a large animal model. Eur Radiol. 2010 Apr; 20(4): 862-869

Smits ML, Nijsen JF, van den Bosch MA, Lam MG, Vente MA, Huijbregts JE, van het Schip AD, Elschot M, **Bult W**, de Jong HW, Meulenhoff PC, Zonnenberg BA. Holmium-166 radioembolization for the treatment of patients with liver metastases: design of the first-in-man HEPAR trial. J Exp Clin Cancer Res. 2010 Jun 15;29:70

**Bult W**, Varkevisser R, Soulimani F, Seevinck PR, de Leeuw H, Bakker CJ, Luijten PR, van het Schip AD, Hennink WE, Nijsen JF. Holmium Nanoparticles: preparation and in vitro characterization of a new device for Radioablation of Solid Malignancies. Pharm Res. 2010 Oct;27(10):2205-12.

Oerlemans C, **Bult W**, Bos M, Storm G, Nijsen JF, Hennink WE. Polymeric Micelles in Anticancer Therapy: Targeting, Imaging, and Triggered Release. Pharm Res. 2010 Aug 20. (Epub ahead of print)

**Bult W**, de Leeuw H, Steinebach OM, Wolterbeek W Th, Hennink WE, van het Schip AD, Nijsen JF. Radioactive holmium acetylacetonate microspheres for interstitial microbrachytherapy: an *in vitro* and *in vivo* stability study. *Submitted*

**Bult W**, Kroeze SG, Elschot M, Seevinck PR, Beekman FJ, Luijten PR, Hennink WE, de Jong HW, van het Schip AD, Bosch JL, Nijsen JF, Jans JJ. Radioactive microspheres for treatment and multimodality imaging in a mouse model of kidney cancer. *In preparation*

**Bult W**, Vente MA, Vandermeulen E, Seevinck PR, Saunders J, van het Schip AD, Bakker CJ, Krijger GC, Peremans K, Nijsen FJ. Interstitial microbrachytherapy using holmium-166 acetylacetonate microspheres: a feasibility study in feline liver cancer patients. *Submitted*

**Abstracts (first and second authorship only)**

Zielhuis SZ, **Bult W**, Vente MA, Nijsen JF, de Wit TC, Krijger GC, Seevinck PR, de Roos R, Zonnenberg BA, van Rijk PP, van het Schip AD. Preliminary studies on holmium-166 loaded liposomes for diagnostic and therapeutic purposes. European Association of Nuclear Medicine Annual Meeting 2006, Athens, Greece

Vente MA, **Bult W**, de Wit TC, Seevinck PR, Seppenwoolde JH, Zonnenberg BA, de Roos R, Krijger GC, van het Schip AD, Nijsen JF. Holmium-166 poly-L-lactic acid microspheres for treatment of liver malignancies: treatment procedure testing in a large animal model. International Researchgroup on Immuno-Scintigraphy and Therapy "Beta Days" 2007, Capri, Italy

Seevinck PR, **Bult W**, Nijsen JF, Vente MA, de Roos R, van het Schip AD, Bakker CJ. Highly loaded holmium microspheres for test dose detection and biodistribution prediction in internal radiation therapy of liver tumors. International Society of Magnetic Resonance in Medicine Annual Conference 2008, Toronto, Canada

**Bult W**, Krijger GC, Hennink WE, van het Schip AD, Nijsen JF. New microspheres with high holmium-166 content for microbrachytherapy. World Biomaterials Conference 2008, Amsterdam, The Netherlands

**Bult W**, Vente MA, Vandermeulen E, Vermeire S, de Roos R, Hennink WE, van het Schip AD, Peremans K, Nijsen JF. Intratumoral radioablation of liver tumors using holmium-166 microspheres: a pilot study. Biomaterials Asia 2009, Hong Kong, China

**Bult W**, Seevinck PR, Krijger GC, Bakker CJ, Hennink WE, van het Schip AD, Nijsen JF. Multifunctional microspheres with ultrahigh holmium load for imaging and therapy. International Society of Magnetic Resonance in Medicine Annual Conference 2009, Honolulu, Hawaii

**Bult W**, Vente MA, Zonnenberg BA, Kirpensteijn J, Meij BP, van der Bovenkamp CG, Peremans K, Vermeire S, Vandermeulen E, Dekkers E, Krijger GC, de Roos R, van het Schip AD, Nijsen JF. Interstitial microbrachytherapy in veterinary patients using small holmium-166 microspheres. European Association of Nuclear Medicine Annual Meeting 2009, Barcelona, Spain

**Bult W**, Kroeze SG, Beekman FJ, Bosch JL, Nijsen JF, Jans JJ. Holmium Loaded Microspheres as novel minimally invasive therapy for kidney cancer. International Researchgroup on Immuno-Scintigraphy and Therapy Biannual conference 2010, Groningen, The Netherlands

**Patent application**

Nijsen JF, **Bult W**, van het Schip AD. A microsphere comprising an organic lanthanide metal complex. EP2178817.







**Dankwoord**



Hooggeleerde Prof. dr. ir. Hennink, beste Wim, tijdens mijn promotie heb ik je inzicht, meedenken, directheid en gevoel voor humor heel erg gewaardeerd. Hartelijk dank voor de 2-maandelijke meetings, het snel en grondig nakijken van manuscripten en natuurlijk de gastvrijheid op het Biofarmacie lab!

Hooggeleerde Prof. dr. Luijten, beste Peter, al kwam je wat later aan boord, mede dankzij je praktische en gestructureerde aanpak werd het project succesvol afgerond. Bedankt!

Hooggeleerde Prof. dr. van Rijk, beste Peter, je ging al snel na mijn aanstelling met emiraat. Dank voor de overlegmomenten die we hebben gehad.

Dan kom ik bij mijn twee co-promotores, die samen de ruggengraat vormen van **de** Holmiumgroep.

Dr. Nijsen, beste Frank, je tomeloze enthousiasme en de wil om dingen gedegen uit te zoeken hebben ertoe geleid dat dit werk is afgesloten met een *happy ending*. Bedankt! Ditzelfde enthousiasme en doorzettingsvermogen hebben ertoe geleid dat er inmiddels patiënten met leverkanker in studieverband worden behandeld met holmium microsferen, wat een hele prestatie is!

Dr. van het Schip, beste Fred, *meticulous, concise, determined* en *resourceful* zijn woorden die je mijns inziens typeren. *Less is more*, al was ik misschien soms wat al te kort door de bocht. Hartelijk dank voor de discussies, het woord voor woord doorpluizen van manuscripten en de rustige, praktische en doortastende aanpak bij veel probleemstellingen. Bedankt!

De leden van de leescommissie, Prof. dr. J.L.H.R. Bosch, Prof. dr. J. Kirpensteijn, Prof. dr. J.J.W. Lagendijk, Prof. dr. G. Storm, en Prof. dr. C. van de Wiele wil ik graag bedanken voor hun bereidheid mijn manuscript te beoordelen.

Dr. Zonnenberg, beste Bernard, als internist-oncoloog ben je betrokken bij **het** Holmiumproject. Je deskundigheid op velerlei gebieden, je inventiviteit, creativiteit en gevoel voor humor heb ik zeer gewaardeerd.

Dr. Vente, beste Maarten, met jou heb ik drie jaar op één kamer *ups, downs, strikes* en *gutters* gedeeld. Het was heel fijn om je kennis van radio-embolisatie, kanker, (proef)dieren en (archaïsch) Engels te kunnen aanspreken. Bedankt ook voor de inhoudelijke input, en ideeën voor experimenten. Bovendien delen we een licht gestoord gevoel voor humor, waardoor de grootste “rampen” (uiteindelijk) weggelachen konden worden. Ook de uitjes naar het WK Superbikes in Assen heb ik heel erg gewaardeerd! Heel veel succes met je carrière in de radiotherapie (zowel humaan als veterinair)!

De held van menig aio van **de** Holmiumgroep is Remmert – “Rembo” – de Roos. Als ik je met één zin zou typeren: “Remmert regelt het wel!” En dat was ook zo, geen vraag te moeilijk, of je wist het binnen een dag te regelen door je eindeloze netwerk binnen het UMC. Hartelijk dank voor de hulp bij mijn experimenten!

Dan komen we bij de “nieuwe helden” van **het** Holmiumproject. Allereerst Chris – “spieren in rust” – Oerlemans, bedankt voor je humoristische inbreng en het te pas en te onpas citeren van Family Guy. Succes met je onderzoek, laat je niet gek maken! Plezierig! Onze Grieks/Franse Agnes – “Gallo, goe gaat get?” – Paradissis wens ik sterkte met het verpakken van holmium nanoparticles in micellen, en natuurlijk met het (steeds beter) leren van de Nederlandse taal. De jongste aanwinst voor **de** Holmiumgroep is Mattijs – “Mooie Mattie” – Elschot, met wie ik de laatste maanden de kamer heb gedeeld. Bedankt voor de humor, de voorkeur voor StuBru, de squashavondjes en de passie voor ‘bakken’! Sterkte met de dosimetrie-vraagstukken! Ook zou ik Dr. Sander Zielhuis willen bedanken: ik heb je meermalen lastig gevallen met rare vragen. Dank voor je bereidheid deze te beantwoorden! Succes in de ziekenhuisapotheek van het AMC!

Verder wil ik alle medewerkers van de afdeling Nucleaire Geneeskunde bedanken die de werkomgeving iedere dag stralend maakten. De heren (klinisch) fysici en klinisch fysici i.o. (Hugo, Tim, Aááánold, Bartje en Alan) zou ik ook graag willen bedanken voor de gezelligheid, het squashen en de discussies tijdens de lunch.

Multimodale beeldvorming is een belangrijk onderdeel van dit proefschrift.

Dr. Bakker, beste Chris, je drang tot wetenschap is aanstekelijk! Dank voor de interessante discussies, rappe en duidelijke commentaren op manuscripten en droog gevoel voor humor. Bedankt!

*Fore!* Dr. Seevinck, beste Peter, bedankt voor de avonden MRI en CT scannen van gelen met bollen. De (quasi)wetenschappelijke gesprekken onder het genot van een biertje, al dan niet na het slaan van ballen, heb ik erg gewaardeerd! Da ge bedankt zet, da witte.

Hendrik de Leeuw, bedankt voor al die avonden scannen van fantomen, maar vooral voor het eindeloos scannen van konijnen! Wat konden we dat toch goed op het laatst... Succes met het vergaren van voldoende wetenschappelijke data voor jezelf! Gerrit van de Maat, bedankt voor het meten van menig fantoom op 4,7 Tesla en gerelateerde discussies. Sterkte met het afronden van je eigen promotie. Martijn van der Bom zou ik willen bedanken voor de verrassend snelle CT acquisities, de gezellige diners in “*Le Brinque*” en de flauwe grappen...

Mijn tweede werkplek was de afdeling Biofarmacie en Farmaceutische Technologie. De rots in de branding daar is Mies van Steenbergen. Mies, jij bent de redder van AIO’s in nood. Je optimisme, behulpzaamheid en kunde zijn legendarisch! Hartelijk dank voor al je hulp.

De mooie jongens van kamernummer Z735A: Marcel, Raymond en Enrico. Bedankt voor de flauwe grappen en de samenwerking met de uitdagende muizenstudie, die helaas niet is opgenomen in dit proefschrift. In het bijzonder Marcel: je optimisme, gevoel voor humor en praktische aanpak van onderzoek zijn ongeëvenaard. Vat geen kou boy daar in de VS, het is geen Italië!

De groep is verder zo leuk, gezellig en behulpzaam dat ik jullie allen wil bedanken voor de leuke tijd, gezellige uitjes en spetterende borrels, en een paar mensen in het bijzonder: Albert de G., Amir G., Cristianne, Ellen, Ethlinn, Frank, Inge, Joost, Joris, Marina, Marion, Marjan, Niels, Pieter, Roel, Roberta, Rolf, Roy, Sophie, Tina. Bedankt!

Dr. Wally Müller, Chris Schneidenberg en Hans Meeldijk wil ik bedanken voor de *no-worries* mentaliteit, eindeloze geduld en de onbegrensde hulpvaardigheid bij de SEM acquisities. Dr. Tom Visser van de afdeling Anorganische Chemie wil ik graag bedanken voor zijn hulpvaardigheid en kennis van IR en RAMAN spectroscopie, zelfs tot na je pensioen heb je me erg fijn geholpen. Bedankt! Fouad Soulimani wou ik bedanken voor het uitvoeren van de IR en RAMAN metingen. Dr. Loes Kroon-Batenburg van de afdeling Kristal- en Structurele Chemie wil ik graag bedanken voor de fijne discussies over de structuur van *de* bollen. Prof. dr. Ron Heeren, bedankt voor het *last-minute* vergaren van essentiële informatie!

Dr. Gerard Krijger wil ik bedanken voor het bestralen van bollen, de avonden met bier en het lepeltje-lepeltje liggen op Capri ;-). Anneke Koster-Ammerlaan wil ik bedanken voor de prettige samenwerking en vooral de precisie waarmee er bestraald werd! René Nouse, wil ik graag bedanken voor zijn ritten bij nacht en ontij om ons de “hete” bollen te komen brengen in ruil voor hete “koffie”. Olav Steinebach zou ik willen bedanken voor zijn hulp bij de ICP-OES metingen en het meedenken over de destructie van holmiumbevattende monsters.

Zonder biotechnici en diervverzorgers geen dierexperimenten!! In het bijzonder wil ik Nico, Hester, Hans en Anja bedanken voor hun excellente biotechnische assistentie tijdens de konijnenexperimenten.

De afdeling Stralingshygiëne van het UMC (Carolien, Kitty, Michel, Marlies en Huub) en die van het GDL (Jannico en Hans) zou ik ook graag willen bedanken voor het meedenken en het beoordelen/doorrekenen van alle aanvragen.

Hoofdstuk 5 zou er niet zijn gekomen zonder de inzet en het meedenken van onze collega's van de afdeling Nucleaire Diergeneeskunde in Gent, België. Dr. Kathelijne Peremans, dr. Eva Vermeulen, dr. Ingrid Gielen, en (bijna-)dr. Simon Vermeire, heel hartelijk dank voor de gastvrijheid, samenwerking en voor jullie aangename aanwezigheid.

Hoofdstuk 6 zag het levenslicht dankzij een prettige samenwerking met Stephanie Kroeze en dr. Judith Jans van de afdeling Urologie van het UMC Utrecht. Ik zou jullie graag willen bedanken voor de aangename samenwerking, de telefoontjes, de daadkrachtige experimentele aanpak en de zgn. KGB's. Ruud Ramakers wil ik graag bedanken voor zijn geduld, zijn hulp met SPECT-acquisities, en het registreren van de mooie plaatjes. Sorry voor de flauwe grappen...;-).

Raymond Toelanie wil ik bedanken voor de mooie illustraties, en Karin van Rijnbach voor het opmaken van vele mooie posters en dit proefschrift!

Laten we ook de studenten niet vergeten die hun onderzoeksstages op de afdeling Nucleaire Geneeskunde van het UMC Utrecht hebben overleefd: Albert de G., Maria, Filipe, Lara ('Laers'), Xandra, Judith, Mira ('Miers'), en Rosanne. Bedankt voor jullie aanwezigheid en bijdrage, ik heb veel van jullie geleerd! Leuk te zien dat een aantal van jullie ook de wetenschap zijn ingedoken, ondanks jullie onderzoeksproject onder mijn hoede...

Ik zou ook graag mijn nieuwe collegae van de afdeling Klinische Farmacie en Apotheek van het UMC Groningen willen bedanken voor de gezelligheid, de prettige werkomgeving en voor het mogelijk maken van de ICP-MS metingen.

*Last but **not** least* zou ik mijn familie en vrienden willen bedanken. Allereerst mijn paranimfen (en hun partners): Michiel ('Mikkus') en Sefik ('Zole'). Michiel, het was een hele eer ceremoniemeester te zijn op je trouwdag. Fijn dat je mij nu bijstaat! Zole, de nasi-avonden waren/zijn super, maar laten we op mijn promotiefeest wel alles heel?! Willem, Wybren, Alexander, Koen, de Leeuw, Ed, Bob, Rutger en Niels (en natuurlijk jullie partners), bedankt voor de gezellige avonden, borrels, diners, weekendjes weg, golfuitjes, flauwe films etc., etc. Bedankt! Laten we er snel weer een paar drinken!

Dan komen we bij de familie. Allereerst mijn schoonfamilie, Hans, Marian, Merel en Roeland. Bedankt voor de gastvrijheid, de gezelligheid tijdens uitdagende, inspirerende, ongelofelijk mooie reizen naar verre oorden, de potjes golf en de overheerlijke diners.

Mijn lieve zus Merel en haar man 'nonkel' Barry: bedankt voor de gezelligheid, de morele steun, de gezellige feestjes, asperge/BBQ-avonden, de mooie bruidsauto, de flauwe grappen etc., etc. Mijn dankbaarheid grenst aan hondsdelheid! Lieve Papa en Mamma (sPa/Bompa en sMa/Bomma), dank voor jullie eindeloze steun, liefde en vertrouwen! Ook al ben ik er niet meer zo vaak, naar Putte gaan is altijd thuiskomen. Jullie zijn echt te gek! Bedankt voor alles!

En dan als laatste mijn gezin: Rosemarie en Sophie. Lieve Roosje, na 5 jaar promotie-onderzoek en 2 jaar een LAT relatie te hebben gehad, ben ik dan ook eindelijk geëmigreerd naar Groningen. Voor mij geen avondjes meer achter de computer, geen ritjes naar de Uithof, geen weekenden meer typen of pipetteren, maar gewoon rust. Bedankt voor je eindeloze steun in soms barre tijden. Lieve Sophie, welkom in mijn leven! Laten we er wat moois van maken samen met mamma! Ik heb er zin in!



